



**COMILLAS**  
UNIVERSIDAD PONTIFICIA

ICAI

# GRADO EN INGENIERÍA EN TECNOLOGÍAS INDUSTRIALES

TRABAJO FIN DE GRADO

Numerical and experimental study of novel heat flux  
measurement in turbomachinery

Autor: Yago García Cucala

Director: Isak Jonsson

Co-Director: Valery Chernoray

Madrid

Declaro, bajo mi responsabilidad, que el Proyecto presentado con el título  
Numerical and experimental study of novel heat flux measurement in turbomachinery  
en la ETS de Ingeniería - ICAI de la Universidad Pontificia Comillas en el  
curso académico 2019/20 es de mi autoría, original e inédito y  
no ha sido presentado con anterioridad a otros efectos.  
El Proyecto no es plagio de otro, ni total ni parcialmente y la información que ha sido  
tomada de otros documentos está debidamente referenciada.



Fdo.: Yago García Cucala

Fecha: 20/ 08/ 2020

Autorizada la entrega del proyecto

Director:

Isak Jonsson

isak.jonsson@chalmers.se



Fecha: 23/ 08/ 2020





**COMILLAS**  
UNIVERSIDAD PONTIFICIA

ICAI

# GRADO EN INGENIERÍA EN TECNOLOGÍAS INDUSTRIALES

TRABAJO FIN DE GRADO

Numerical and experimental study of novel heat flux  
measurement in turbomachinery

Autor: Yago García Cucala

Director: Isak Jonsson

Co-Director: Valery Chernoray

Madrid



# **NUMERICAL AND EXPERIMENTAL STUDY OF NOVEL HEAT FLUX MEASUREMENT IN TURBOMACHINERY**

**Autor: García Cucala, Yago.**

Director: Jonsson Isak.

Entidad Colaboradora: Chalmers University of Technology.

## **RESUMEN DEL PROYECTO**

**Palabras clave:** flujo de calor, transferencia de calor, coeficiente de transferencia de calor, experimento, diseño.

### **1. Introducción**

El objetivo de este proyecto de fin de grado es diseñar un experimento que se utilizará para averiguar cómo de bien se puede medir el flujo de calor en el laboratorio utilizando una técnica de infrarrojos [1]. Un estudio reciente e innovador [2] ha mostrado resultados prometedores en la medición de transferencia de calor en las palas de salida de una turbina de baja presión [3]. En este estudio, la incertidumbre estimada es relativamente baja, que suscita escepticismo. Por lo tanto, las suposiciones aplicadas y el método deben verificarse utilizando casos más fundamentales donde existe una solución analítica precisa.

Este nuevo método parece ser muy preciso y rentable. Se basa en una técnica de medición de temperatura por infrarrojos que ayuda a reducir una de las principales fuentes de incertidumbre. Se quiere comparar este método usando un caso fundamental, la medición del flujo de calor a través de una placa plana. Para probar este método con este caso fundamental, es necesario diseñar un experimento apropiado donde el método de infrarrojos usado en el estudio anterior [2] pueda compararse con otros métodos experimentales.

En este proyecto se ha diseñado, construido y probado un experimento apropiado para poder comparar el método de infrarrojos.

### **2. Metodología**

El proyecto se divide en tres partes: el diseño y construcción del experimento, un cálculo de las incertidumbres de las mediciones y prueba de la instalación midiendo con la cámara de infrarrojos la temperatura superficial de la placa y midiendo el gradiente de presiones de la misma.

## 2.1 Diseño

Las condiciones que se desean simular dónde se realizarán todos los experimentos y mediciones adicionales es uno de los casos de transferencia de calor más básicos, el flujo de calor a través de una placa plana precalentada con flujo laminar. La placa plana se calentará con una corriente de agua a una determinada temperatura, el calor pasará mediante convección desde el agua  $T_w$  hasta la pared interior de la placa plana  $T_1$ , luego cruzará la placa plana por conducción llegando a la parte superior de la misma  $T_2$ . Una corriente de viento a una temperatura  $T_3$  atravesará la superficie de la placa enfriando su superficie por convección y radiación.

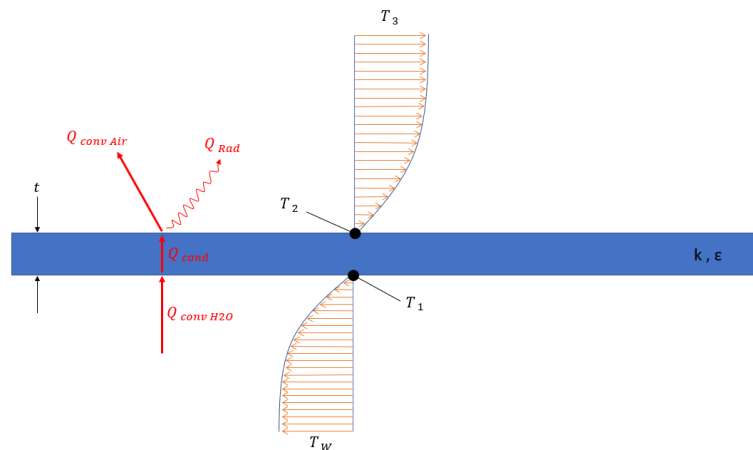


Figura 1. Representación teórica del experimento a diseñar

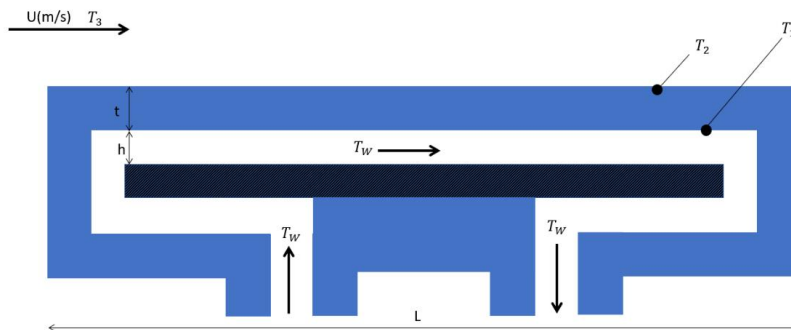


Figura 2. Idea básica del diseño del experimento.

Los principales parámetros que se deben definir para diseñar esta placa son la longitud y el espesor de la misma. Debe ser lo suficientemente larga para poder ver la evolución del flujo de calor a través de su superficie y para que la capa límite térmica e hidrodinámica se desarrollen por completo. Al mismo tiempo hay que tener en cuenta que su precio dependerá directamente del tamaño. Por otro lado, se ha de mantener lo más fina posible para minimizar las pérdidas de calor a través de las paredes para que tengan una temperatura superficial  $T_2$  lo más similar posible a la temperatura de la pared interior  $T_1$ .

Para calcular estos parámetros se realizó un estudio teórico tanto para flujo laminar como turbulento del experimento a diseñar.

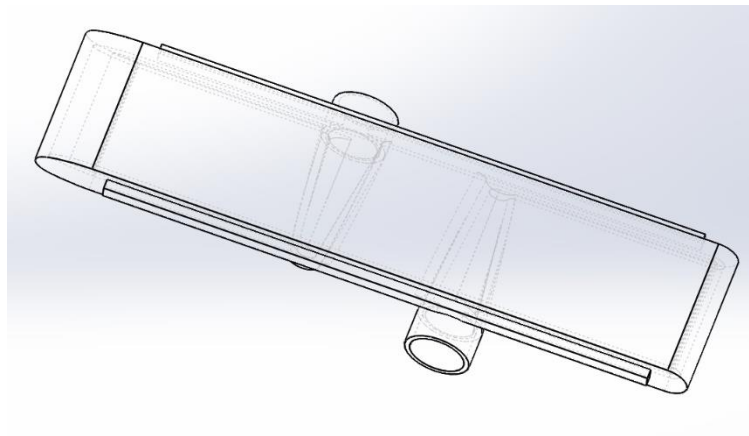


Figura 3. Diseño final de la placa

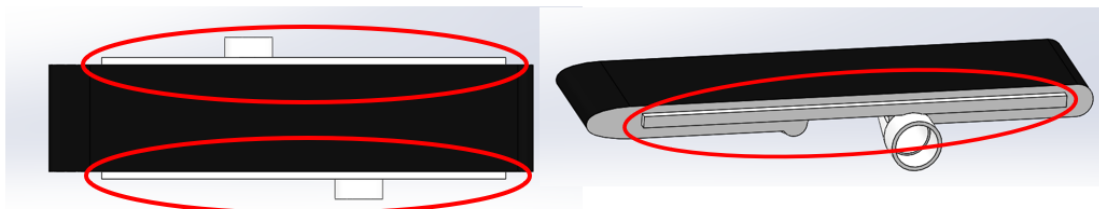


Figura 4. Salientes para sujetar la placa rodeados en rojo

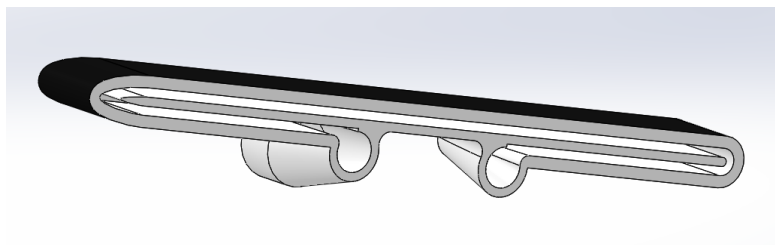


Figure 5. Canales internos de la placa.

Para sujetar la placa plana, dos soportes de aluminio idénticos fueron diseñados. Estos soportes son dos placas metálicas en forma de L con un orificio con la forma del contorno lateral de los salientes de la placa como se puede apreciar en la Figura 6. Estos salientes se introducirán en los soportes metálicos que luego se atornillan al suelo del túnel de viento.

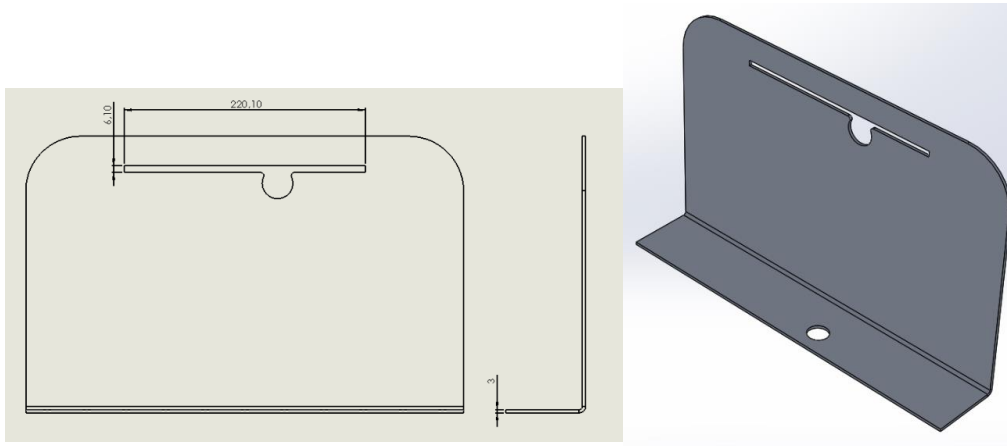


Figure 6. Diseño de los soportes de aluminio.

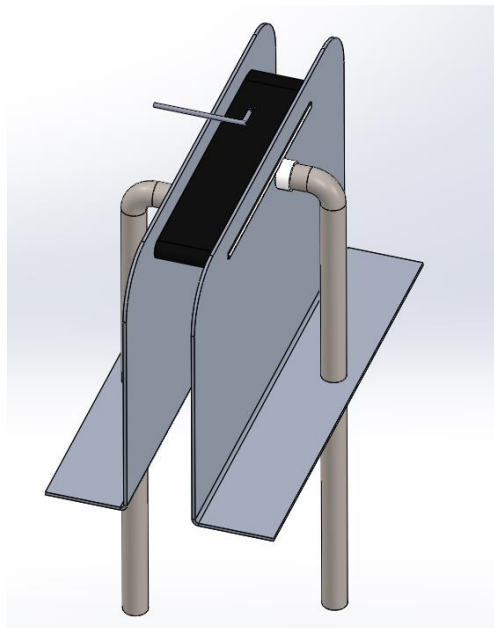


Figure 7. Diseño final del experimento

Las piezas diseñadas para el experimentado fueron encargadas. Una vez obtenidas, se construyó la estructura del experimento sobre una plataforma móvil que luego se instaló en el túnel de viento. El circuito de agua consiste en tubos de cobre cubiertos por un material aislante que se conecta a un tanque de agua donde se calienta y se bombeaba la

misma a través del circuito. Además, se colocaron distintos sensores para medir temperaturas y presiones, así como la cámara IR en el techo del túnel de viento.

## 2.2 Uncertainties calculations

Se realizó un cálculo de incertidumbres para que en futuras investigaciones se tenga una idea aproximada de qué tan precisas deben ser sus mediciones y para que puedan saber de dónde es más probable que vengan esos errores. Para ello, todas las variables que afectan al cálculo de transferencia de calor en el experimento diseñado se agruparon en la ecuación 1. Esta se obtiene de la combinación del cálculo del coeficiente de transferencia de calor a partir de los flujos de calor y el cálculo del coeficiente de transferencia de calor a partir del número de Nusselt para flujo laminar donde C es la constante  $C=0.332$ .

$$\text{Ecuación 1. } C = \left( \frac{1}{T_2 - T_3} \right) \left( \frac{k_w}{t} (T_1 - T_2) - \sigma (\epsilon T_2^4 - T_3^4) \right) \rho^{-\frac{1}{2}} x^{\frac{1}{2}} k_{air}^{\frac{2}{3}} \mu^{\frac{1}{6}} C p^{-\frac{1}{3}} U_{\infty}^{-\frac{1}{2}}$$

Para cuantificar la propagación del error para cada variable independiente de la Ecuación 1. Se utilizó el método de la serie de Taylor como se especifica en ASME PTC19.1 [4] Este método se basa en la Ecuación 2:

$$\text{Ecuación 2. } \epsilon_{tot}(x_1, x_2, \dots, x_n) = \left\{ \sum_{i=1}^n \left( \frac{\partial h}{\partial x_i} * \delta x_i \right)^2 \right\}^{\frac{1}{2}} = \left\{ \sum_{i=1}^n \epsilon_i^2 \right\}^{\frac{1}{2}}$$

$$x_i = (T_1, T_2, T_3, t, \epsilon, x, U_{\infty}, \rho, \mu, k_w, k_{air})$$

Los errores absolutos para cada variable introducidos en la ecuación 2 se calcularon utilizando una simulación de Monte Carlo y de estudios [2] análisis y estimaciones previas. Los errores absolutos se calcularon utilizando este método y fueron representados según la posición x en la superficie de la placa plana:

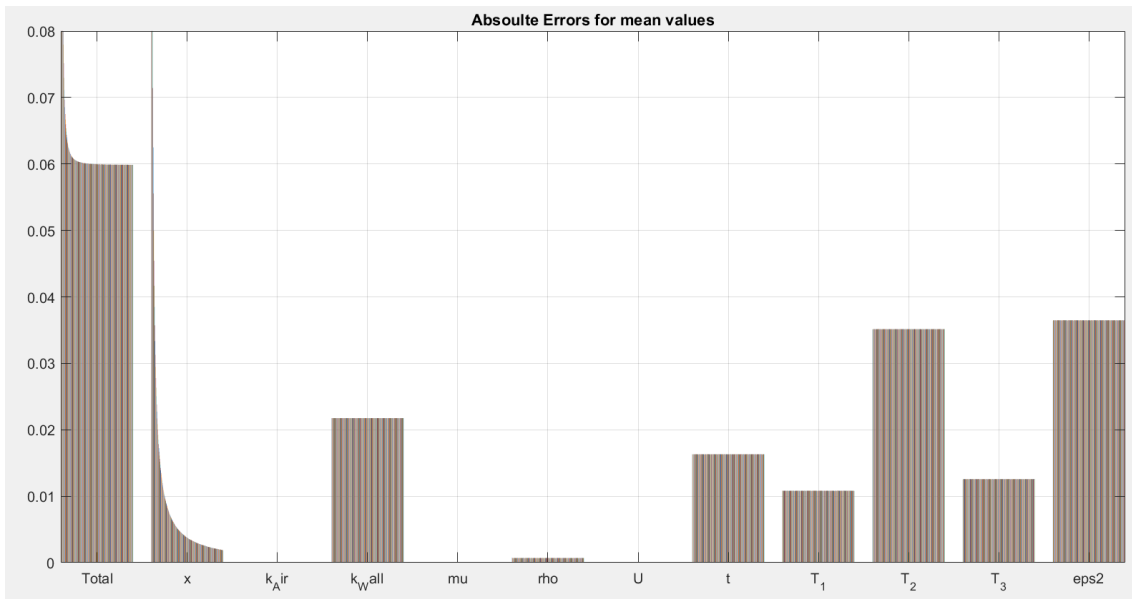


Figura 8. Errores absolutos para valores medios de las variables a través de la placa plana.

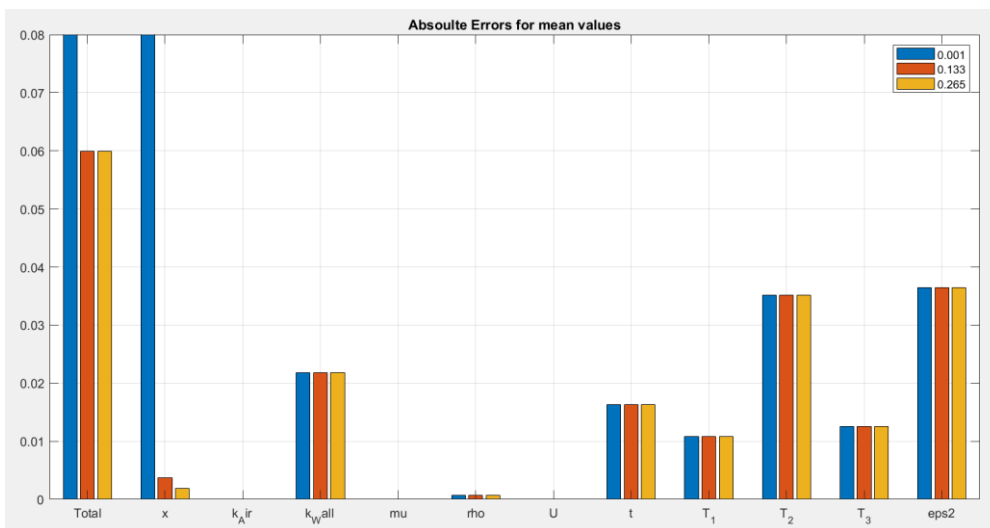


Figure 9. Errores absolutos para valores medios de las variables en  $x=0.001m$ ,  $x=0.133m$  y  $x=0.265m$ .

### 2.3 Testeo

Finalmente, el experimento diseñado se probó con una corriente de aire a  $25 \text{ m/s}$  y una temperatura en torno a los  $25^\circ\text{C}$ . En estas condiciones, se midió la temperatura de la superficie de la placa con la cámara de infrarrojos y se calculó el coeficiente de transferencia de calor, también se calculó la capa límite hidrodinámica con las medidas de presión a lo largo de la superficie con un tubo de Pitot conectado a una estructura

motorizada que se podía desplazar muy cerca de la superficie del experimento. Estos experimentos se repitieron para diferentes velocidades del agua y del viento para verificar diferentes suposiciones teóricas.

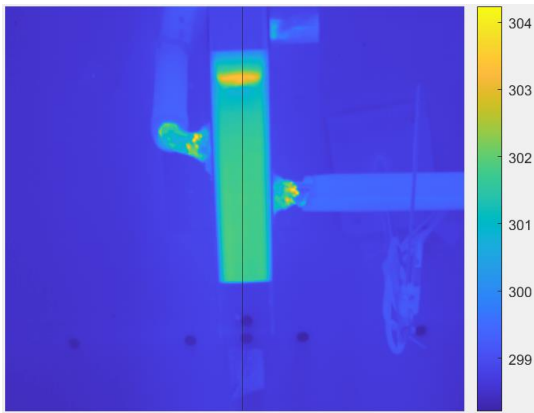


Figura 10. Temperaturas medidas por la cámara de infrarrojos en °K.

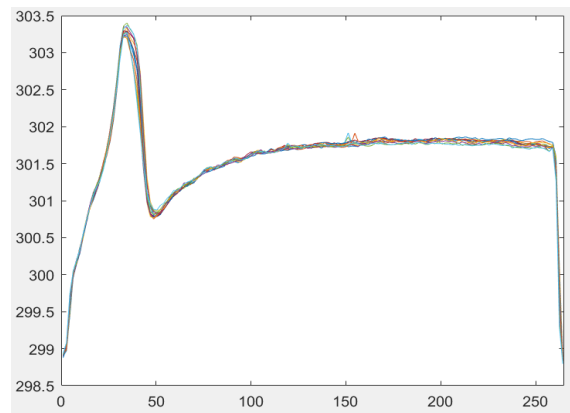


Figura 11. Representación de las temperaturas alrededor del centro de la placa a lo largo de su superficie

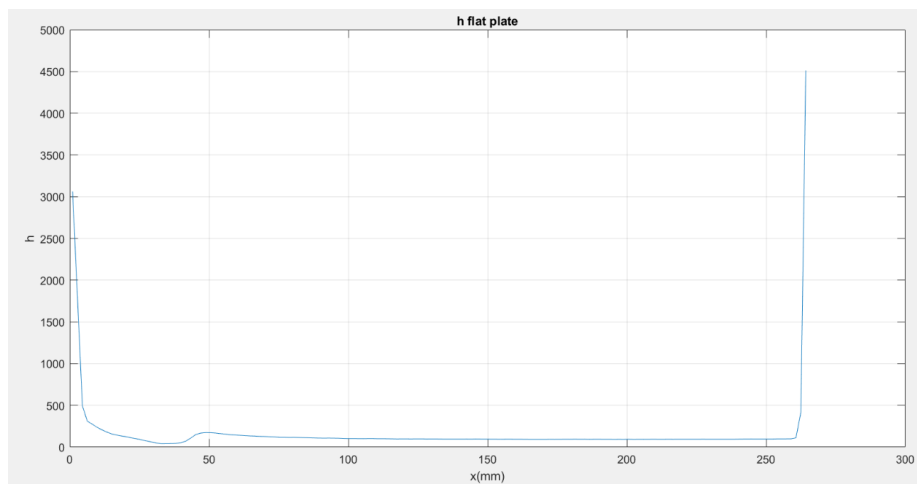


Figura 12. Coeficiente de transferencia de calor calculado con las mediciones de la cámara de infrarrojos.

También se midió la presión total y estática en distintos puntos de la placa y con los resultados obtenidos se calcularon los perfiles de velocidades en cada punto de medida

como  $u = \sqrt{2 \frac{q}{\rho}}$  donde q es la presión dinámica obtenida al restar la presión estática de la presión total.

La capa límite hidrodinámica se calculó como la altura donde la velocidad del fluido es el 99% de la velocidad del fluido de la corriente libre.

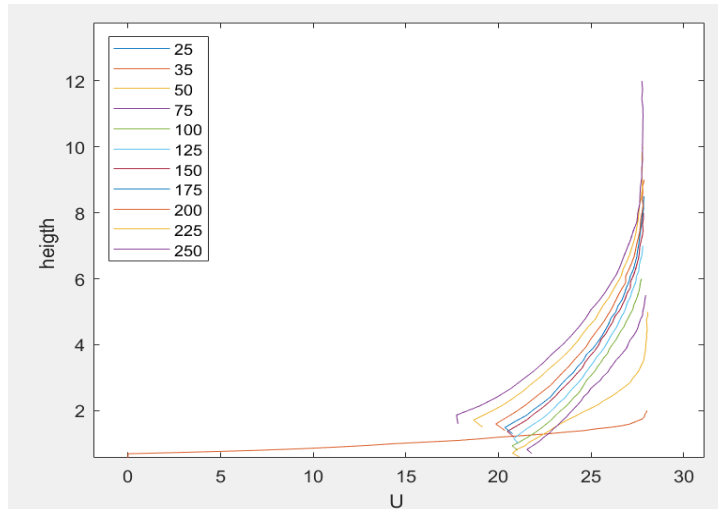


Figura 13. Perfil de velocidades(m/s) dependiendo de la altura(mm) y de la posición en la placa (mm).

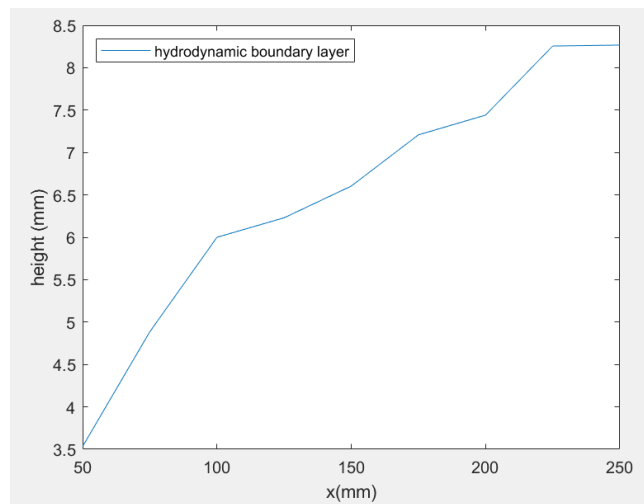


Figura 14. Capa limite hidrodinámica.

### 3. Resultados

En este capítulo se mostrarán los resultados obtenidos. En este proyecto, se desarrolló un experimento para probar un método innovador para medir el flujo de calor. Se construyó el experimento diseñado y se realizaron algunas pruebas para asegurar su funcionamiento y utilidad. El diseño y construcción final de la placa plana, los soportes y todo el circuito se puede encontrar en las figuras 15 y 16.



Figura 15. Montaje final del experimento visto desde el interior del túnel de viento.



Figura 16. Montaje final del experimento visto desde fuera del túnel de viento.

Se realizaron algunas pruebas en el experimento diseñado donde se midieron mediante la cámara de infrarrojos las temperaturas de la superficie de la placa plana y por otro lado el gradiente de presión utilizando un tubo de Pitot movido a través de la superficie de la placa plana. Para las pruebas de infrarrojos, se realizaron diferentes mediciones con diferentes velocidades del agua y del viento.

Se demostró experimentalmente que se puede suponer que la temperatura de la pared interior de la placa  $T_1$  es la misma que la temperatura del agua  $T_w$  si el coeficiente de transferencia de calor del agua es mucho más alto que el coeficiente de transferencia de calor del viento. Esto se consigue aumentando el flujo de agua tras incrementar la potencia de la bomba que la impulsa.

| Potencia de la Bomba | 20%    | 40%    | 60%     | 80%    | 100%   |
|----------------------|--------|--------|---------|--------|--------|
| $T_w$                | 307.11 | 307.13 | 307.046 | 307.12 | 307.22 |
| $T_2$                | 301.5  | 301.42 | 301.21  | 301.11 | 301.59 |

Tabla 1. Temperaturas del agua y de la superficie de la placa plana dependiendo de la potencia de bombeo.

En la tabla 1 se comparan las medidas para diferentes potencias de la bomba, la variación máxima en la temperatura superficial  $T_1$  es de 0.38 K, 1.3% y en el lado del agua,  $T_w$  varía 0.174 K, 0.056% de la  $T_w$  máxima.

Esto prueba el supuesto de que la temperatura de la pared interior de la placa plana se puede relacionar como  $T_1 = T_w$  y que la temperatura de la superficie,  $T_2$ , no se ven muy afectadas por la velocidad del flujo de agua. El resto de los experimentos se realizaron con la máxima potencia de la bomba.

Con el supuesto previamente verificado:  $T_1 = T_w$  y sabiendo que  $Q_{cond} = Q_{convAire} + Q_{Rad}$ ,  $h_2$  se calculó con las medidas de la cámara IR como:

$$h_2 = \frac{1}{T_2 - T_3} \left( \frac{k}{t} (T_1 - T_2) - \sigma (\epsilon T_2^4 - T_3^4) \right)$$

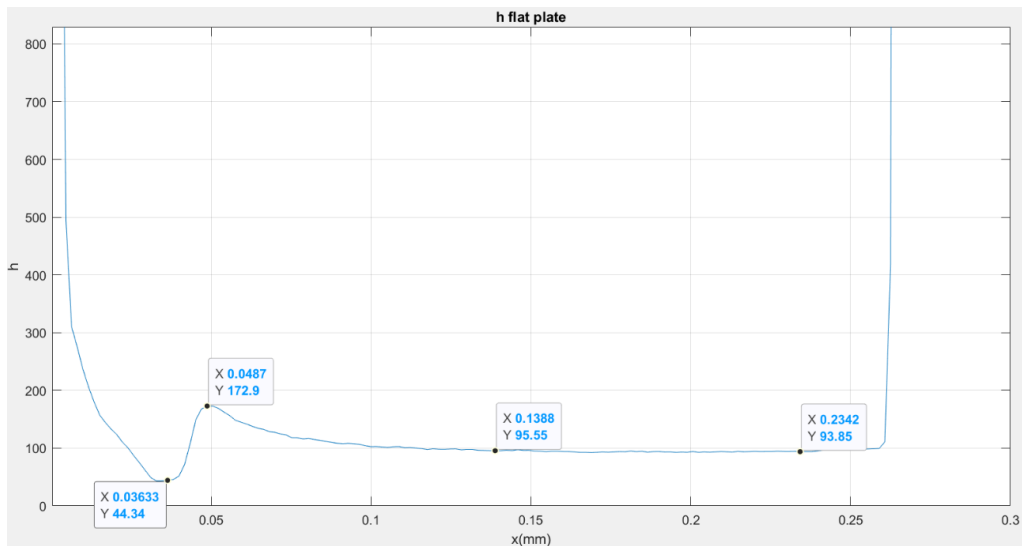


Figura 17.  $h_2$  calculado con las medidas de la cámara de infrarrojos.

Midiendo los gradientes de presión, se calculó el perfil de velocidad y la capa límite hidrodinámica.

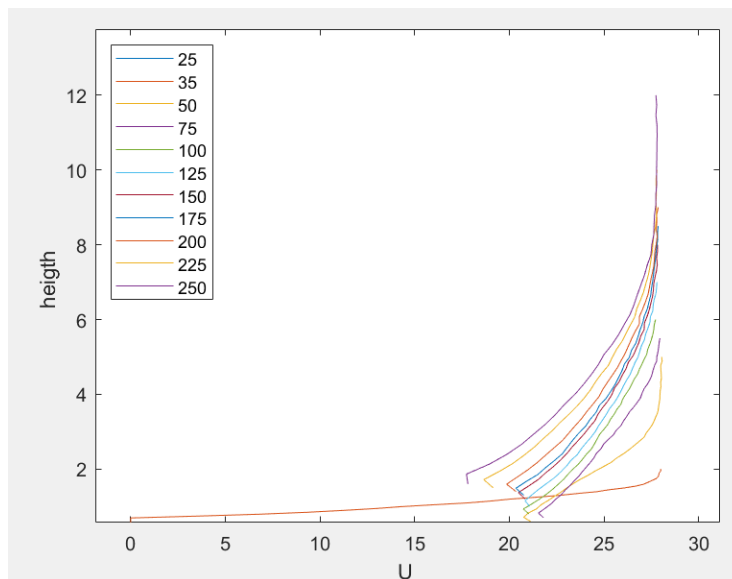


Figura 18. Perfil de velocidades(m/s) dependiendo de la altura(mm) y de la posición en la placa (mm)..

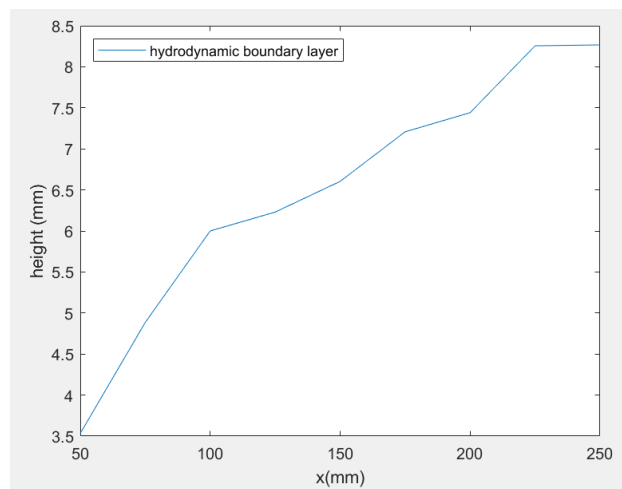


Figura 19. Capa limite hidrodinámica.

Resultados de los cálculos de incertidumbres para futuras investigaciones:

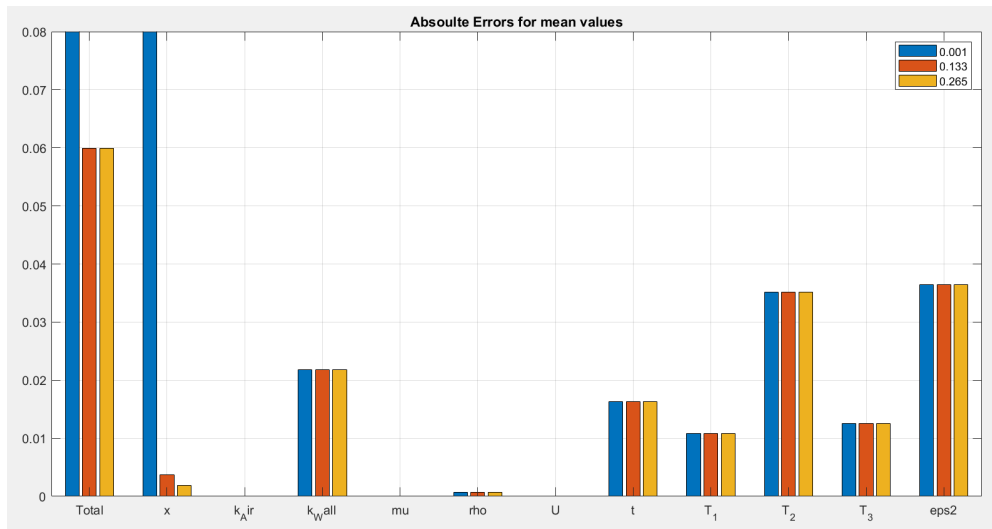


Figura 20. Errores absolutos para valores medios de las variables en  $x=0.001m$ ,  $x=0.133m$  y  $x=0.265m$ .

Se puede observar la temperatura superficial proporciona uno de los mayores errores junto con su emisividad. Además, la conductividad del material, proporcionada por el fabricante, añade un error considerable a la hora de calcular el coeficiente de transferencia de calor.

#### 4. Conclusiones

El experimento se diseñó con éxito, fue montado y colocado dentro del túnel de viento donde se pudieron realizar algunas mediciones. Durante estos experimentos, se encontraron algunos problemas que deberían resolverse para futuras investigaciones y para poder comprar de forma precisa esta forma de medición con infrarrojos.

Primero, como puede verse en los resultados de las mediciones de presión a través de la superficie de la placa plana, El flujo del viento se aceleró hasta casi 28 m / s cuando debería de ser de 25 m/s. Los soportes de aluminio son los que podrían estar interfiriendo en el flujo natural de la corriente de viento, acelerando esta corriente. Por lo tanto, las paredes de soporte deberían de ser recortadas para que no superen la superficie de la placa plana sin necesidad de comprar unos nuevos. Cortando toda la parte superior 4 mm por encima de la ranura diseñada como se puede ver en la figura 21.

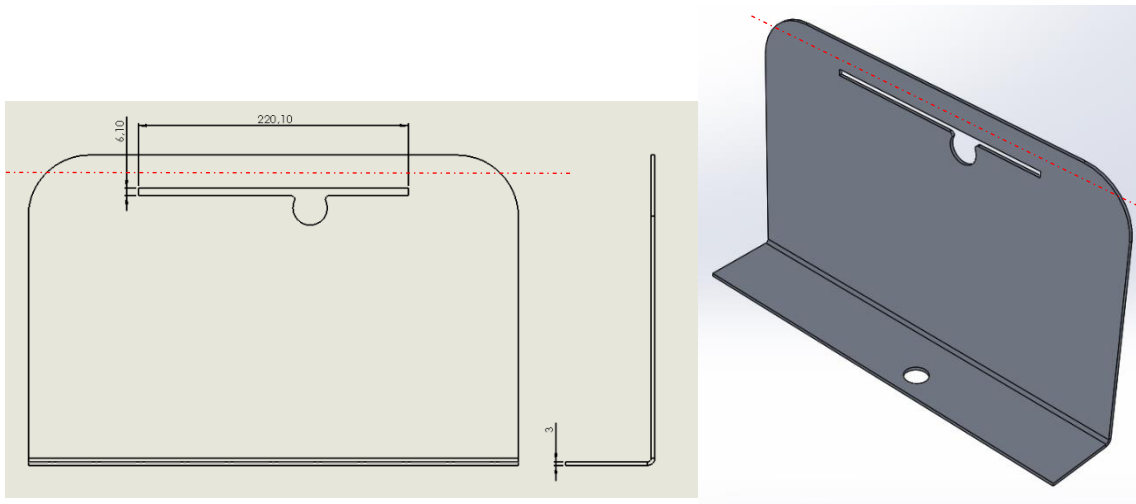


Figura 21. Representación del corte que debe aplicarse a los soportes en rojo, 4 mm sobre la ranura ya existente.

Además, como se puede ver en la figura 22, todas las mediciones que se realizaron muestran resultados no esperados en el borde donde incide la corriente de aire. Este fenómeno podría estar sucediendo debido a los soportes de aluminio que ya se ha explicado cómo deberían ser modificadas y debido al choque del fluido en el borde de ataque a pesar del redondeo que ya se le aplico en el diseño original para evitar este fenómeno. Para futuras investigaciones, la placa plana debería rediseñarse tratando de tener un borde de ataque más afilado para que la corriente del viento siga la superficie de la placa sin separarse con un flujo laminar.

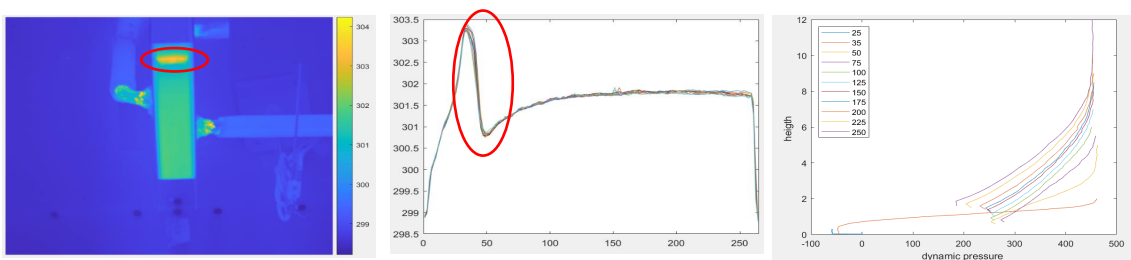


Figura 22. separación de la corriente de viento en el inicio de la placa.

## 5. Referencias

- [1] Benjamin Kirollos; Thomas Povey, «High-accuracy infra-red thermography method using reflective marker arrays,» IOP publishing, Oxford, 2017.
- [2] Isak Jonsson; Valery Chernoray; Radheesh Dhanasegaran, "INFRARED THERMOGRAPHY INVESTIGATION OF HEAT TRANSFER ON OUTLET GUIDE VANES IN AN ENGINE EXIT MODULE," MDPI, Gothemburg, 2020.
- [3] «World unique single turbine stage low-temperature steady-state test facility for TRS and LPT studies,» [En línea]. Available: <https://www.chalmers.se/en/departments/m2/simulator-labs/labs/chalmerswindtunnels/facility/Pages/OGV-LPT.aspx>.
- [4] A. ASME International, «Test Uncertainty PTC 19.1. Technical report,» ASME International ASME, 2005.

# NUMERICAL AND EXPERIMENTAL STUDY OF NOVEL HEAT FLUX MEASUREMENT IN TURBOMACHINERY

**Author: García Cucala, Yago.**

Supervisor: Jonsson Isak.

Collaborating Entity: Chalmers University of Technology.

## SUMMARY OF THE PROJECT

**Keywords:** heat flux, heat transfer, heat transfer coefficient, experiment, design.

### 1. Introduction

The aim of this final bachelor's project is to design an experiment that will be used to figure out how good heat flux can be measured in the laboratory by using an Infra-Red technique [1]. A recent and innovative study [2] have shown promising results in heat transfer on an OGV (Outlet guide vane) of a LPT (Low pressure turbine) [3]. In this study the estimated uncertainty is relatively low, sufficiency low, so that skepticism internally and along peers existed. Therefore, assumption and method needed to be verified using more fundamental cases where analytical solution exist or with high confidence in the numerical simulations.

This new method seems to be highly accurate and cost effective. This method feeds on infrared thermography technique which helps reducing one of the major sources of uncertainty. A fundamental case, heat flux measurement trough a flat plate will be used to benchmark this. To test this method with this fundamental case, an appropriate experiment needs to be designed where the method used in the OGV paper [2] can be compared with other experimental methods.

In this project an appropriate experiment has been designed, built and tested to benchmark the IR method.

## 2. Methodology

The project was divided in the design of the experiment, uncertainties calculations to check the future measurements that will be performed and testing of the facility with the IR camera and by measuring the pressure gradient.

### 2.1 Design

The experiment that is wanted to simulate where all the further experiments and measurements will be done is one of the most basic heat transfer cases, heat flux through a pre heated flat plate with laminar flow. The flat plate will be heated with a water current at a certain temperature, heat will go through convection from the water  $T_w$  to the inner wall of the flat plate  $T_1$ , then it will cross the flat plate by conduction reaching the upper part of the flat plate  $T_2$ . A wind current at a temperature  $T_3$  will be running through the flat plate surface cooling its surface by convection and radiation.

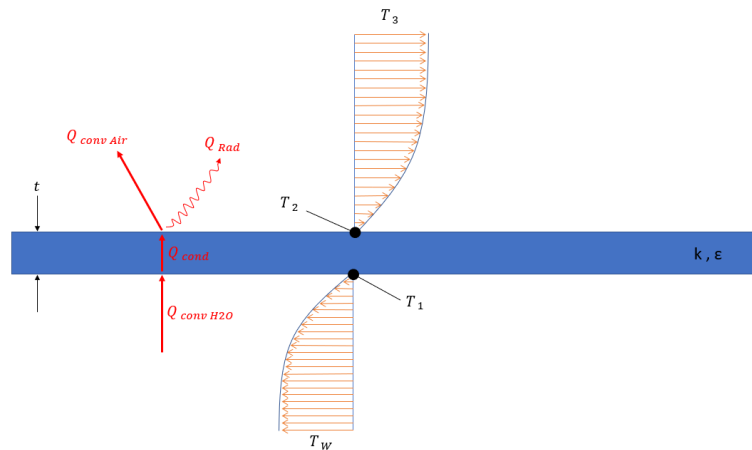


Figure 1. theoretical experiment approach

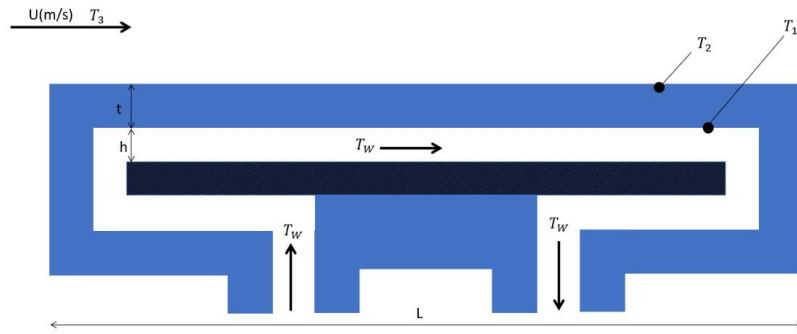


Figure 2. flat plate basic experiment design approach.

The main parameters that must be defined are the length and the thickness of the flat plate. It must be long enough to see the evolution of heat flux through its surface and for the thermal and hydrodynamic boundary layer to be fully developed but as longer as it gets, it will be more expensive. It was also tried to be kept as thin as possible to minimize heat losses through the walls having a surface temperature  $T_2$  as similar as possible to the inner wall temperature  $T_1$ . Also, as less material is used, the flat plates will be cheaper.

To calculate these parameters, a theoretical approach of the experiment was made for both laminar and turbulent flow on the case of study.

The flat plate final design can be seen in figure 3. It consists of a rectangular formed brick with rounded edges and two bosses at the sides to hold the plate. It has two holes on the sides that are connected through inside cooling channels of the plate structure.

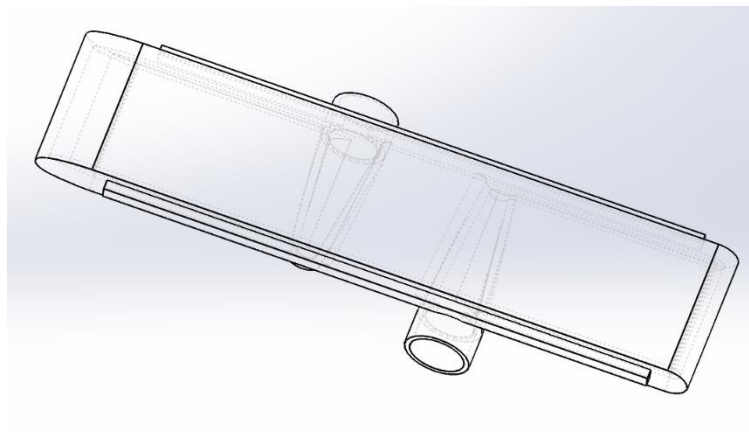


Figure 3. Final Flat plate design

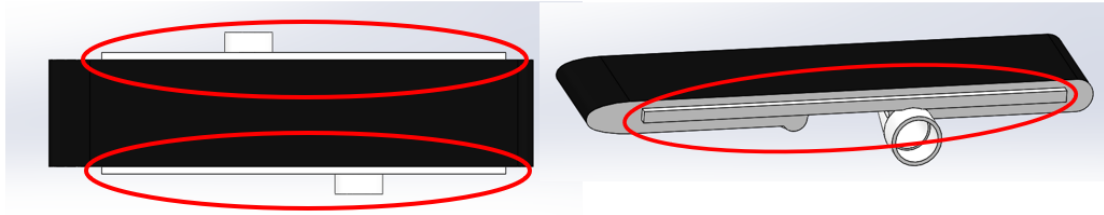


Figure 4. Flat plate Bosses in the red circles

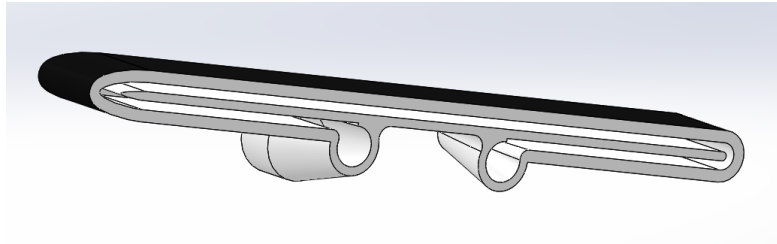


Figure 5. Flat plate internal channels design

To hold the flat plate on place two identical aluminum supports where used. These supports are two metallic plates L shaped with a hole in the shape of the side outline of the plate as can be seen in Figure 6. The flat plate bosses are introduced in the metallic supports that are later screwed to the wind tunnel ground.

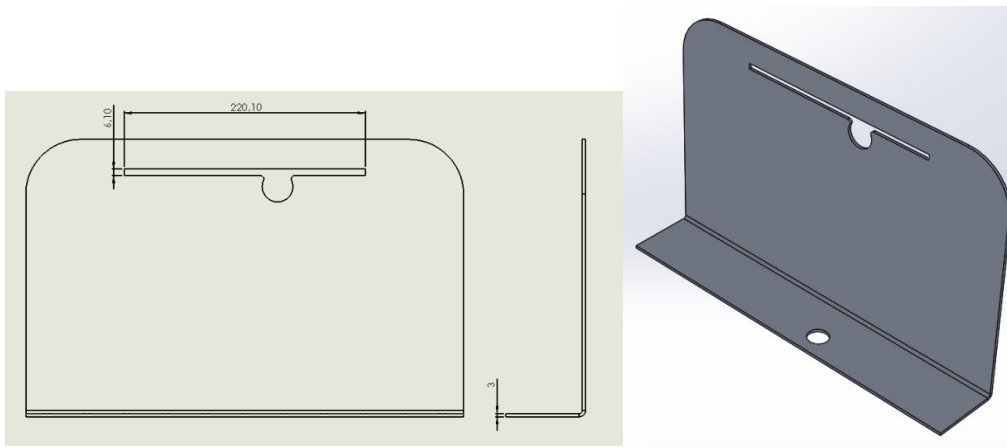


Figure 6. Supports design.

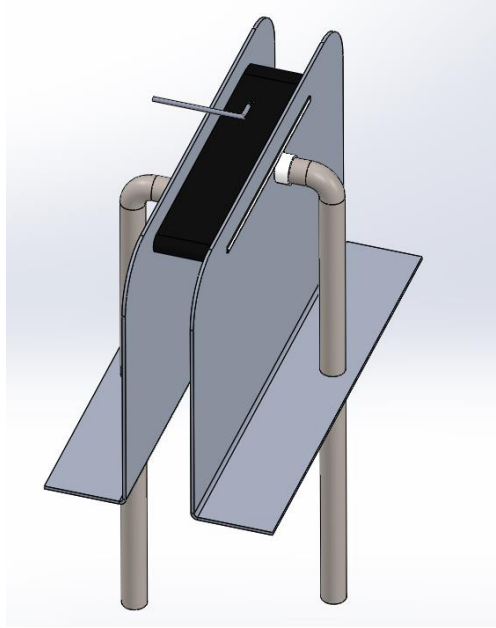


Figure 7. Final experiment design.

The parts designed for the experiment were bought and the experiment was built on a moving platform that was later fitted in the wind tunnel. The water circuit consisted in copper tubes covered by an isolating material that were connected to a water tank where the water was heated and pumped through the circuit. Also, different sensors were added to measure temperatures and pressures as well as the IR camera on the roof of the wind tunnel.

## 2.2 Uncertainties calculations

An uncertainty calculation was performed for further researchers to know how accurate their measurements should be and for them to know where the errors of their measurements come from. To do so, all the variables that can affect a heat transfer calculation were grouped in equation 1. It was obtained from combining heat transfer coefficient calculation from the heat fluxes and heat transfer coefficient calculation from the Nusselt number for laminar flow.

$$\text{Equation 1. } C = \left( \frac{1}{T_2 - T_3} \right) \left( \frac{k_w}{t} (T_1 - T_2) - \sigma (\epsilon T_2^4 - T_3^4) \right) \rho^{-\frac{1}{2}} x^{\frac{1}{2}} k_{air}^{-\frac{2}{3}} \mu^{\frac{1}{6}} C_p^{-\frac{1}{3}} U_\infty^{-\frac{1}{2}}$$

An analysis to quantify the error propagation was made for each independent variable from Equation 1. To do so, the Taylor series method was used as specified in ASME PTC19.1 [4] this method is based in Equation 2:

$$\text{Equation 2. } \epsilon_{tot}(x_1, x_2, \dots, x_n) = \left\{ \sum_{i=1}^n \left( \frac{\partial h}{\partial x_i} * \delta x_i \right)^2 \right\}^{\frac{1}{2}} = \left\{ \sum_{i=1}^n \epsilon_i^2 \right\}^{\frac{1}{2}}$$

$$x_i = (T_1, T_2, T_3, t, \epsilon, x, U_{\infty}, \rho, \mu, k_w, k_{air})$$

The absolute errors for each variable that are introduced in the equation 2 where either calculated using a Monte Carlo simulation or obtained from previous studies [2]. The absolute errors where calculated using this method and plotted depending on the x position through the flat plate:

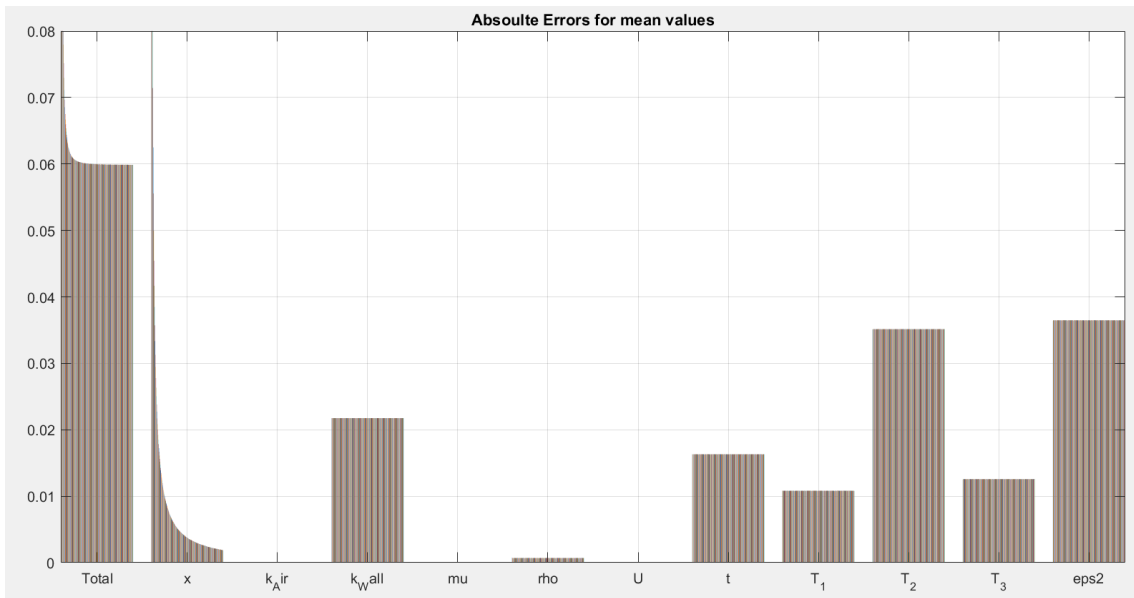


Figure 8. Absolute errors for mean values through the whole flat plate

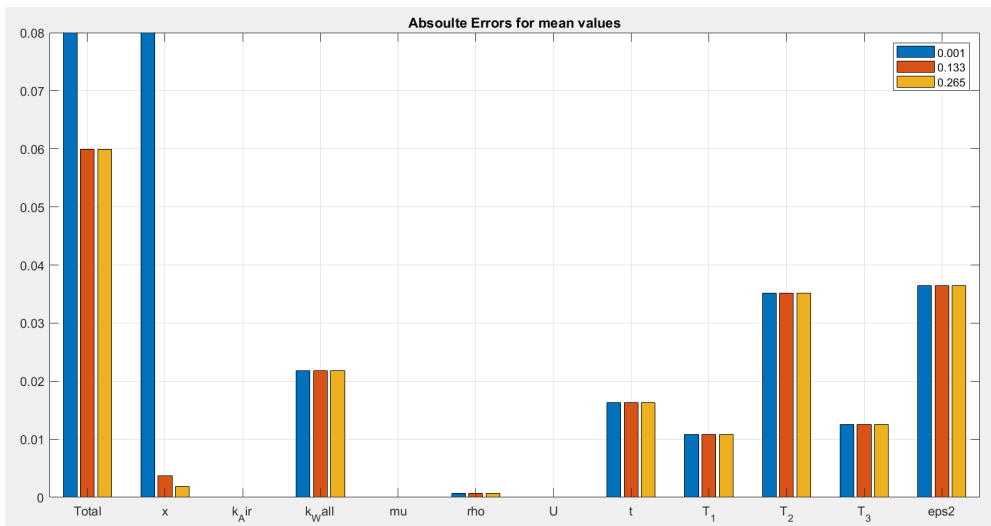


Figure 9. Absolute errors for mean values at x=0.001m, x=0.133m and x=0.265m.

### 2.3 Testing

Finally, the designed experiment was tested with an air current of 25 m/s and wind temperature around 25°C. Under this conditions, surface temperature was measured with the IR camera and heat transfer coefficient was calculated, also the hydrodynamic boundary layer was calculated with the pressure measurements over the flat plate surface with a pitot's tube connected to a motorized structure that was moved through the decided measurement points. These experiments were repeated for different water speeds and wind speeds to verify different theoretical assumptions

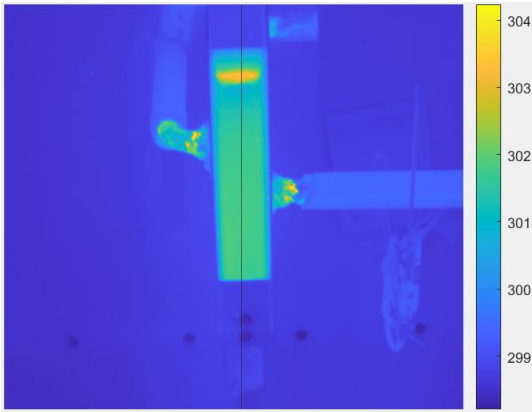


Figure 10. Temperatures measured (kelvins) with the IR-camera.

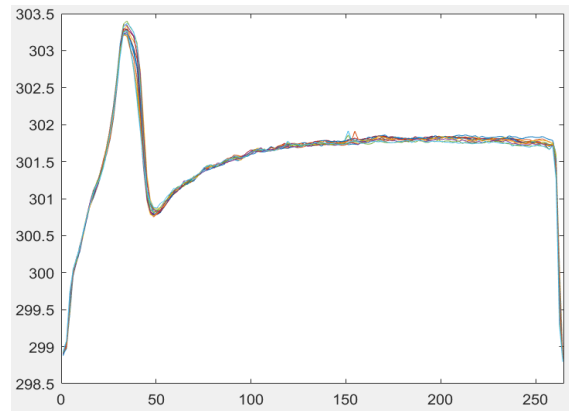


Figure 11. Flat plate surface temperature (kelvins) measured with the IR camera through the surface (mm).

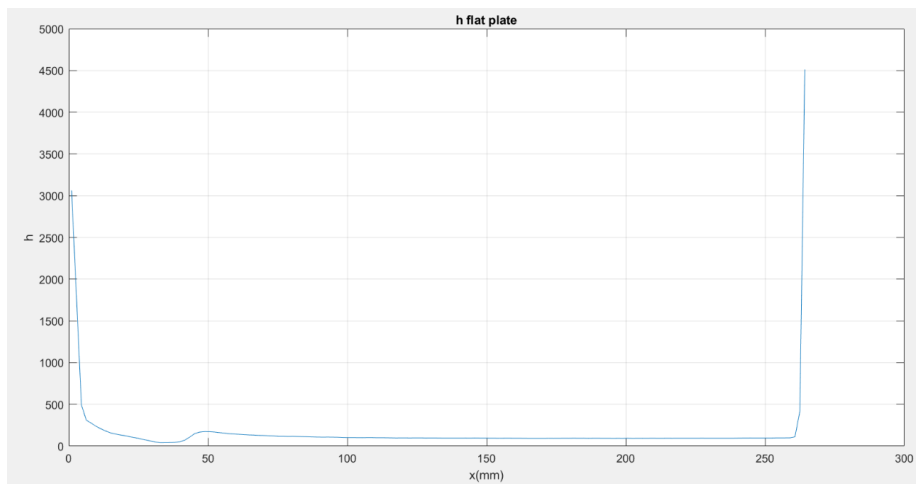


Figure 12. heat transfer coefficient obtained from IR measurements.

The pressure gradient was also measured and with the data obtained, the speed profiles were calculated for each measure point as  $u = \sqrt{2 \frac{q}{\rho}}$  where q is the dynamic pressure obtained from subtracting the static pressure from the total pressure. And the hydrodynamic boundary layer defined as the height where the fluid speed is 99% of the free current fluid speed.

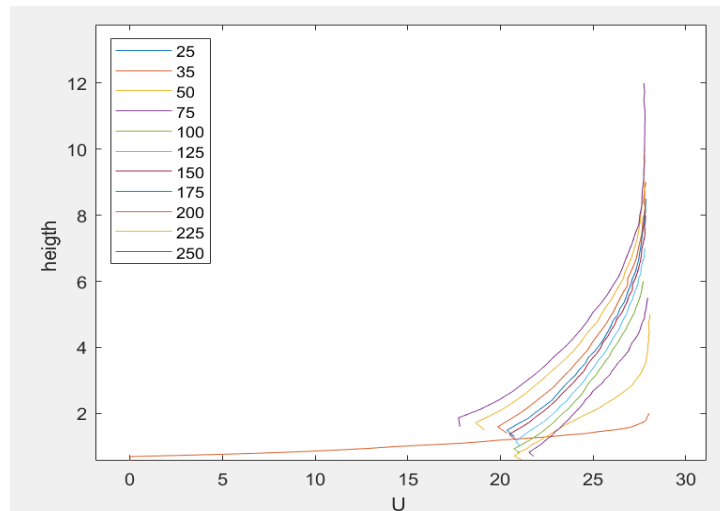


Figure 13. velocity profile(m/s) depending on height and x location in millimeters.

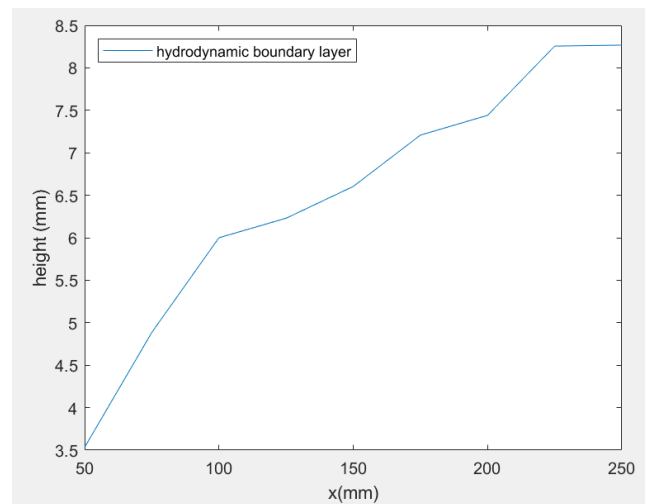


Figure 14. Hydrodynamic boundary layer at the flat plate

### 3. Results

In this chapter the results obtained will be shown. In this project, an experiment to test a special method to measure heat flux was developed. The experiment designed was built

and some tests were performed to ensure its utility and to verify a theoretical assumption. The final design and build of the flat plate, the supports and the whole circuit can be found in figures 15 and 16.



Figure 15. Final Experiment Build from inside the wind tunnel.



Figure 16. Final Experiment Build from outside the wind tunnel.

The designed experiment was done to benchmark an IR based heat transfer measurement method. Some tests were performed on the designed build where flat plate surface temperatures were measured with the IR method and pressure gradient was also measured using a pitot's tube moved through the flat plate surface vicinity. For the IR tests, different measurements were done with different water speeds and wind speeds.

It was experimentally proved that the inner wall temperature can be assumed to be the same as the water temperature if the water heat transfer coefficient is much higher than the wind heat transfer coefficient:

| Pump Power | 20%    | 40%    | 60%     | 80%    | 100%   |
|------------|--------|--------|---------|--------|--------|
| $T_w$      | 307.11 | 307.13 | 307.046 | 307.12 | 307.22 |
| $T_2$      | 301.5  | 301.42 | 301.21  | 301.11 | 301.59 |

Table 1. Water and surface temperatures for varying pump power.

In table 1, measurements for different pump powers are compared together, the maximum variation on the surface temperature  $T_1$  is of 0.38 K, 1.3% and in the water side,  $T_w$  varies 0.174 K, 0.056% of the maximum  $T_w$ .

This proves the assumption that the inside wall temperature of the flat plate  $T_1 = T_w$  and therefore the surface temperature,  $T_2$  is not affected much by water flow speed. The rest of the experiments where made with full pump power.

With the previously verified assumption:  $T_1 = T_w$  and knowing  $Q_{cond} = Q_{conv Air} + Q_{Rad}$ ,  $h_2$  was calculated with the measurements of the IR camera as:

$$h_2 = \frac{1}{T_2 - T_3} \left( \frac{k}{t} (T_1 - T_2) - \sigma (\epsilon T_2^4 - T_3^4) \right)$$

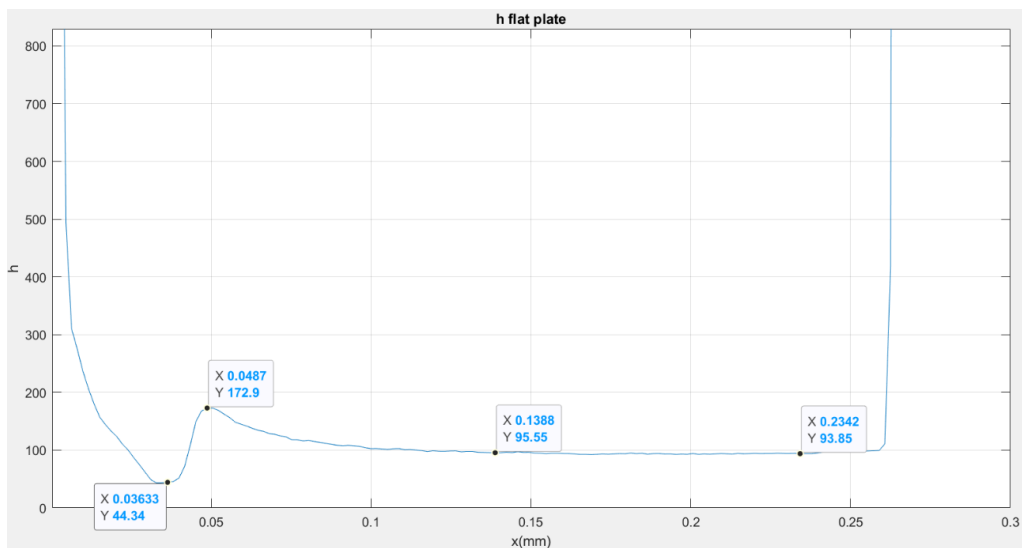


Figure 17.  $h_2$  calculated with IR measurements.

By measuring the pressure gradients, the velocity profile was calculated and the hydrodynamic boundary layer.

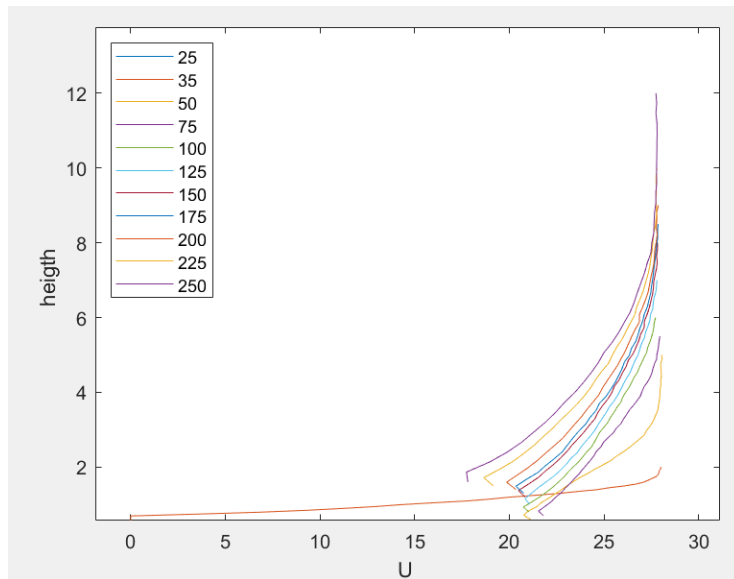


Figure 18. velocity profile(m/s) depending on height and x location in millimeters.

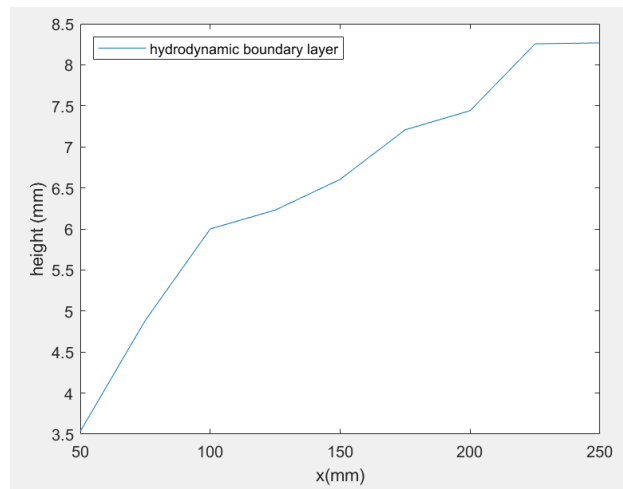


Figure 19. Hydrodynamic boundary layer at the flat plate.

Uncertainties results for further research:

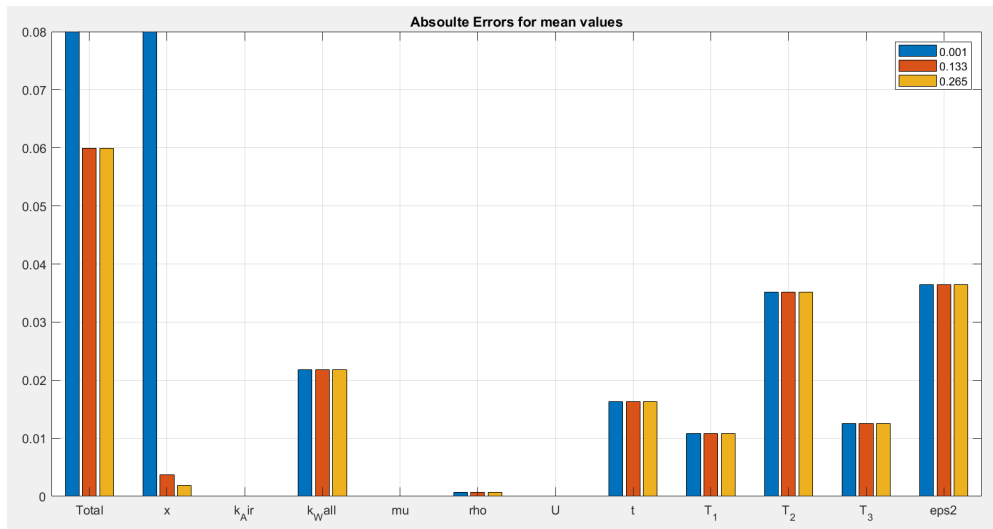


Figure 20. Absolute errors for mean values at  $x=0.001m$ ,  $x=0.133m$  and  $x=0.265m$ .

It was found that the surface temperature provides one of the biggest errors together with the surface emissivity. Also, the material conductivity provided by the fabricant provides a considerable error when calculating the heat transfer coefficient.

#### 4. Conclusions

The experiment was successfully designed and some experiments were tested in the facility built and placed inside the wind tunnel. During these experiments, some issues were found that should be solved for further research and benchmark IR method.

First, as can be seen on the results of the pressure measurements through the flat plate surface, the wind speed goes up to almost 28 m/s. the wind flow was accelerated. The support walls could be interfering on the natural flow of the wind current, accelerating this current and breaking the laminar flow. Therefore the support walls should be cut down so they do not surpass the flat plate surface. This can be done with the already built supports, cutting all the upper part from 4mm over the slot as can be seen in figure 21.

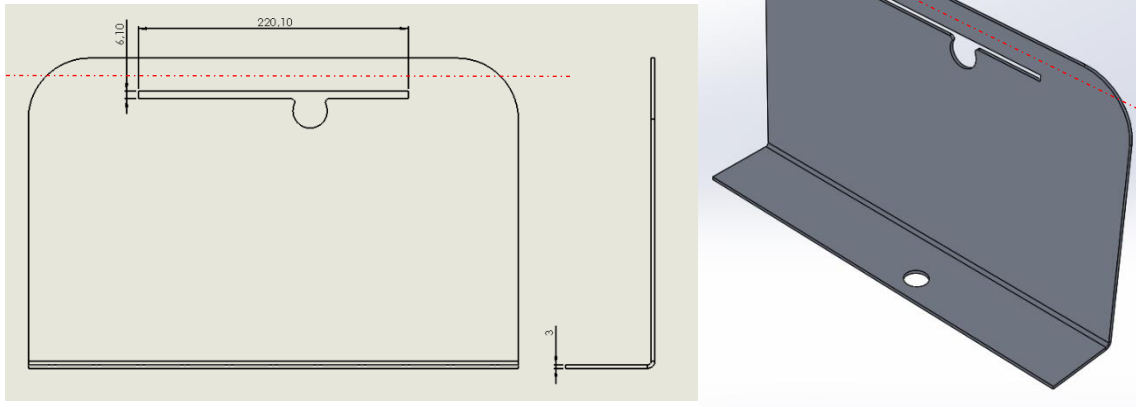


Figure 21. Supports top part removal represented with the red line 4mm over the original slot.

Also, as can be seen in figure 22, all the measurements that were done showed weird results in the incident edge of the wind flow. This phenomenon could be happening because of the support walls and because of the fluid crashing in the leading edge. For further research, the flat plate should be redesigned trying to have a sharper leading edge so the wind current follows the flat plate with a flow as similar as possible to a perfect laminar flow.

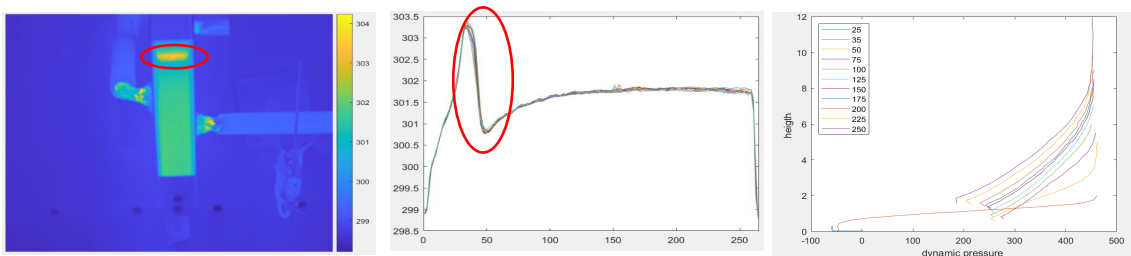


Figure 22. Separation / transition of the wind current in the leading edge.

## 5. References

- [1] Benjamin Kirollos; Thomas Povey, «High-accuracy infra-red thermography method using reflective marker arrays,» IOP publishing, Oxford, 2017.
- [2] Isak Jonsson; Valery Chernoray; Radheesh Dhanasegaran, "INFRARED THERMOGRAPHY INVESTIGATION OF HEAT TRANSFER ON OUTLET GUIDE VANES IN AN ENGINE EXIT MODULE," MDPI, Gothemburg, 2020.
- [3] «World unique single turbine stage low-temperature steady-state test facility for TRS and LPT studies,» [Online]. Available: <https://www.chalmers.se/en/departments/m2/simulator-labs/labs/chalmerswindtunnels/facility/Pages/OGV-LPT.aspx>.
- [4] A. ASME International, «Test Uncertainty PTC 19.1. Technical report,» ASME International ASME, 2005.

# Index

|  |     |
|--|-----|
| 1. Introduction .....  | 39  |
| 1.1 Sustainable development goals .....                          | 40  |
| 2. State of the art .....  | 41  |
| 3. Technologies Description .....                                | 42  |
| 3.1 Infra-Red Thermography Method .....                          | 42  |
| 3.2 Measurement of the Boundary Layer Method .....               | 44  |
| 4. Theoretical approach .....                                    | 49  |
| 5. Experiment design .....                                       | 53  |
| 5.1 Design .....   | 54  |
| 5.1.1 Flat Plate design .....                                    | 55  |
| 5.1.1.1 Laminar flow over an isothermal flat plate: .....        | 59  |
| 5.1.1.2 Turbulent flow over an isothermal flat plate: .....      | 60  |
| 5.1.2 Supports Design .....                                      | 61  |
| 6. Experiment Build .....  | 62  |
| 7. Experiments .....   | 74  |
| 7.1 Internal flat plate wall temperature assumptions prove ..... | 74  |
| 7.2 IR-camera Experiment .....                                   | 82  |
| 7.3 Measurement of the Boundary Layer Experiment .....           | 85  |
| 8. Results .....   | 91  |
| 9. Conclusions .....   | 96  |
| Annexes .....  | 100 |
| Bibliography .....   | 98  |

## Tables and figures index

Figure 3.1. Hydrodynamic boundary layer.

Figure 3.2. Thermal boundary layer.

Figure 3.3. Temperature profile of the experiment.

Figure 3.4. Representation of pressure measurement points marked in red.

Figure 4.2. Absolute errors for mean values through the whole flat plate.

Figure 4.3. Absolute errors for mean values at  $x=0.001\text{m}$ ,  $x=0.133\text{m}$  and  $x=0.265\text{m}$

Figure 5.1. basic study case sketch.

Figure 5.2. flat plate basic experiment design approach.

Figure 5.3. Final experiment design

Figure 5.4. Flat plate design

Figure 5.5. swirls appearing on the flat plate edge with a flat edge on the left and rounded edge on the right

Figure 5.6. Flat plate Bosses in the red circles

Figure 5.7. Flat plate internal channels design

Figure 5.8. Theoretical boundary layer calculation sketch

Figure 5.9. Theoretical thermal and hydrodynamic boundary layer thicknesses for laminar flow

Figure 5.10. Theoretical thermal and hydrodynamic boundary layer thicknesses for turbulent flow

Figure 5.11. Supports design

Figure 6.1. Flat plates

Figure 6.2. velvet-coating 811-21

Figure 6.3. Painted Flat Plates

Figure 6.4. Original copper tubes Left. sanded joined tubes with plastic couplings and flat plate Right

Figure 6.5. Flat plate and aluminum supports joined

Figure 6.6. Flat plate and aluminum supports screwed to the floor.

Figure 6.7. View of the experiment build from the bottom of the wind tunnel

Figure 6.8. experiment structure with both copper tubes connected

Figure 6.9. experiment structure with copper tubes isolated.

Figure 6.10. Pitot tube and temperature sensor for wind flow

Figure 6.11. temperature sensor under the wind tunnel for outgoing water temperature.

Figure 6.12. Pitot tube used to measure hydrodynamic boundary layer.

Figure 6.13. Final build of the experiment seen from the inside of the wind tunnel

Figure 6.14. Final build of the experiment seen from the outside of the wind tunnel with water heater mechanism rounded in red.

Figure 6.15. IR-camera placement.

Figure 6.16. Final build of the experiment from the outside of the wind tunnel.

Figure 6.17. Final build of the experiment from the inside of the wind tunnel.

Figure 7.1. Temperatures measurement [kelvins] with the IR-camera example.

Figure 7.2. 1D representation from the data in the black line in figure 7.1.

Figure 7.3. Fixed 1D representation from the data in the black line in figure 7.1

Figure 7.4. Fixed 1D representation from the data in the black line and surroundings in figure 7.1.

Figure 7.5. Flat plate surface temperature for 20% pump power with 25 m/s windspeed.

Figure 7.6. Flat plate surface temperature for 40% pump power with 25 m/s windspeed.

Figure 7.7. Flat plate surface temperature for 60% pump power with 25 m/s windspeed.

Figure 7.8. Flat plate surface temperature for 80% pump power with 25 m/s windspeed.

Figure 7.9. Flat plate surface temperature for 100% pump power with 25 m/s windspeed.

Table 7.1. Water and surface temperatures for varying pump power.

Figure 7.10. Experiment sketch.

Figure 7.11.  $h_2$  obtained from IR measurements

Figure 7.12. thermal picture from the IR-camera at the left and surface temperature representation through the flat plate around the midspan at the right with flow separation/transition rounded in red.

Figure 7.13. Pitot's tube scheme.

Figure 7.14. Pitot's tube used for the experiment.

Figure 7.15. Pitot's tube used for the experiment scheme.

Figure 7.16. Static pressure measurements depending on height normalized and x location in millimeters.

Figure 7.17. Dynamic pressure [Pascals] measurements depending on height and x location in millimeters.

Figure 7.18. velocity profile(m/s) depending on height and x location in millimeters.

Figure 7.19. velocity profile normalized.

Figure 7.20. Hydrodynamic boundary layer at the flat plate.

Figure 8.1. Final Experiment Build 1

Figure 8.2. Final Experiment Build 2

Figure 8.3. Final Experiment Build 3.

Figure 8.4. Final Experiment Build 4.

Table 8.1. Water and surface temperatures for varying pump power.

Figure 8.5.  $h_2$  calculated with IR measurements.

Figure 8.6. velocity profile(m/s) depending on height and x location in millimeters.

Figure 8.7. Hydrodynamic boundary layer at the flat plate.

Figure 9.1. Supports top part removal represented with the red line 4mm over the original slot.

Figure 9.2. Separation / transition of the wind current in the leading edge.



# 1. Introduction

The aim of this final bachelor's project is to design an experiment that will be used to figure out how good heat flux can be measured in the laboratory by using an Infra-Red technique [1]. A recent and innovative study [2] have shown promising results in heat transfer on an OGV (Outlet guide vane) of a LPT (Low pressure turbine) [3]. In this study the estimated uncertainty is relatively low, sufficiency low, so that skepticism internally and along peers existed. Therefore, assumption and method needed to be verified using more fundamental cases where analytical solution exist or with high confidence in the numerical simulations.

This new method seems to be highly accurate and cost effective. This method feeds on infrared thermography technique which helps reducing one of the major sources of uncertainty. To be verified, a holistic approach of all the variables that are considered on heat flux measurements will be done. A fundamental case, heat flux measurement trough a flat plate will be used to benchmark this. To test this fundamental case, an appropriate experiment is needed to be designed where the method used in the OGV paper [2] can be compared with other experimental methods

The implementation of this method will help in further development and future studies improving accuracy and reducing the uncertainty of the measurements done. It can be applied in modern aeroengines development that leads to more affective and better performing turbofans.

In this project an appropriate experiment has been designed, built and tested for the IR method. Some measurements where done using the IR technique. Also, the pressure gradient was measured to verify the proper design of the experiment.

## 1.1 Sustainable development goals

In this section, the project is related to one or more of the sustainable development objectives established on September 25, 2015 to eradicate poverty, protect the planet and guarantee prosperity for all countries. To achieve these objectives, there must be participation from all sectors of society.

Climate change affects every country in every continent producing a negative impact on their economy, on people's life and societies.

Weather patterns are changing, sea levels are rising, weather events are becoming more extreme, and greenhouse gas emissions are now at the highest levels in history.

Nowadays, we have viable solutions at our disposal so that countries can have a more sustainable and more environmentally friendly economic activity.

Programs such as Clean Sky [6] try to develop innovative technology to reduce CO<sub>2</sub>, gas emissions and noise levels produced by aircraft.

This project could help to improve aeroengine industry to develop more efficient and less polluting turbofans keeping them quiet and powerful.

## **9) Industries, Innovation and Infrastructure [7]**

It has long been recognized that investments in infrastructure (transport, irrigation, energy, information, and communication technology) are needed to achieve a robust economy. These are essential to achieve sustainable development, empower the societies of many countries, promote greater social stability, and make cities more resistant to climate change.

Technological progress must be one of the main concerns to achieve environmental goals, such as increased resources and energy efficiency. Without technology and innovation, industrialization will not occur, and without industrialization, there will be no development. More investment is needed in high-tech products that dominate manufacturing production to increase efficiency.

Managing to measure heat flux precisely, with little uncertainty can lead to more advanced and efficient technology. Such as for example in the aerospace industry, it will allow to manufacture more efficient, reliable and durable turbofans. This method also gives a much more cost-effective, highly accurate solution for heat flux measurement using infrared thermography technique (IRT) [1].

## 2. State of the art

At the current state of the art there exist plenty of different methods to measure heat flux but these measurements have a relatively high acceptance of uncertainty, especially when these experiments are done in challenging environments and not on ideal conditions. This situation repeats most of the times in any fluid dynamics study due to the complexity around the nature of the experiments.

Through the years plenty of methods have been invented trying to make measurements easier and more accurate.

There are plenty of studies in which different methods focus some of the measurement uncertainties trying to reduce them. But until none of them has done a holistic approach to all these uncertainties. On “INFRARED THERMOGRAPHY INVESTIGATION OF HEAT TRANSFER ON OUTLET GUIDE VANES IN AN ENGINE EXIT MODULE” [2] a systematic error mitigation method is presented to implement a cost-effective and accurate method for heat flux measurement using infrared thermography technique (IRT) [1]. This study relays on techniques previously established at Chalmers that took hand of the infrared thermography Technique such as the work done [5] [6] [7] [8]

## 3. Technologies Description

### 3.1 Infra-Red Thermography Method

In this section, the Infra-red technique (IRT) will be briefly explained. This method is deeply explained and demonstrated in “High-accuracy infra-red thermography method using reflective marker arrays” [1] This IR method reduces the errors that appear due to estimated parameters such as the surface emissivity.

To do so a Reflective marker technique (RMA) is used. It is common to divide the radiance measured by the IR-camera coming from three different components: the radiance emitted by the target surface, the radiance reflected coming from the background surroundings or also possibly from the own surface, and the radiance coming from the atmosphere between the lens and the target surface.

In order to calculate the surface temperature, the *Equation 2.1* is used where  $T_{bb}$  is the equivalent black body temperature. This is the temperature measured by the camera.  $T_R$  is the background temperature,  $T_{atm}$  is the temperature of the atmosphere between the lens and the target surface,  $\varepsilon$  is the surface emissivity and  $\tau$  is the transmittance of the air between the camera and the target surface. In this case, a single effective value will be assumed for  $T_R$  and  $T_{atm}$ .

$$\text{Equation 2.1 } \frac{q_{cam}}{\sigma} = T_{bb}^4 = \tau\varepsilon T_s^4 + \tau(1 - \varepsilon)T_R^4 + (1 - \tau)T_{atm}^4$$

In order to extract the real surface temperature  $T_s$  all the terms in *Equation 2.1* must be known. The most challenging value to estimate is  $T_R$  as it depends on the own experiment geometry, the surroundings temperature as well as its radiative and geometric properties. Since  $T_R$  depends on so many different factors that depend on the position on the target surface,  $T_R$  also depends on the position  $T_R(x)$

As it was mentioned before, the camera gives a temperature value equivalent to a black body  $T_{bb}$  and from the *Equation 2.1* we can extract the real temperature of the target object. Assuming  $T_R=T_{atm}$ , the *Equation 2.1* is simplified to:

$$\text{Equation 2.2 } \frac{q_{\text{cam}}}{\sigma} = T_{\text{bb}}^4 = \tau \varepsilon T_s^4 + [\tau(1 - \varepsilon) + (1 - \tau)] * T_R^4$$

This equation is the one that would be used to calculate the real temperature  $T_s$  but, to do so, the value of  $T_R$  must be known instead of that, this method suggests covering the target surface with two coatings of different emissivity. This would divide *Equation 2.1* in the following two equations:

$$T_{\text{bb1}}^4 = \tau \varepsilon_1 T_s^4 + [\tau(1 - \varepsilon_1) + (1 - \tau)] * T_R^4$$

$$T_{\text{bb2}}^4 = \tau \varepsilon_2 T_s^4 + [\tau(1 - \varepsilon_2) + (1 - \tau)] * T_R^4$$

Assuming  $\tau = 1$  as Atmospheric absorption is almost negligible and extracting  $T_R$  and  $T_s$ :

$$T_s^4 = \frac{1 - \varepsilon_2}{\varepsilon_1 - \varepsilon_2} T_{\text{bb1}}^4 - \frac{1 - \varepsilon_1}{\varepsilon_1 - \varepsilon_2} T_{\text{bb2}}^4$$

$$T_R^4 = \frac{\varepsilon_1}{\varepsilon_1 - \varepsilon_2} T_{\text{bb2}}^4 - \frac{\varepsilon_2}{\varepsilon_1 - \varepsilon_2} T_{\text{bb1}}^4$$

This way, the value of  $T_R$  does not need to be estimated, and it is obtained on the same measurement. Giving a fast and accurate method to measure the surface temperature of an object. These equations would be the ones used for an accurate measurement if the necessary materials are available.

In the case of study developed in this project, the target surface was painted with a high emissivity coating with  $\varepsilon = 0.991$  meaning that in *Equation 2.2* assuming  $\tau = 1$  the term  $(1 - \varepsilon) = 0.009 \approx 0$ . This leads to a furthermore simplified equation:

$$\text{Equation 2.3 } \frac{q_{\text{cam}}}{\sigma} = T_{\text{bb}}^4 = \varepsilon T_s^4$$

*Equation 2.3* is the one that will be used for this case of study to compare heat flux measurement with this method with other ones. For further research, the use of two emissivity coatings should be tested, and even better accuracy will be achieved.

### 3.2 Measurement of the Boundary Layer Method

The measurement of the hydrodynamic boundary layer will also be implemented on the designed experiment. When a flat plate is immersed in a fluid current that runs at a speed  $U_\infty$  parallel to the plate. The viscosity “ $\mu$ ” of the fluid gives rise to a shear stress in the vicinity of the plate that causes a reduction in flow velocity near the plate.

The hydrodynamic boundary layer is the region in which there is a velocity gradient. The thickness “ $\delta$ ” of the hydrodynamic boundary layer is such that the fluid experiences a speed variation ranging from 0 in the wall to 99% of the fluid speed,  $0.99 * U_\infty$ .

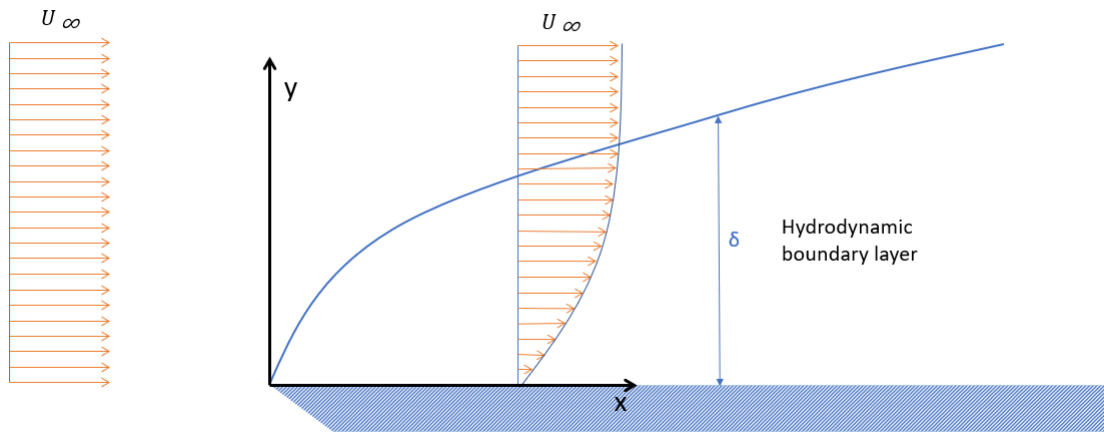


Figure 3.1. Hydrodynamic boundary layer.

If the temperature  $T_\infty$  of the incident current is different from the temperature  $T_s$  of the plate, a transition zone between the two temperatures will appear on the vicinity of the plate. The thermal boundary layer is defined as the region in which there is a temperature gradient. The thickness “ $\delta_T$ ” of the thermal boundary layer is such that the fluid experiences a temperature variation ranging from  $T_s$  in the wall to 99% of the fluid temperature,  $0.99 * T_\infty$ .

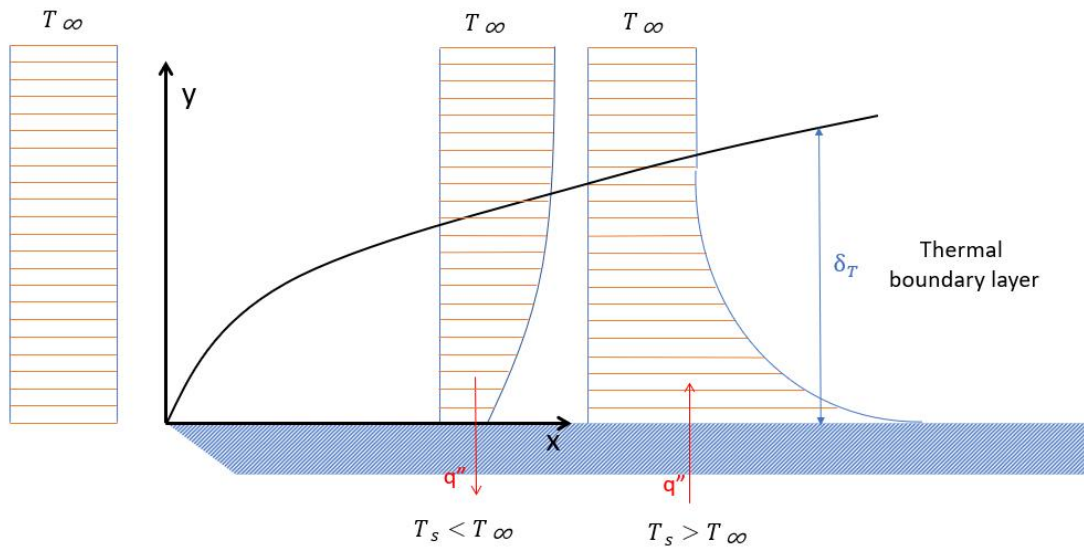


Figure 3.2. Thermal boundary layer.

Depending on the kind of flow, laminar or turbulent and the relation between the plate temperature  $T_s$  and the flow temperature  $T_\infty$ . The gradient of temperatures and the relation between hydrodynamic boundary layer and the thermal boundary layer might vary. In the case of the experiment that will be done, the plate temperature  $T_s$  is higher than the flow temperature  $T_\infty$  so the temperatures profile will look like in figure 3.3.

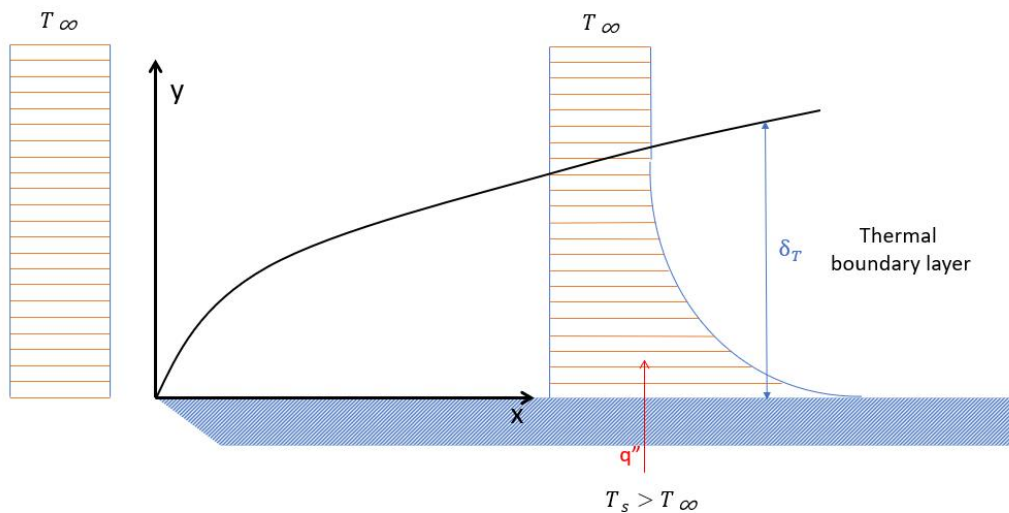


Figure 3.3. Temperature profile of the experiment.

To measure this phenomenon, a pitot's tube will be used. This sensor measures static pressure  $P_s$  and Total pressure  $P_T$  wherever it is placed. To have a representation of the hydrodynamic boundary layer, this sensor will be moved through the flat plate in longitudinal and transversal directions. Taking measurements through a couple of representative points as can be seen in figure 3.4.

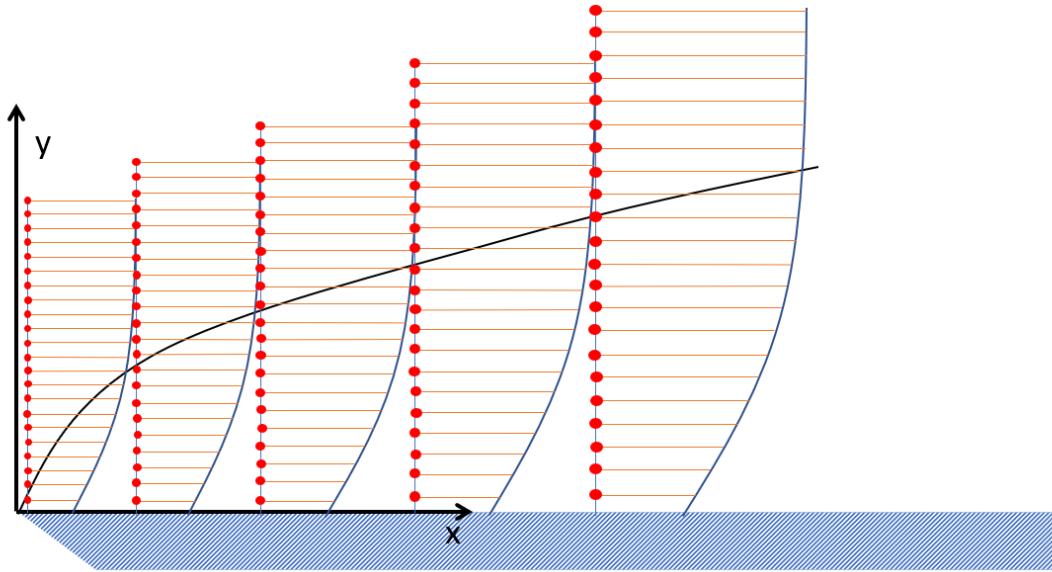


Figure 3.4. Representation of pressure measurement points marked in red.

Once measurements are done in all this points, there will be enough data to calculate the boundary layer. To do so, first the dynamic pressure " $q$ " must be calculated. Using equation 3.1:

$$\text{Equation 3.1 } q = P_T - P_s$$

Knowing the relation between the dynamic pressure " $q$ " and the flow velocity " $u$ " represented in equation 3.2:

$$\text{Equation 3.2 } q = \frac{1}{2} \rho u^2$$

U can be easily obtained as:

$$u = \sqrt{2 \frac{q}{\rho}}$$

Knowing the velocity profile, the hydrodynamic boundary layer can be obtained knowing  $\delta = u = 0.99 * U_{\infty}$ , and depending on the flow properties relations for the thermal boundary layer can be easily obtained.

## 4. Theoretical approach

For this study, heat flux through a heated flat plate was measured using separate methods in different conditions. To carry out these experiments, first a theoretical approach and an experiment design is required.

For this theoretical approach the problem was modeled in two dimensions for better understanding and easier calculations. The sketch on which this approach will be based can be seen in figure 4.1. water with temperature  $T_w$  is pumped through the internal channels of a flat plate. The channels have a height " $h$ " and the flat plate thickness is " $t$ ". The water will heat up the internal walls of the flat plate  $T_1$  and the heat will go through the plate to its surface  $T_2$ . Then, a wind current is blown through the surface of the flat plate at a speed " $U$ " and temperature  $T_3$ . Heat transfer will occur from the water to the wind current.

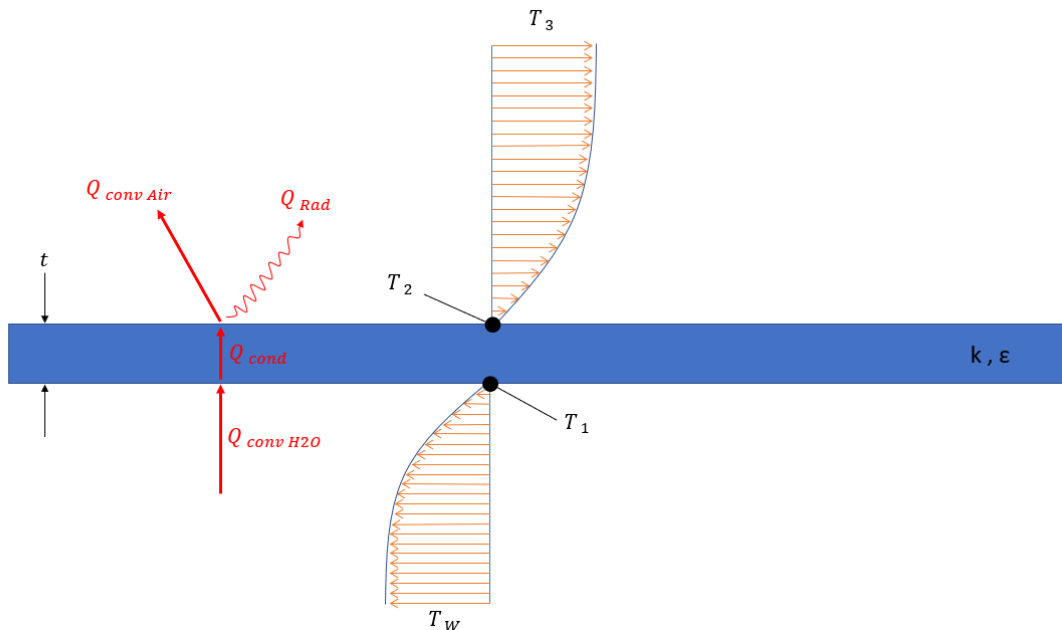


Figure 4.1. theoretical experiment approach.

The heat goes from the water current to the internal wall through convection  $Q_{conv H_2O}$ , then it crosses the flat plate by conduction  $Q_{cond}$  and ends in the air by convection  $Q_{conv Air}$  and radiation  $Q_{Rad}$ . Where:

$$Q''_{conv H_2O} = h_1(T_W - T_1)$$

$$Q''_{conv Air} = h_2(T_2 - T_3)$$

$$Q''_{cond} = \frac{k}{t}(T_1 - T_2)$$

$$Q''_{Rad} \approx \sigma(\varepsilon T_2^4 - \tau \varepsilon_b T_b^4)$$

Knowing  $Q''_{cond} = Q''_{conv Air} + Q''_{Rad}$ ,  $h_2$  can be solved as:

$$h_2 = \frac{Q''_{cond} - Q''_{Rad}}{T_2 - T_3} = \frac{1}{T_2 - T_3} \left( \frac{k}{t}(T_1 - T_2) - \sigma(\varepsilon T_2^4 - \tau \varepsilon_b T_b^4) \right)$$

In these equations  $h_1$  and  $h_2$  are the heat transfer coefficients on the water side and the air side respectively. The conductivity of the material is represented as " $k$ ". the Stefan-Boltzmann constant is " $\sigma$ ", " $\varepsilon$ " is the emissivity of the flat plate surface, " $\tau$ " is the air reflectivity, " $\varepsilon_b$ " is the background emissivity and " $T_b$ " the background temperature.

The radiation heat flux was simplified as the air reflectivity was approximated as  $\tau \approx 1$  and the background emissivity was also approximated as  $\varepsilon_b \approx 1$  and the  $T_b \approx T_3$  this was done knowing with the designed experiment most of the heat flux will occur through conduction between the flat plate and the wind current.

The final equation used can be find below:

$$\text{Equation 4.1 } h_2 = \frac{1}{T_2 - T_3} \left( \frac{k}{t}(T_1 - T_2) - \sigma(\varepsilon T_2^4 - T_3^4) \right)$$

$h_2$  is normally calculated from the definition of the Nusselt number. The Nusselt number represents the dimensionless temperature gradient of the fluid in contact with the wall and is calculated as:

$$\text{Equation 4.2 } Nu(x) = \frac{h(x)}{k_f} * x$$

Where  $k_f$  is the fluid conductivity, air in this case.

For Prandtl numbers  $Pr > 0.6$  and laminar flow, the Nusselt number can be calculated as:

$$\text{Equation 4.3 } Nu(x) = 0.332 R_e^{\frac{1}{2}}(x) Pr^{\frac{1}{3}}$$

To include all the variables in an error estimation, including air properties, the constant  $C=0.332$  was used as a target value combining equations 4.1, 4.2, and 4.3 the equation 4.4 is obtained:

$$\text{Equation 4.4 } C = \left( \frac{1}{T_2 - T_3} \right) \left( \frac{k_w}{t} (T_1 - T_2) - \sigma (\varepsilon T_2^4 - T_3^4) \right) \rho^{-\frac{1}{2}} x^{\frac{1}{2}} k_{air}^{-\frac{2}{3}} \mu^{\frac{1}{6}} C p^{-\frac{1}{3}} U_{\infty}^{-\frac{1}{2}}$$

An analysis to quantify the error propagation was made for each independent variable from Equation 4.4. To do so, the Taylor series method was used as specified in ASME PTC19.1 [4] this method is based in Equation 4.5:

$$\text{Equation 4.5 } \epsilon_{tot}(x_1, x_2, \dots, x_n) = \left\{ \sum_{i=1}^n \left( \frac{\partial h}{\partial x_i} * \delta x_i \right)^2 \right\}^{\frac{1}{2}} = \left\{ \sum_{i=1}^n \epsilon_i^2 \right\}^{\frac{1}{2}}$$

$$x_i = (T_1, T_2, T_3, t, \varepsilon, x, U_{\infty}, \rho, \mu, k_w, k_{air})$$

The value of  $k_w$  is known as it is provided by the manufacturer [12] of the flat plates with 2% of uncertainty.

One of the assumptions that was made already shown in previous work [2] was the fact that  $T_1=T_w$ . The theory deeply explained in that work is based in the idea that the heat transfer coefficient in the water side is infinitely large. This assumption will be proved experimentally later. The estimated uncertainty was calculated and shown to be between 2% and 5%

Surface temperature  $T_2$  total error estimation is of 7.5% [2]

The wind temperature  $T_3$  measurement error was also calculated and shown to be around 5%

The flat plate thickness “t” total error is of 1.5% after painting its surface with the matt paint.

Matt paint total error emissivity depending on temperature and vision angle  $\varepsilon=0.991$ , was estimated to be around 2%.

The location does not scale to the size of the length, it is in absolute 1mm = 0.001 m is the assumption as for now, 0.1%.

$U_{\infty}$  is roughly 0.2% for all span.  $U_{\infty, \text{error}} = 0.0002$

The air properties error estimations were calculated using a Monte Carlo simulation and later added to equation 4.5.

The absolute errors were calculated using the Taylor series method shown in equation 4.5 and plotted depending on the x position through the flat plate:

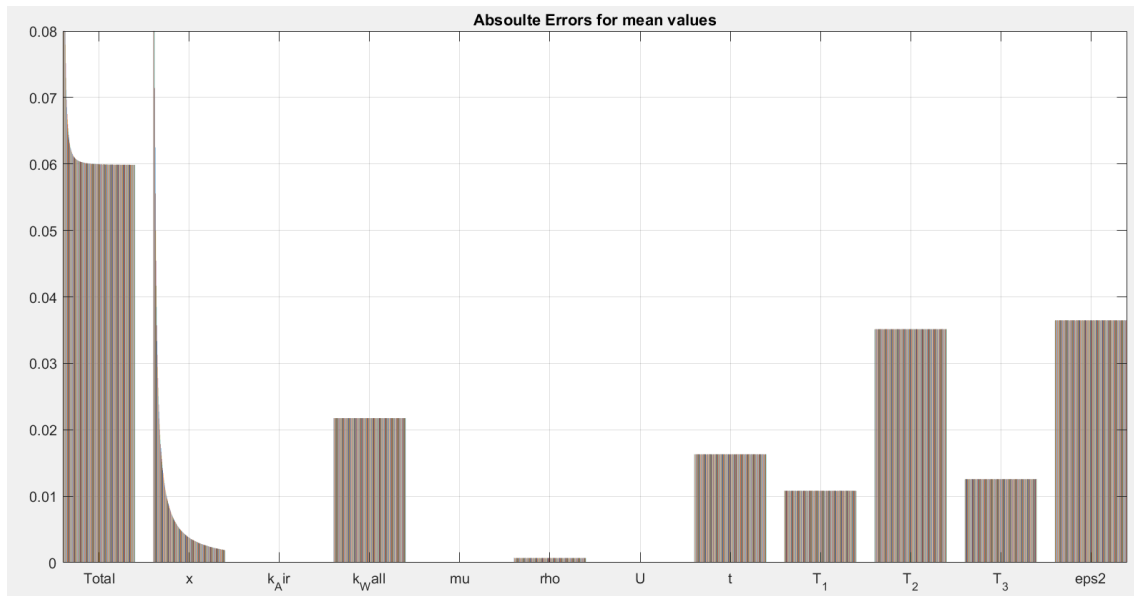


Figure 4.2. Absolute errors for mean values through the whole flat plate.

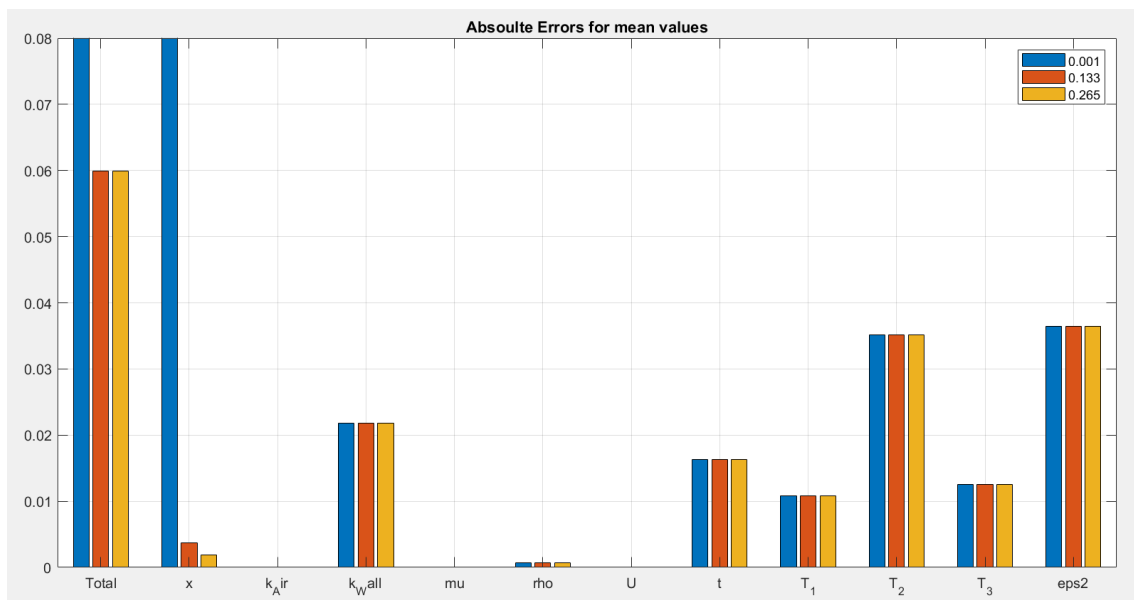


Figure 4.3. Absolute errors for mean values at  $x=0.001\text{m}$ ,  $x=0.133\text{m}$  and  $x=0.265\text{m}$ .

Viewing the errors calculated following the Taylor series method as specified in ASME PTC19.1 [10] it can be seen how at the leading edge the errors almost only depend on the positioning rapidly dropping through the plate surface being almost null at the end. In the rest of the cases most of the error's calculations depend on the surface temperature and its emissivity.

## 5. Experiment design

In order to benchmark the IR method, a simple case of heat flux needed to be designed. Therefore, heat flux through a flat plate was chosen as it can be solved theoretically relatively easy, and the experiment design does not give hard drawbacks.

On figure 5.1 the basic case that wants to be tested can be appreciated easily. A flat plate will be heated up from the bottom and wind will be pumped through the surface of the plate to cool it down. Heat flux will go from the bottom of the flat plate to the upper part where convection and radiation phenomena will be measured using the IR method and by measuring the hydrodynamic boundary layer.

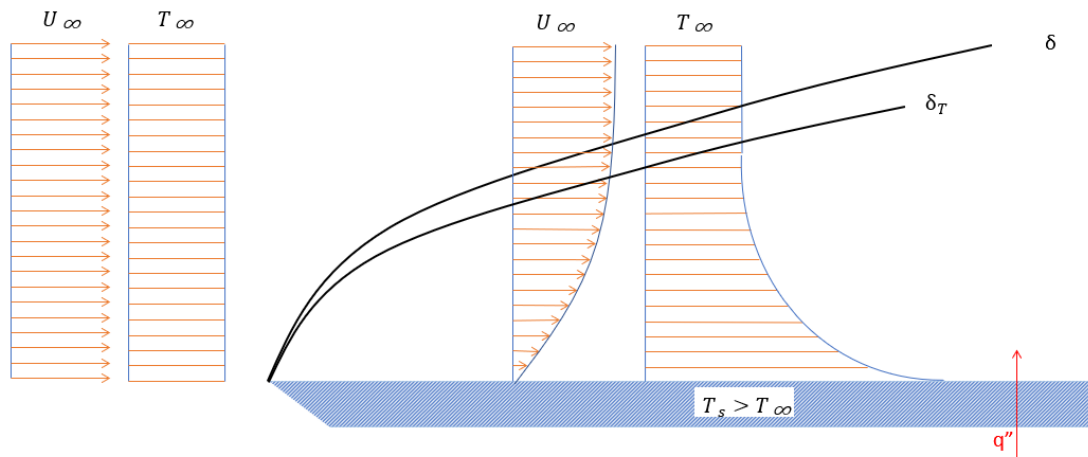


Figure 5.1. basic study case sketch

For the design of the experiment, the SolidWorks software was used. The design was tried to be kept as simple as possible. To do so a two-dimensional approach was made. On figure 5.2 a first sketch of the experiment can be seen. It consists of a flat plate with some internal channels where hot water will be pumped to heat the flat plate up. At the same

time wind at different speeds,  $U$ , and temperatures,  $T_3$ , will go through the plate surface where the heat transfer measurements will be done.

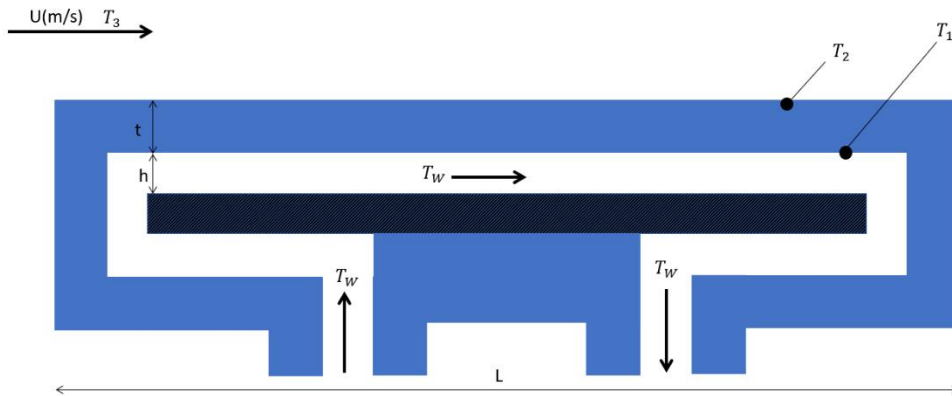


Figure 5.2. flat plate basic experiment design approach.

Water was chosen as the method to heat up the flat plate as it simplifies some calculations that will be explained later. It also leads to less uncertainties and a more regular heat transfer from the water to the flat plate than a thermal resistance.

To take this sketch to reality some limitations had to be considered. First, the whole structure had to be fixed somehow to the floor of the wind tunnel as windspeeds up to 30m/s were tested. Also, water channels from the flat plate to the heater were kept as short as possible to minimize heat losses.

### 5.1 Design

The final design of the experiment structure can be seen in figure 5.3. To hold the flat plate to the floor of the wind tunnel two metallic supports were designed. These supports are attached to the flat plate walls by two bosses that were added to the plate design as can be seen in figure 5.4. these bosses are introduced in the metallic supports that will hold the flat plate on place. The supports are bended on an L form so they can be screwed to the wind tunnel floor. From each side of the flat plate, one cylindrical pipe goes out and was later connected with a water heater and a pump through two plastic tubes.

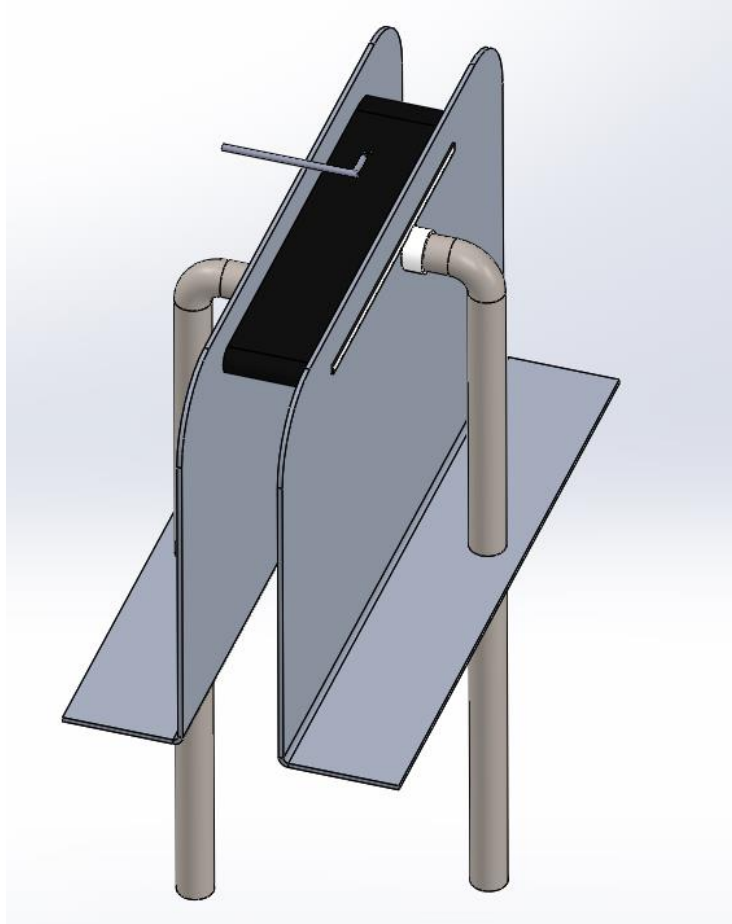


Figure 5.3. Final experiment design.

### 5.1.1 Flat Plate design

The flat plate final design can be seen in figure 5.4, It consists of a rectangular formed brick with rounded edges and two bosses at the sides to hold the plate. It has two holes on the sides that are connected through inside cooling channels of the plate structure that can be seen in figure 5.7.

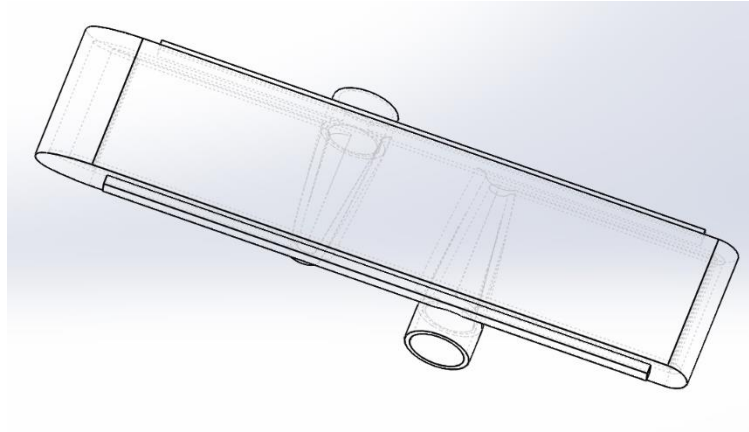


Figure 5.4. Flat plate design

The edges of the plate where rounded in order to have a better flow through the plate. They are intended to prevent turbulences from appearing because of the air flow crashing on the border of the plate as can be seen in figure 5.5. with the rounded edge, some turbulences will also appear but the flow through the flat plate will look more similar to a full laminar flow than in the flat edge case.

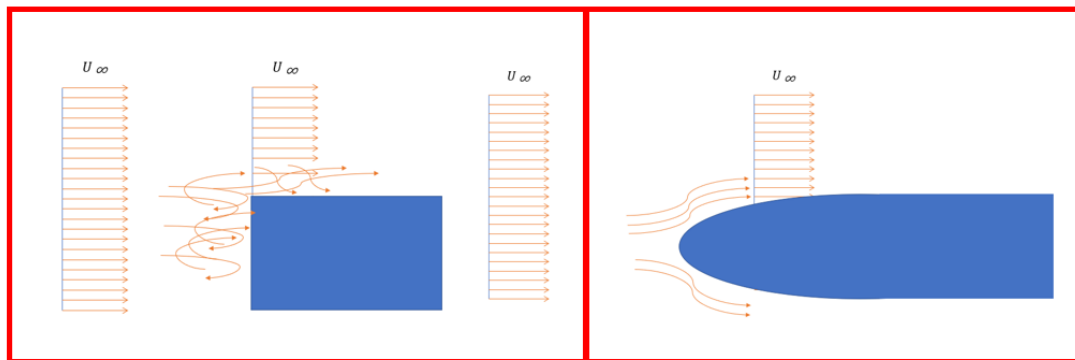


Figure 5.5. swirls appearing on the flat plate edge with a flat edge on the left and rounded edge on the right

On each side of the flat plate two rectangular bosses come out of the main structure of the plate as can be seen in figure 5.6. These bosses are there to join the plate with the supports that hold the structure to the ground.

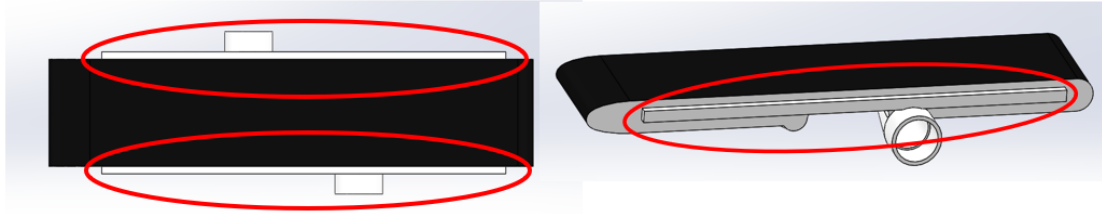


Figure 5.6. Flat plate Bosses in the red circles

The inside design of the plate can be seen in figure 5.7. It consists of small channels that go all around the plate. The water comes in continuously through one of the entrances and goes out through the other one heating up all the structure.

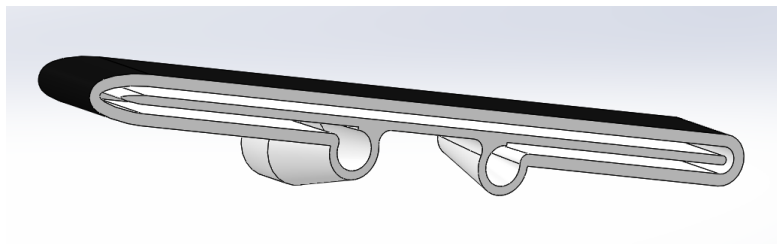


Figure 5.7. Flat plate internal channels design

The length of the flat plate was designed to be 265mm. For both, laminar and turbulent flow, the boundary layer thickness grows through the flat plate span. The hydrodynamic boundary layer thickness  $\delta$  is defined as the value of  $y$  for which  $\frac{u}{u_\infty} = 0.99$  being " $y$ " the distance measured perpendicularly from the flat plate as can be seen in figure 5.8 and the wind speed. The boundary layer thickness was calculated theoretically for turbulent and laminar flow in the case of heat going from a flat plate to the ambient as can be seen on figure 5.8. The experiment is intended to be done with laminar flow as calculations and

results interpretation are easier. But turbulences could appear so both cases will be studied theoretically to calculate the plate length.

For a good measurement of the boundary layer, it is better for it to be as thick as possible, this means that for a longer plate, better results will be obtained. But also, flat plate price increases exponentially as its length increases. This means that the flat plate should be long enough to have a good measurement of the hydrodynamic boundary layer but as short as possible to keep its price low.

For a good measurement with the available material, a hydrodynamic boundary layer thickness between 1 and 2 mm on the plate would be enough.

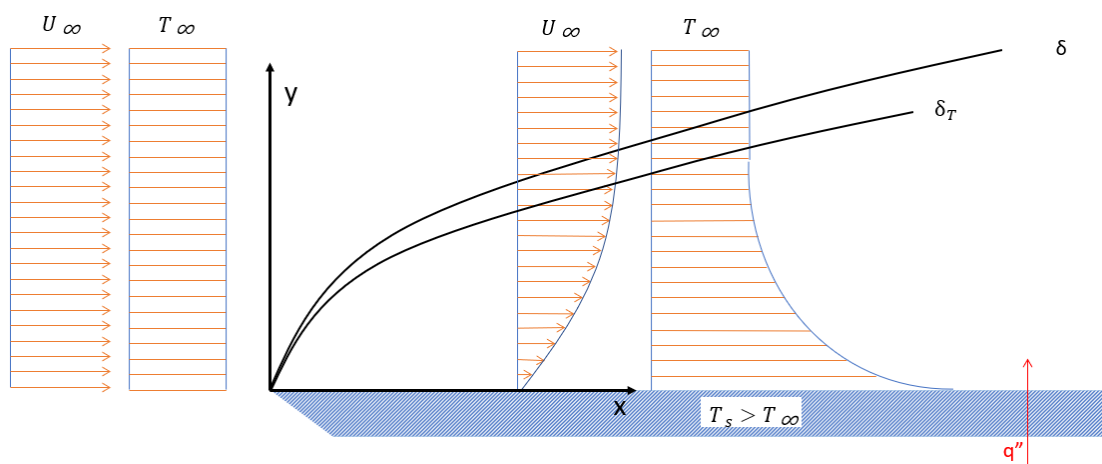


Figure 5.8. Theoretical boundary layer calculation sketch.

To do so, wind speed, and temperature  $T_\infty = 24^\circ\text{C}$  was chosen. The wind temperature on the wind tunnel is between  $23^\circ\text{C}$  and  $26^\circ\text{C}$  so  $T_\infty = 24^\circ\text{C}$  is a good reference and was chosen for the design.

For the boundary layer calculation, some air properties are needed. In order to calculate them a MATLAB script was used. In this script the air temperature  $T_\infty = 24^\circ\text{C}$  is introduced receiving in response the desired air properties.

For this case, the output properties needed where the kinematic viscosity of air ( $\nu_{air}$ ):

$$\nu_{air} = \frac{\mu_{air}}{\rho_{air}} = 1.5497 * 10^{-5} \frac{m^2}{s}$$

and the Prandtl number ( $Pr_{air}$ ) calculated as:

$$Pr_{air} = Cp_{air} * \frac{\mu_{air}}{k_{air}} = 0.7159 \text{ [pag 376 incropera]}$$

Then the Reynolds number was calculated depending on the position  $x$  measured in meters with  $x=0$  starting on the leading edge as can be seen on figure 5.8:

$$Re_x = \frac{\rho_{air} * U_{\infty}}{\mu_{air}} * x = \left( \frac{U_{\infty}}{\nu} \right) * x \text{ [6.23 incropera]}$$

Knowing these values, the thermal boundary layer was calculated for both laminar and turbulent flow.

#### 5.1.1.1 Laminar flow over an isothermal flat plate:

For laminar flow, the hydrodynamic boundary layer can be calculated as

$$\delta = \frac{5}{\sqrt{Re_x}} = \frac{5 * x}{\sqrt{\nu * x}} \quad [7.19 \text{ incropera}]$$

And a good approximation for this case to de thermal boundary  $\delta_T$  layer is:

$$\delta_T = \delta * Pr^{-\frac{1}{3}} \quad [\text{incropera 7.24}]$$

Results can be found in figure 5.9. being the blue graph  $\delta_T$  and the orange graph  $\delta$ . Both boundary layers grow through the plate span as expected giving an estimated hydrodynamic thickness (the one that will be measured) of 1mm at flat plate length of 0.05m and 2mm at  $x=0.25$  m .

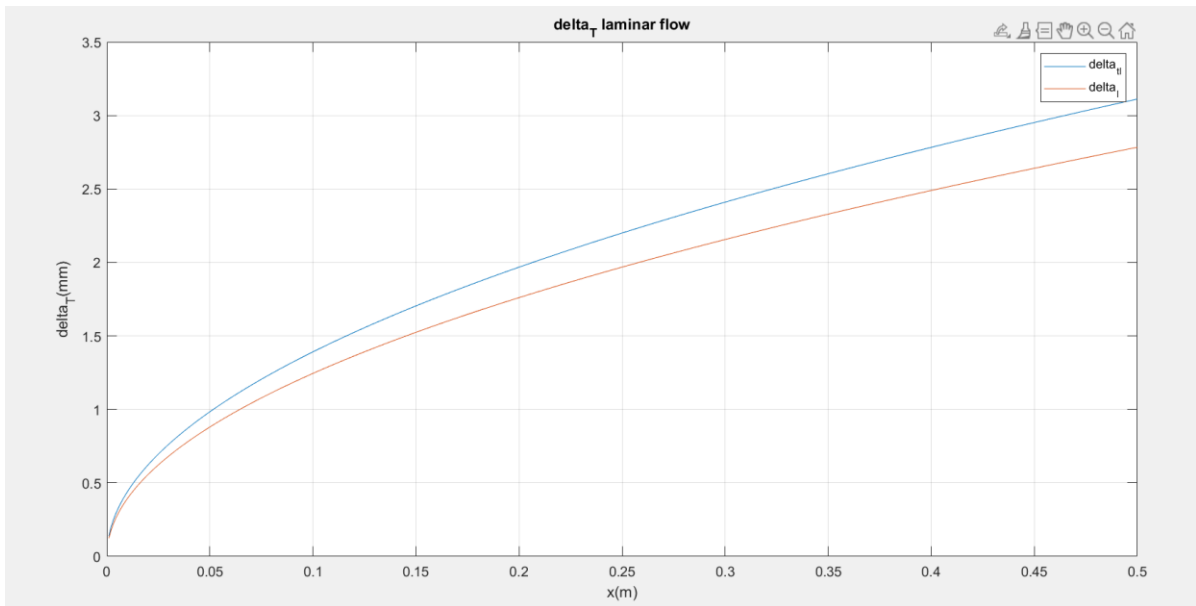


Figure 5.9. Theoretical thermal and hydrodynamic boundary layer thicknesses for laminar flow.

### 5.1.1.2 Turbulent flow over an isothermal flat plate:

For the case of turbulent flow over an isothermal plate, a good hydrodynamic boundary layer approximation can be expressed as:

$$\delta = 0.37 * Re_x^{-\frac{1}{5}} * x \text{ [incropera 7.35]}$$

And also:

$$\delta \approx \delta_T \text{ [411 incropera]}$$

Results from these equations can be found in figure 5.10. For turbulent flow, the boundary layer thickness grows much faster than in the case of laminar flow.

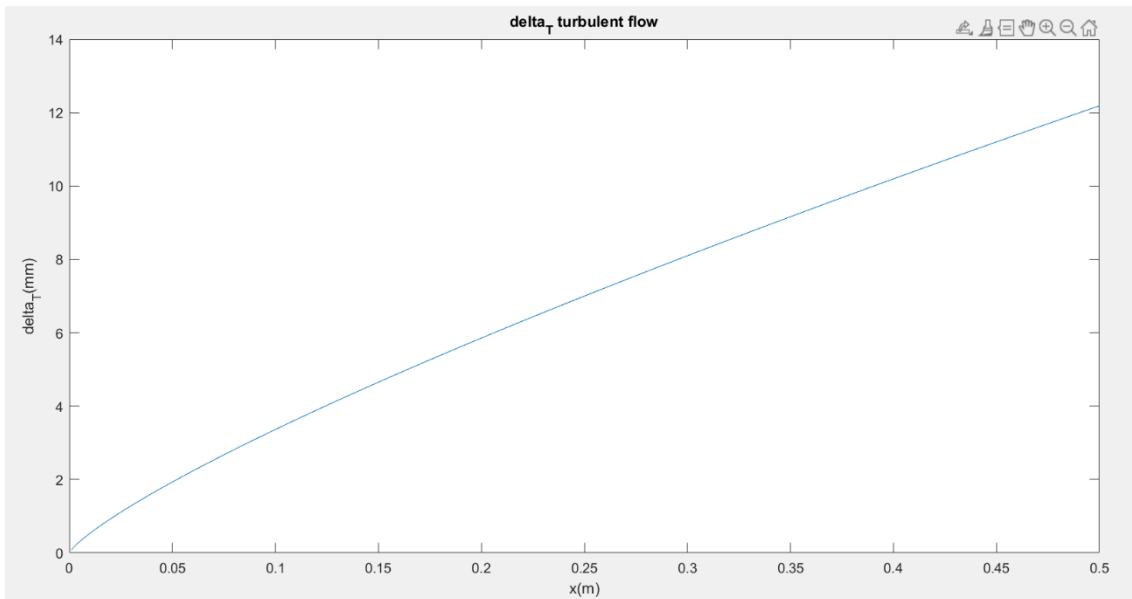


Figure 5.10. Theoretical thermal and hydrodynamic boundary layer thicknesses for turbulent flow.

Knowing the thicknesses values for both laminar and turbulent flow,  $L= 0.265$  was chosen. In the desired case, laminar flow, boundary layer seems to have a good thickness between  $x=0.05\text{m}$  and  $x=0.25\text{m}$ .  $L= 0.25$  could have been chosen but this value was finally increased to  $L=0.265$  to have some margin of error.

The flat plate was made in Figure 4 HI TEMP 300-AMB . It is a plastic suitable for high temperature components testing.

### 5.1.2 Supports Design

To hold the flat plate on place two identical aluminum supports where used. These supports are two metallic plates L shaped with a hole in the shape of the side outline of the plate as can be seen in Figure 5.11. The flat plate bosses are introduced in the metallic supports that are later screwed to the wind tunnel ground.

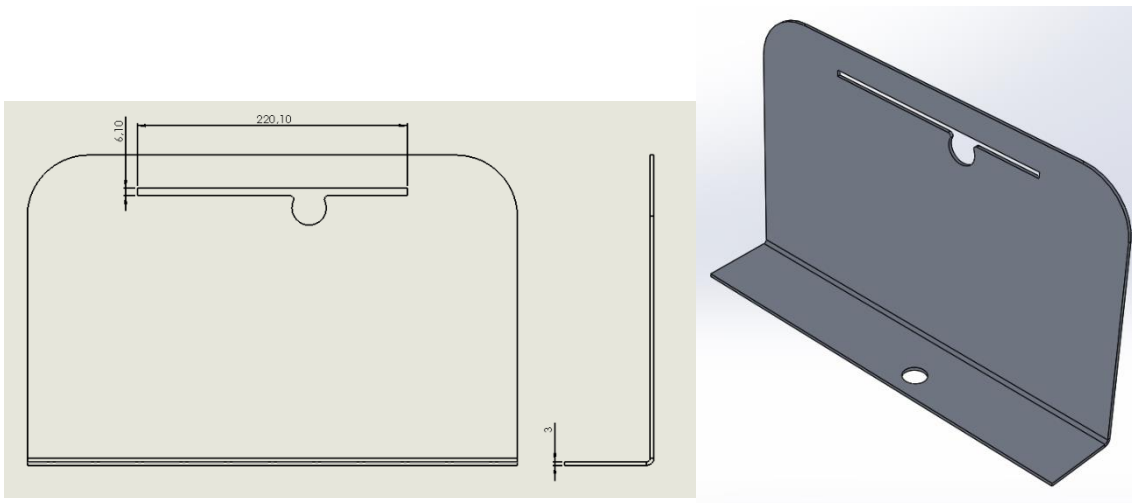


Figure 5.11. Supports design

## 6. Experiment Build

Before the realization of the measurements, the whole structure of the experiment had to be mounted. The main structure consists of: The flat plate, the supports, the copper pipes and the water heater with the pump.

Three flat plates were printed, figure 6.1, in case they broke during experiment build or the measurements.

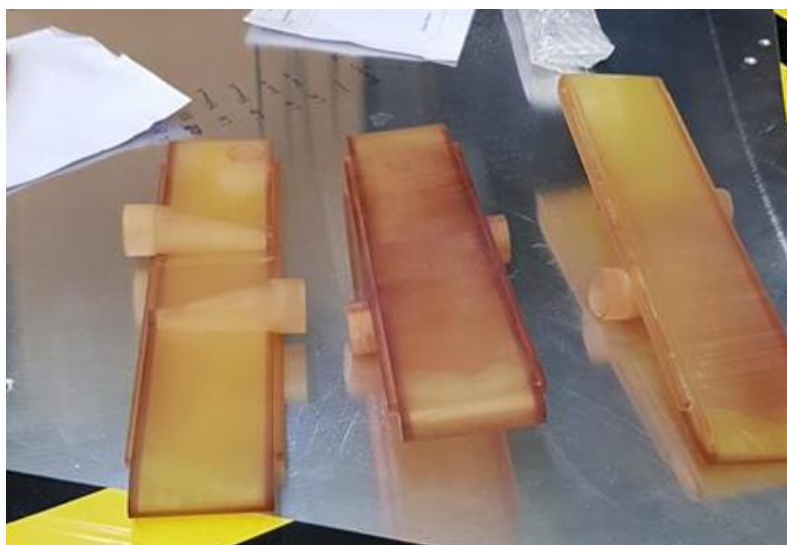


Figure 6.1. Flat plates

The flat plates surfaces were painted, from edge to edge, with a special matt paint used to create matte and completely anti-glare surfaces velvet-coating 811-21 Figure 6.2 The emissivity of this setup is 0.991-1 [13]. In order to have a surface as similar as possible to a black body with a really low reflectivity to reduce the uncertainties at the measurements of the IR camera. The coat paint was kept as thin as possible so the experiment was as similar as possible to the theoretical approach.



Figure 6.2. velvet-coating 811-21

The final result can be seen in figure 6.3



Figure 6.3. Painted Flat Plates

The copper tubes, and the entrance of the water channels to the flat plate where sanded to have a smooth fit and for a better glue performance on the joints.

The result can be seen in figure 6.4.



Figure 6.4. Original copper tubes Left. sanded joined tubes with plastic couplings and flat plate Right.

The metallic supports had to be sanded also as the wholes where the flat plate bosses had to go in where too small for it to fit in with out cracking. One of the painted flat plates was introduced in the supports as can be seen in in figure 6.5.



Figure 6.5. Flat plate and aluminum supports joined.

Then the structure was centered in the wind tunnel and the supports were screwed to a removable wooden floor. One of the copper tubes was introduced in the flat plate using a L-shaped coupling. The result can be found in figure 6.6



Figure 6.6. Flat plate and aluminum supports screwed to the floor.

The copper tube that can be seen in figure 6.6, goes under the wind tunnel where with another a L-shaped coupling is guided where it will be connected to a water heater and a pump. Then it was held by another support that can be rounded in red in figure 6.7.



Figure 6.7. View of the experiment build from the bottom of the wind tunnel

Then, another copper pipe was glued to the other entrance of the flat plate and guided out of the wind tunnel through a hole in the tunnel wall as it was easier than taking it also under the wind tunnel. The copper tube was held with another metallic support. This support is a metallic part crossed by the tube. It was added because one of the flat plates cracked during the build of the experiment. This happened because all the forces that were applied to the copper tube, ended directly in the flat plate that is made of HI TEMP 300-AMB [12], a plastic that is considerably fragile. The result can be seen in figure 6.8



Figure 6.8. experiment structure with both copper tubes connected.

All the copper tubes were covered by an isolating material as can be seen in figure 6.9.

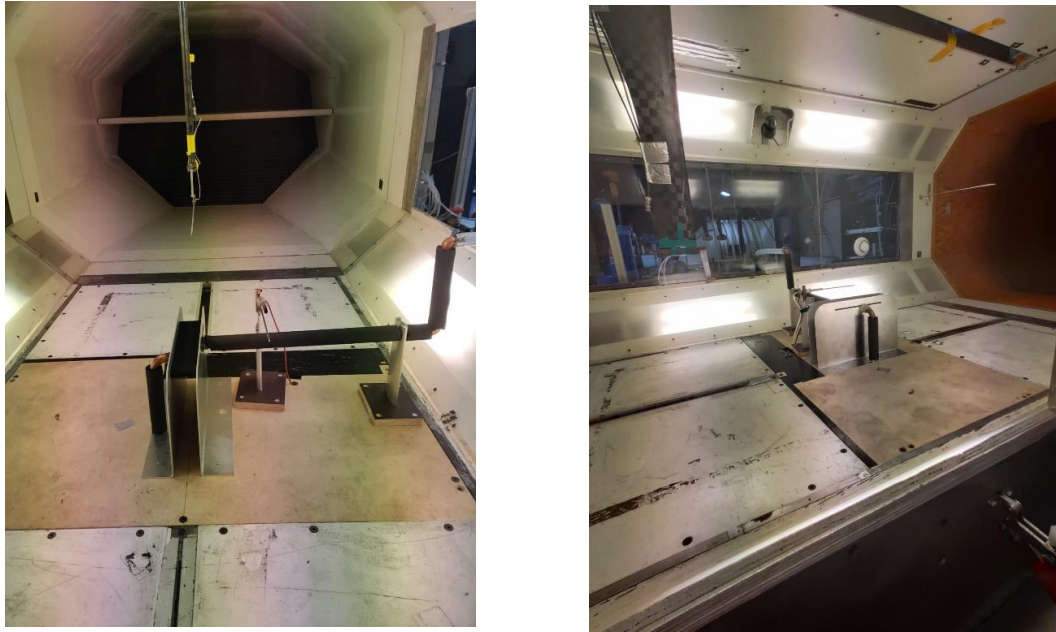


Figure 6.9. experiment structure with copper tubes isolated.

Next to the flat plate, a pitot tube and a temperature sensor were placed to measure wind speed and temperature. Figure 6.10. They were held to a support as the one that was used to hold the copper tube.

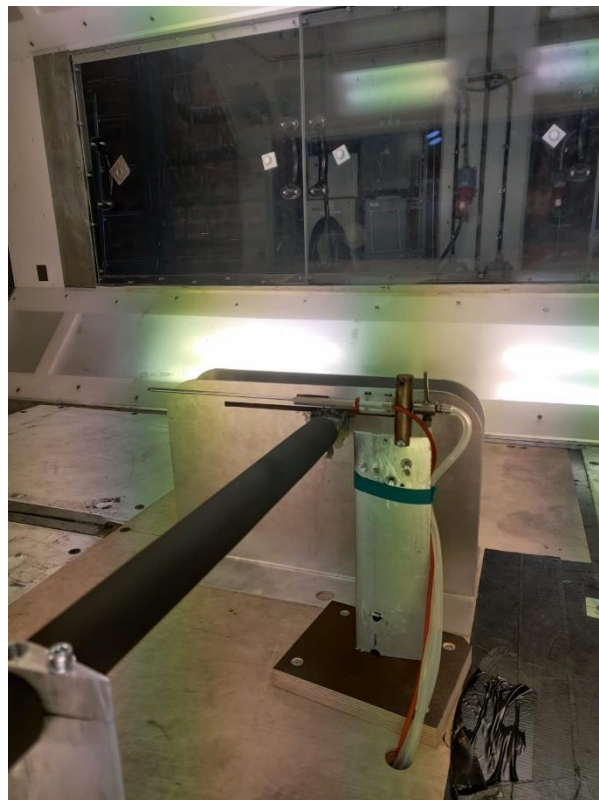


Figure 6.10. Pitot tube and temperature sensor for wind flow.

Another temperature sensor, figure 6.11, was added under the wind tunnel to measure the outgoing water temperature. It was held against the copper tube using duct tape and later covered with an isolating coating.

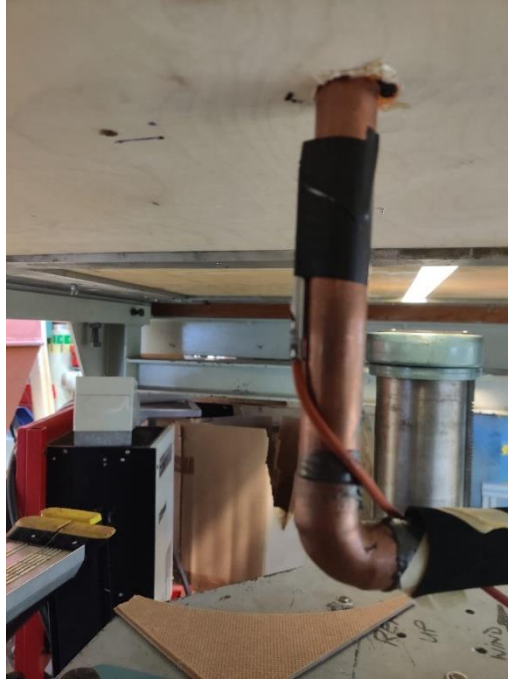


Figure 6.11. temperature sensor under the wind tunnel for outgoing water temperature.

In the roof of the wind tunnel there is an entrance through which a carbon fiber structure connected to two electric engines enters. This structure can be moved by the robot up and down and left and right. This structure holds a pitot tube that will be used to calculate the hydrodynamic boundary layer through the flat plate. The build can be seen in figure 6.12

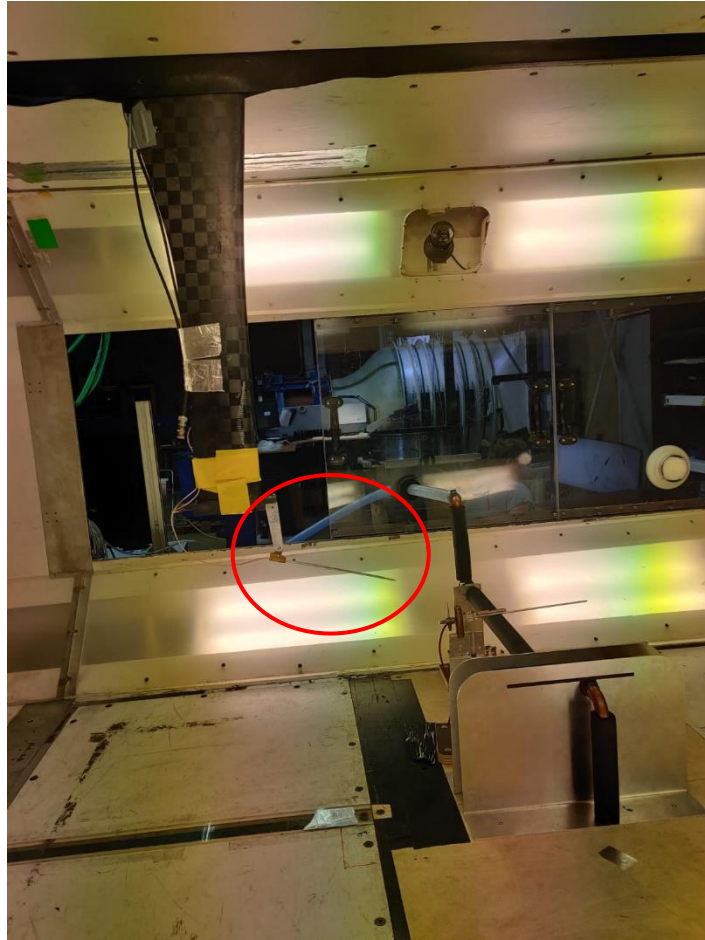


Figure 6.12. Pitot tube used to measure hydrodynamic boundary layer.

Once the main structure was mounted as can be seen in figure 6.13, the water circuit was closed by connecting the open end of the copper tubes to a water heater with a pump. The water heater can be seen in figure 6.14. This water heater consists on an isolated container that looks like a white box on figure 6.14. All the water is placed on the inside where a thermal resistance is placed to heat the water up. From this white box, two tubes go out. One plastic tube is directly connected to one of the copper pipes from the experiment. The other one goes through the back part of this white box; it is connected to a pump and to a valve to stop the flow and then to the other copper tube.

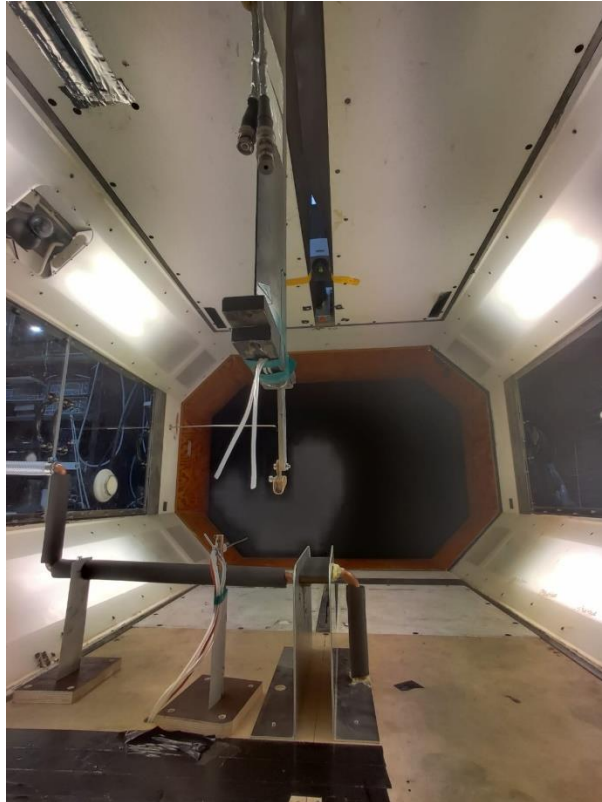


Figure 6.13. Final build of the experiment seen from the inside of the wind tunnel.

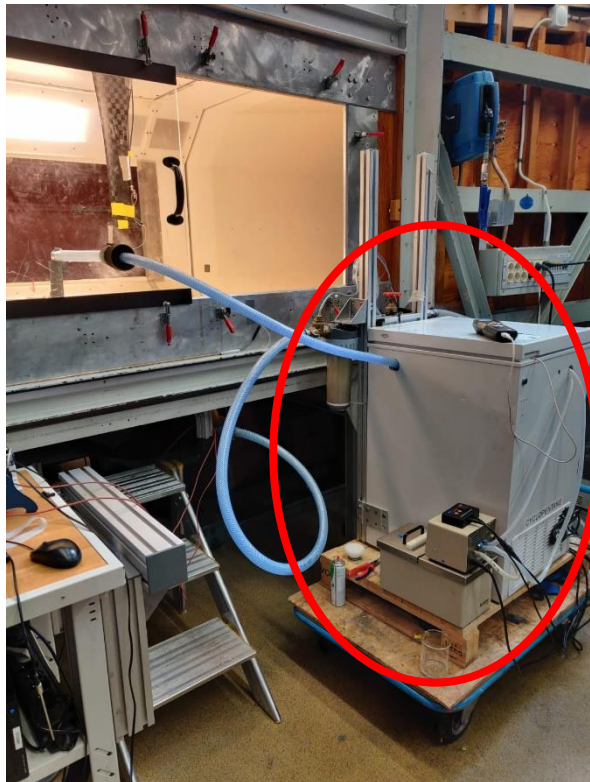


Figure 6.14. Final build of the experiment seen from the outside of the wind tunnel with water heater mechanism rounded in red.

Finally, the IR- camera was placed on the top of the wind tunnel. It was placed on the outside and an aperture was made so the lenses could focus on the flat plate. The camera placement can be seen on figure 6.15.



Figure 6.15. IR-camera placement.

The final build of the whole experiment structure can be seen in figures 6.16. and 6.17:



Figure 6.16. Final build of the experiment from the outside of the wind tunnel.

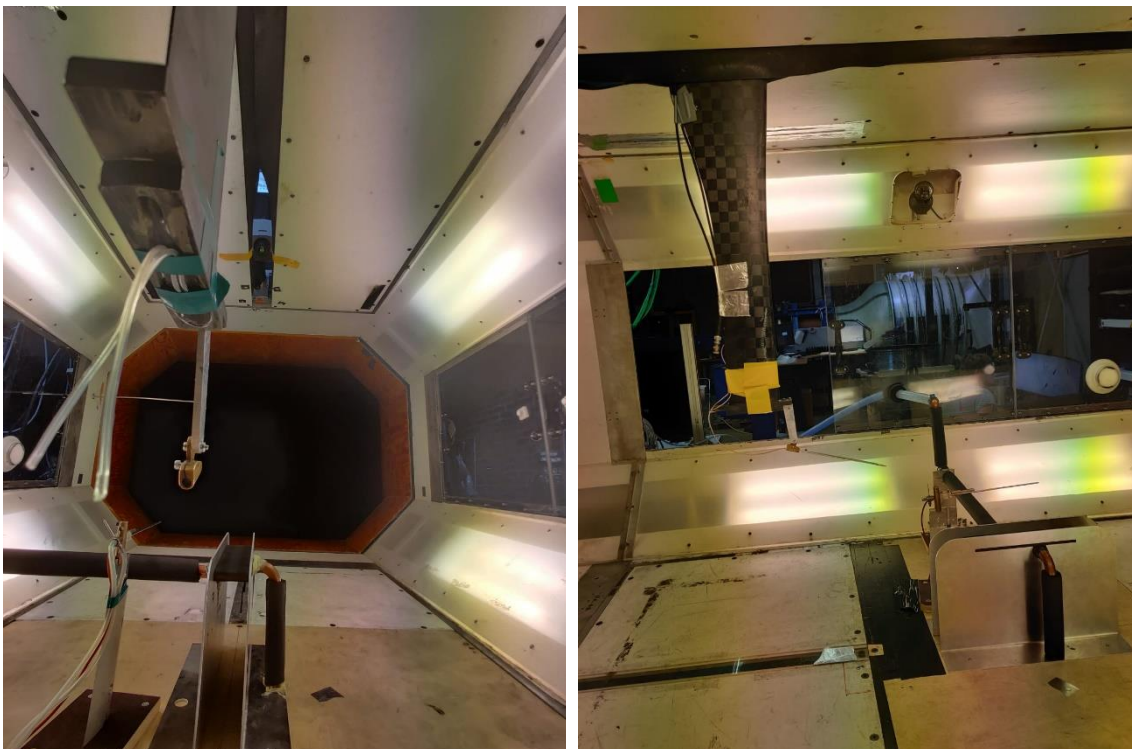


Figure 6.17. Final build of the experiment from the inside of the wind tunnel.

## 7. Experiments

Once everything was mounted and after performing the theoretical approach previously explained, the two experiments, hydrodynamic boundary layer measurement and infrared thermography method were applied.

### 7.1 Internal flat plate wall temperature assumptions prove.

First, the assumption of  $T_1 = T_w$  had to be proved. This assumption consisted in assuming that the inner wall temperature  $T_1$  and the water temperature  $T_w$  are similar because of the flow velocity. This assumption is valid when the heat transfer coefficient is infinitely large or when the water temperature does not change through the water channels. The theoretical approach and bias error calculation can be found in previous work by I. Jonsson, V. Chernoray and R. Dhanasegaran [2]. The assumption made was that the heat transfer coefficient in the water side of the flat plate is big enough compared to the heat transfer coefficient of the air side.

To prove this assumption did not affect the measurements, different tests were made. The surface temperature of the flat plate  $T_2$  was measured with the IR-camera and the water temperature was measured with a Resistance Temperature Detector. Water and air temperature were kept constant for all the experiments and water flow was increased from the minimum that the pump allowed to maximum power. The pump power was divided in 10 steps being 1 dot the minimum power and 10 dots the maximum power.

The camera measured the temperature through the whole flat plate. To simplify the calculations, the data from the midspan and surroundings was taken. This can be seen in figure 7.1 where a black line represents the data that will be taken. Also, some more pixels around this black line will be considered.

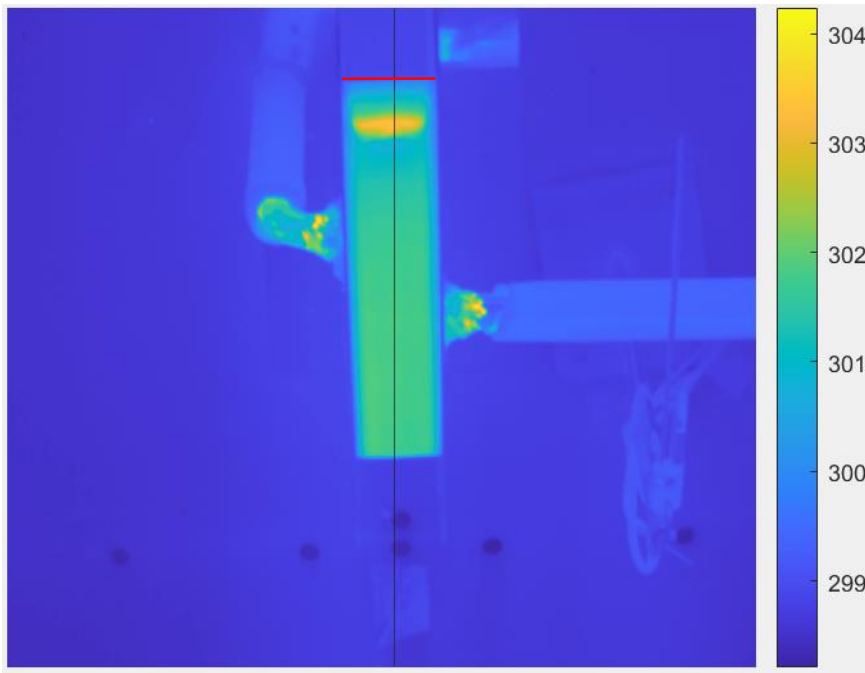


Figure 7.1. Temperatures measurement [kelvins] with the IR-camera example.

The data from this black line is represented on a graph, Figure 7.2 with temperatures in Kelvin's on the Y axis and pixels on the X axis being  $x=0$  the pixel at the bottom and  $x=256$  the pixel at the top of the black line in figure 7.1

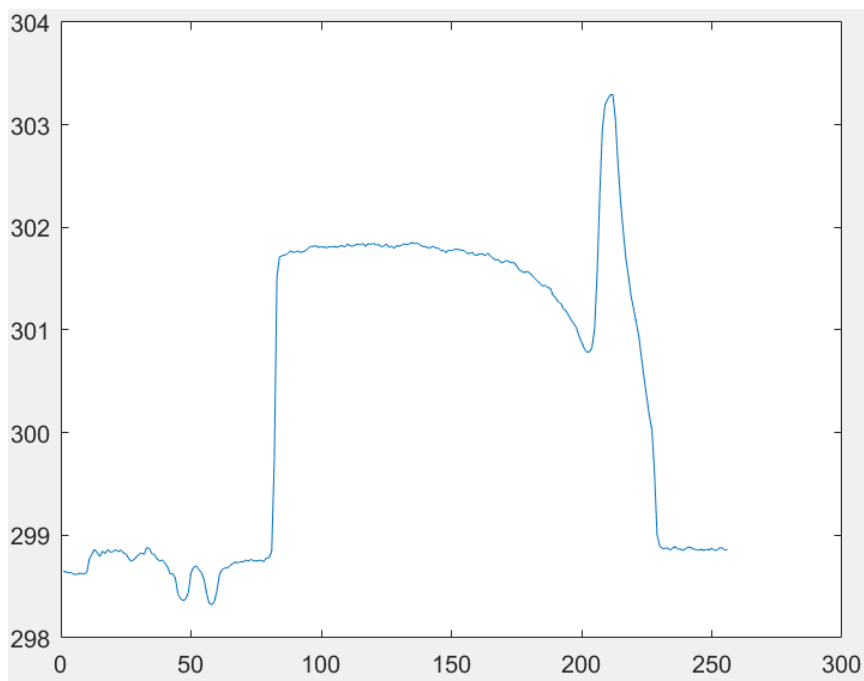


Figure 7.2. 1D representation from the data in the black line in figure 7.1.

This data was fixed and so that the point  $x=0$  in the graph corresponds to the leading edge where the air flow hits, in figure 7.1 the edge represented as a red line. The new data will look like in figure 7.3 and Figure 7.4.

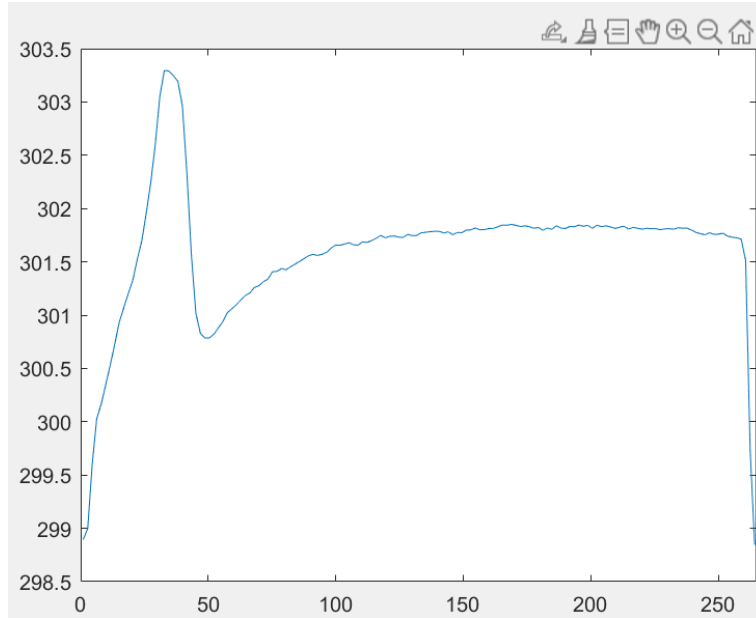


Figure 7.3. Fixed 1D representation from the data in the black line in figure 7.1.

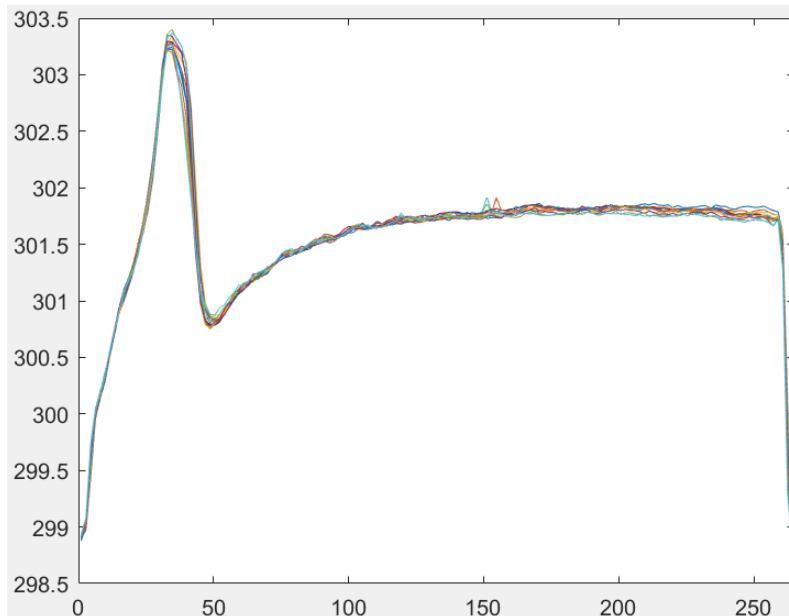


Figure 7.4. Fixed 1D representation from the data in the black line and surroundings in figure 7.1.

On the other hand, the resistance variation measured by the Resistance Temperature Detector where converted into temperatures.

For each measurement, the temperatures measured by the camera and the temperature of the water at the outflow will be shown.

1. 20% pump power with 25 m/s windspeed

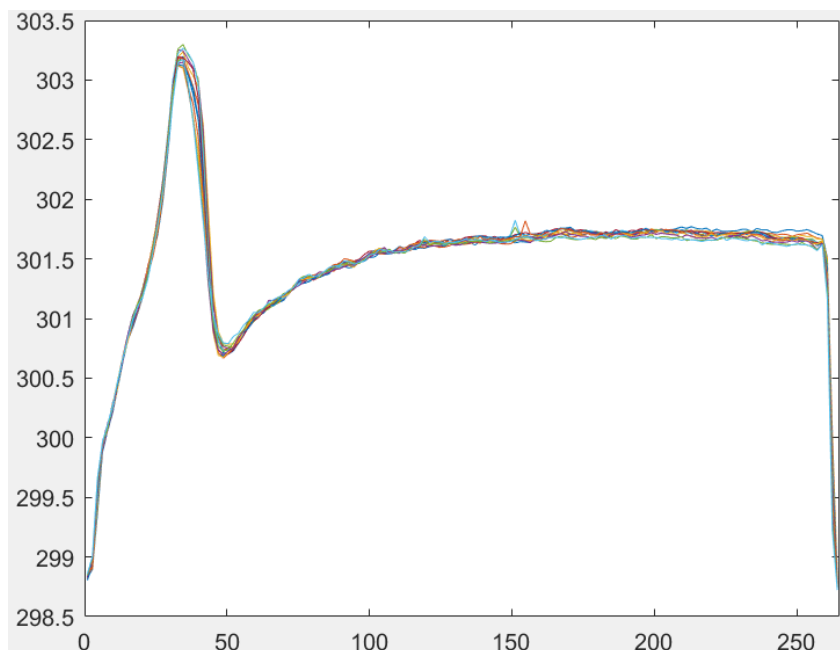


Figure 7.5. Flat plate surface temperature for 20% pump power with 25 m/s windspeed.

Water outflow temperature  $T_w = 307.11 K$

Mean surface temperature  $T_2 = 301.5 K$

2. 40% pump power with 25 m/s windspeed

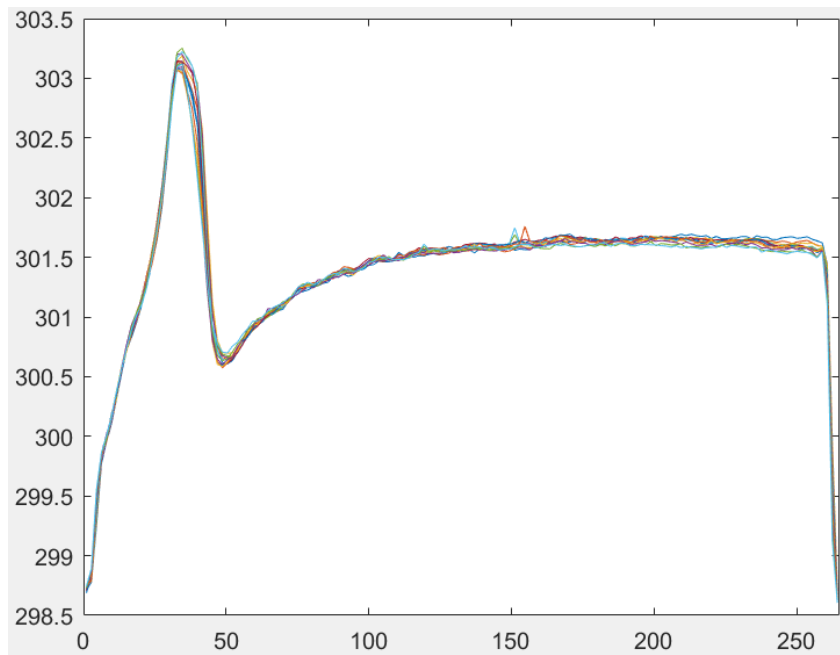


Figure 7.6. Flat plate surface temperature for 40% pump power with 25 m/s windspeed.

Water outflow temperature  $T_w = 307.13 K$

Mean surface temperature  $T_2 = 301.42 K$

3. 60% pump power with 25 m/s windspeed

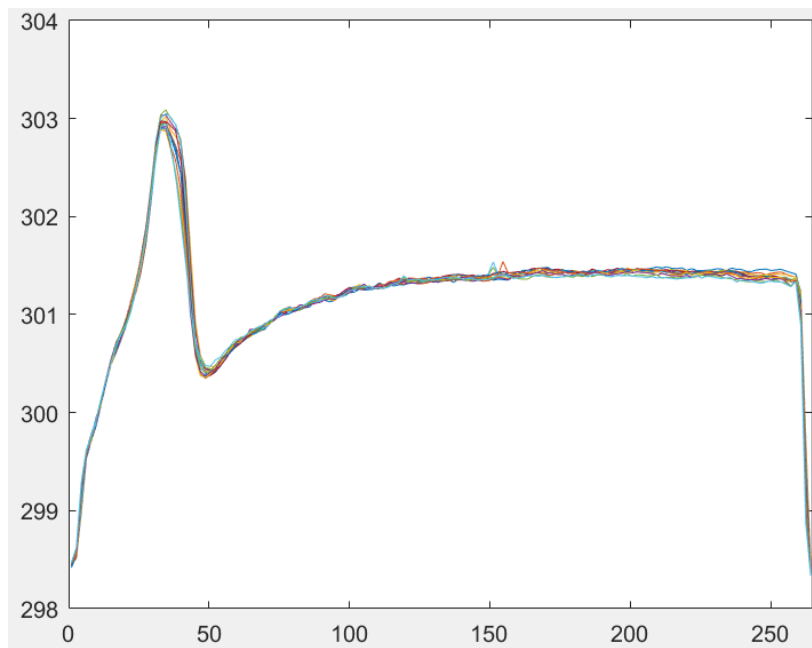


Figure 7.7. Flat plate surface temperature for 60% pump power with 25 m/s windspeed.

Water outflow temperature  $T_w = 307.046 K$

Mean surface temperature  $T_2 = 301.21 K$

4. 80% pump power with 25 m/s windspeed

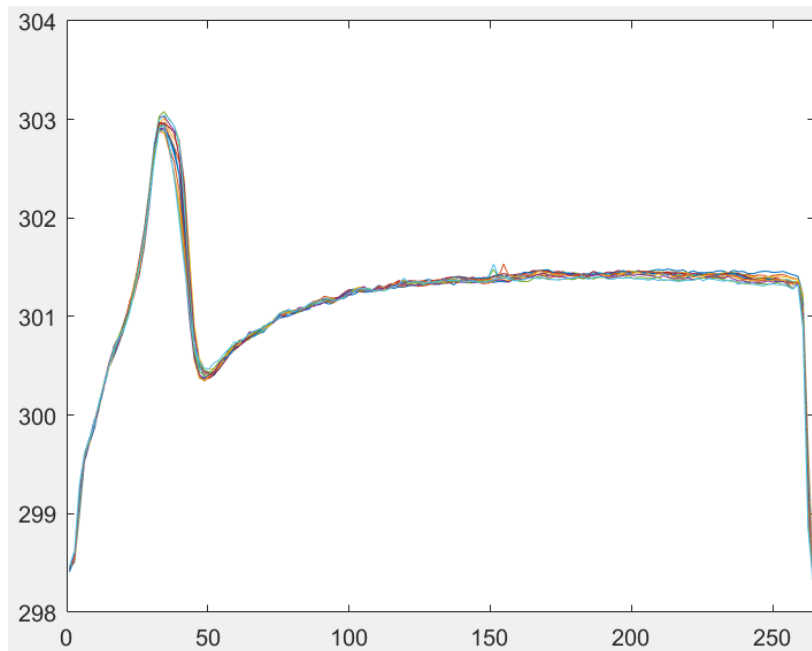


Figure 7.8. Flat plate surface temperature for 80% pump power with 25 m/s windspeed.

Water outflow temperature  $T_w = 307.046 K$

Mean surface temperature  $T_2 = 301.21 K$

5. 100% pump power with 25 m/s windspeed

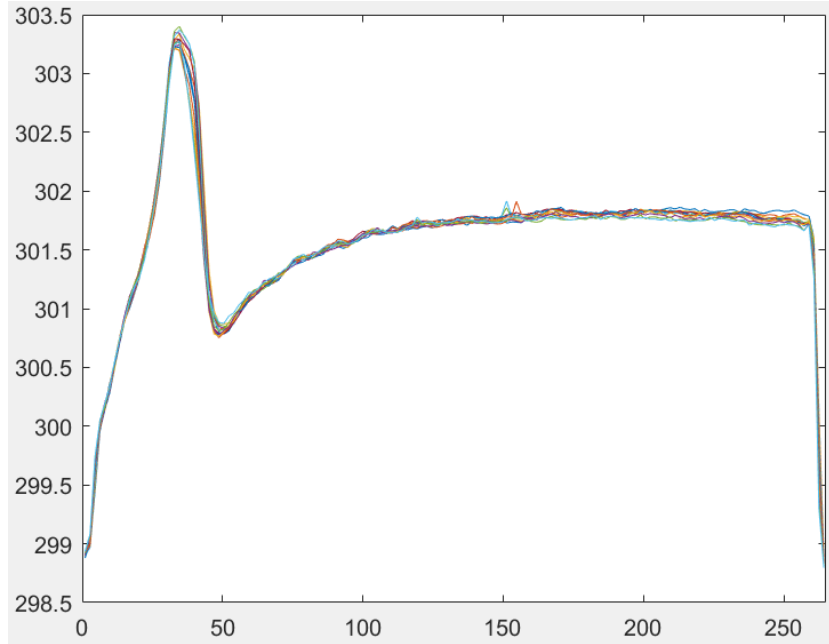


Figure 7.9. Flat plate surface temperature for 100% pump power with 25 m/s windspeed.

Water outflow temperature  $T_w = 307.22 K$

Mean surface temperature  $T_2 = 301.59K$

Representing all the data together:

| Pump Power | 20%    | 40%    | 60%     | 80%    | 100%   |
|------------|--------|--------|---------|--------|--------|
| $T_w$      | 307.11 | 307.13 | 307.046 | 307.12 | 307.22 |
| $T_2$      | 301.5  | 301.42 | 301.21  | 301.11 | 301.59 |

Table 7.1. Water and surface temperatures for varying pump power.

In table 7.1 all the measurements are compared together, the maximum variation on the surface temperature  $T_1$  is of 0.38 K, 1.3% and in the water side,  $T_w$  varies 0.174 K, 0.056% of the maximum  $T_w$ .

This proves the assumption that the inside wall temperature of the flat plate  $T_1 = T_w$  and therefore the surface temperature,  $T_2$  does not depend on the water flow speed. The rest of the experiments where made with full pump power.

## 7.2 IR-camera Experiment

Also, with these results, the heat transfer coefficient on the water side  $h_2$  can be calculated as knowing:

$$Q_{conv\ Air} = h_2(T_2 - T_3)$$

$$Q_{cond} = \frac{k}{t}(T_1 - T_2)$$

For the radiation heat flux, some approximations where also made to simplify calculations: complete black background and  $\tau = 1$  as Atmospheric absorption is almost negligible. This led to:

$$Q_{Rad} \approx \sigma(\varepsilon T_2^4 - T_3^4)$$

With the previously verified assumption:  $T_1 = T_w$  and knowing  $Q_{cond} = Q_{conv\ Air} + Q_{Rad}$ ,  $h_2$  can be solved as:

$$Equation\ 7.1\ h_2 = \frac{Q_{cond} - Q_{Rad}}{T_2 - T_3} = \frac{1}{T_2 - T_3} \left( \frac{k}{t}(T_1 - T_2) - \sigma(\varepsilon T_2^4 - T_3^4) \right)$$

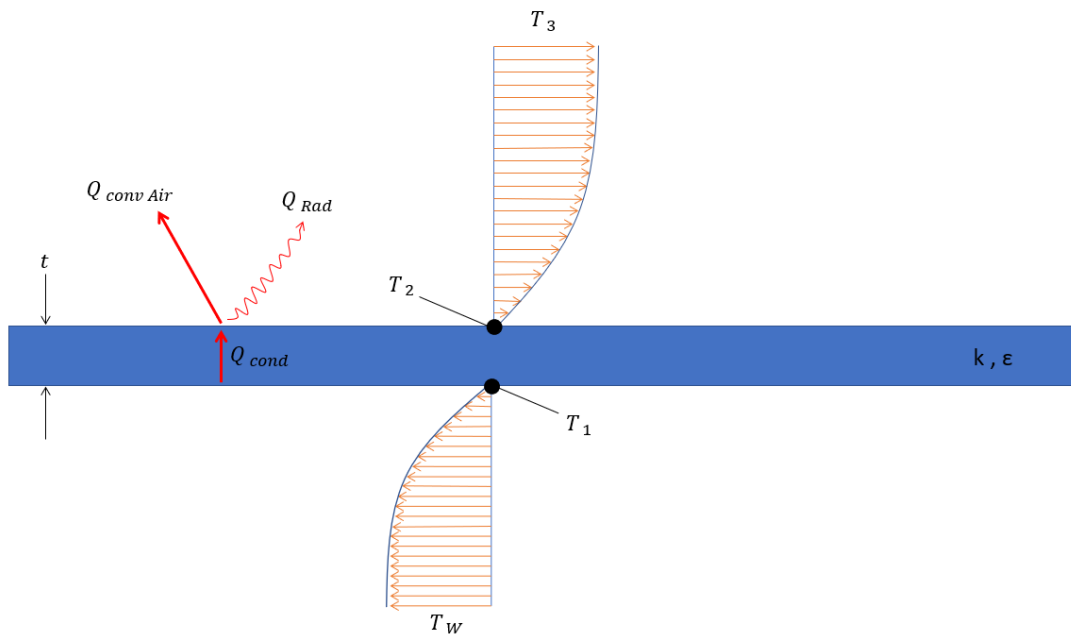


Figure 7.10. Experiment sketch.

In equation 7.1,  $T_1 = T_W$  which was measured at the outlet pipe of the flat plate with a Resistance Temperature Detector placed in the copper tubes under the isolating material as was already shown in the mounting process.

$T_2$  was measured with the IR-camera as shown before to prove the independence of  $h_1$  with the water flow speed.

$T_3$  was measured with another Resistance Temperature Detector also shown in the mounting process.

The thermal conductivity of the flat plate material is represented as " $k$ " and was provided by the flat plate manufacturers.

The flat plate thickness is represented by " $t$ ".

$\sigma = 5.669 \times 10^{-8}$  is the Stefan-Boltzmann constant and  $\varepsilon = 0.991$  is the emissivity of the flat plate surface painted with the matt paint.

By solving this equation for an air flow of 25m/s at  $T_3 = 25.59$  and water temperature of  $T_w \approx 35^\circ$  with full pump power, figure 7.11 is obtained:

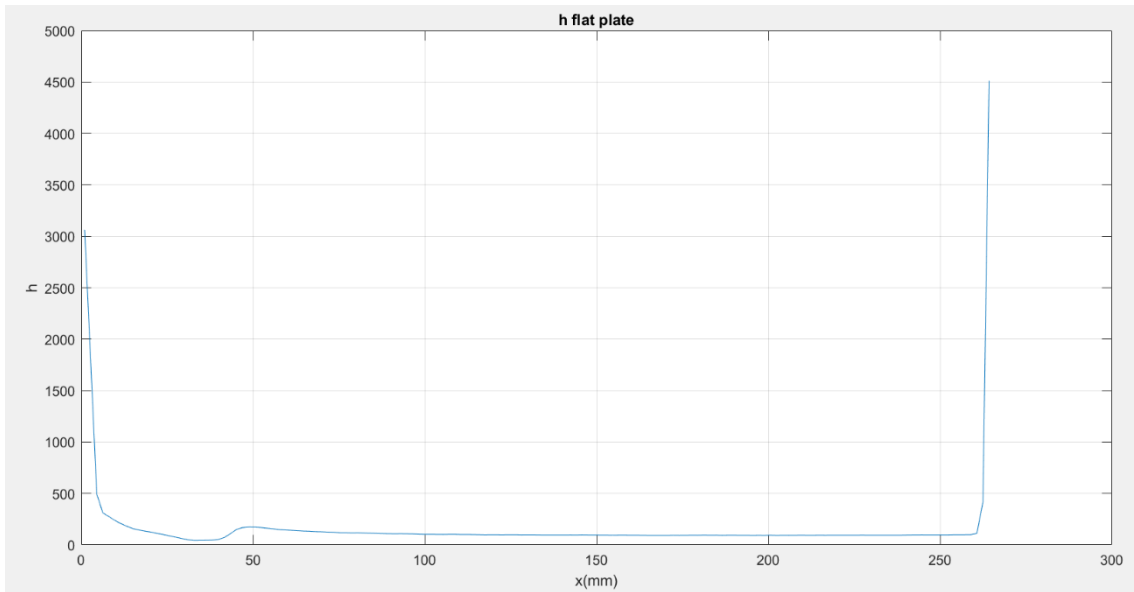
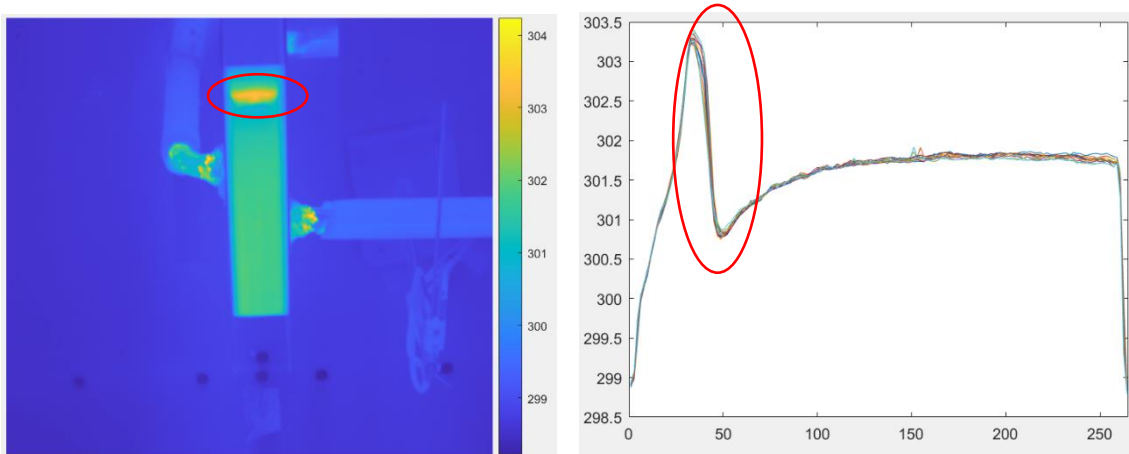


Figure 7.11.  $h_2$  obtained from IR measurements.

In this figure, it can be seen how the heat transfer coefficient rapidly stabilize around 100, then there is a “jump” at around  $x=40\text{mm}$  that can be because of a transition between laminar and turbulent flow, or because of that there is a separation of the flow in that zone. This phenomenon can be appreciated in the thermal picture taken from the camera and in the temperatures-graph shown in figure 7.12. At the end,  $h_2$  rapidly increases, but



those temperature measurements are from outside of the flat plate so they do not have to be considered.

Figure 7.12. thermal picture from the IR-camera at the left and surface temperature representation through the flat plate around the midspan at the right with flow separation/transition rounded in red.

### 7.3 Measurement of the Boundary Layer Experiment

To verify the results obtained with the IR method, pressure gradient was also measured through the flat plate using a pitot's tube. The pitot's tube has two holes. As can be seen in figure 7.13

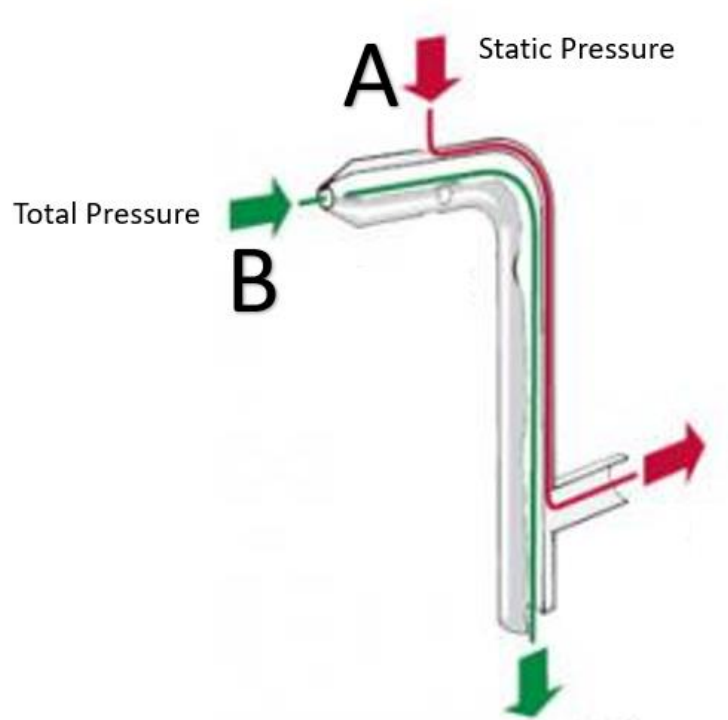


Figure 7.13. Pitot's tube scheme.

The one used for the measurements at Chalmers can be seen in figure 7.14. and schematized in figure 7.15. It was held on a mechanized structure to move it through the different measure points designed for the experiment.

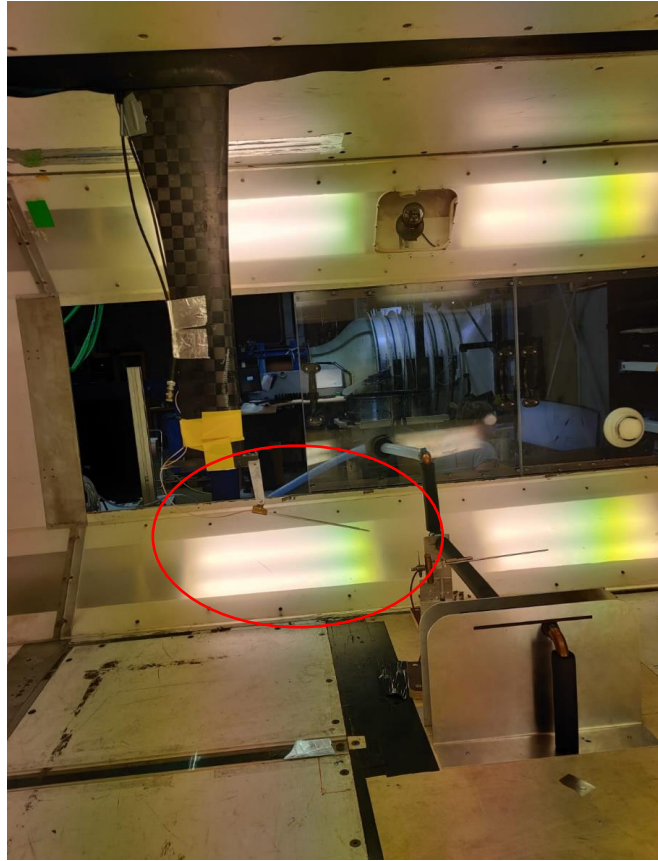


Figure 7.14. Pitot's tube used for the experiment.

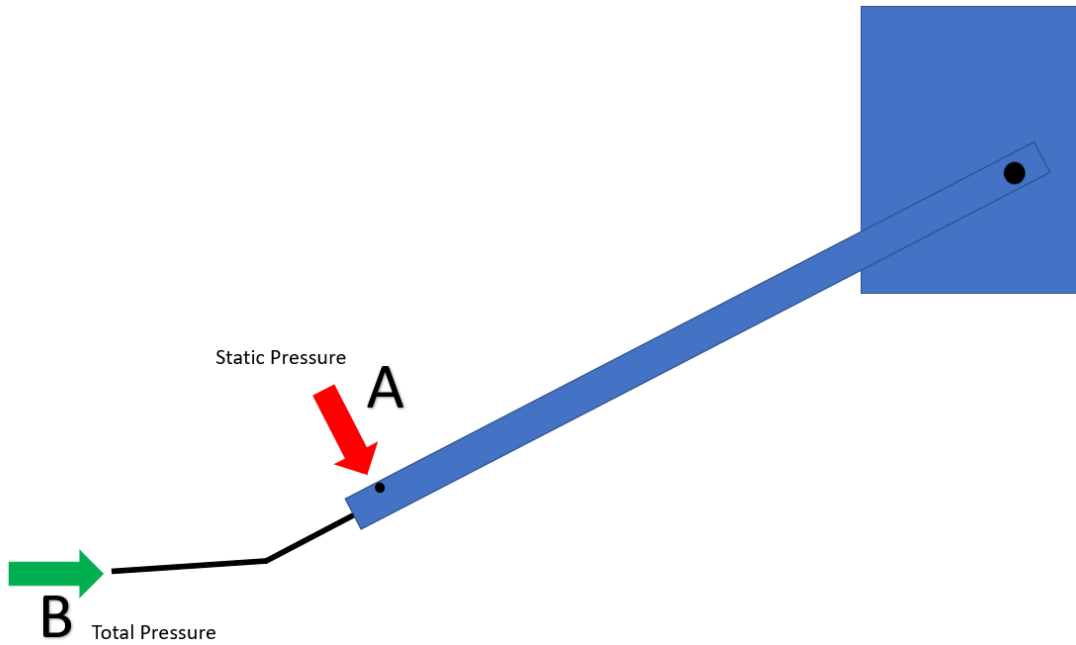


Figure 7.15. Pitot's tube used for the experiment scheme.

As can be appreciated on figure 7.15, the measures of static pressure and total pressure correspond to two different locations as the holes aren't placed in the same position, therefore the experiment was repeated twice, one to measure total pressure and another one to measure static pressure.

Static pressure was measured and as can be seen in figure 7.16, it is almost constant for each measure point.

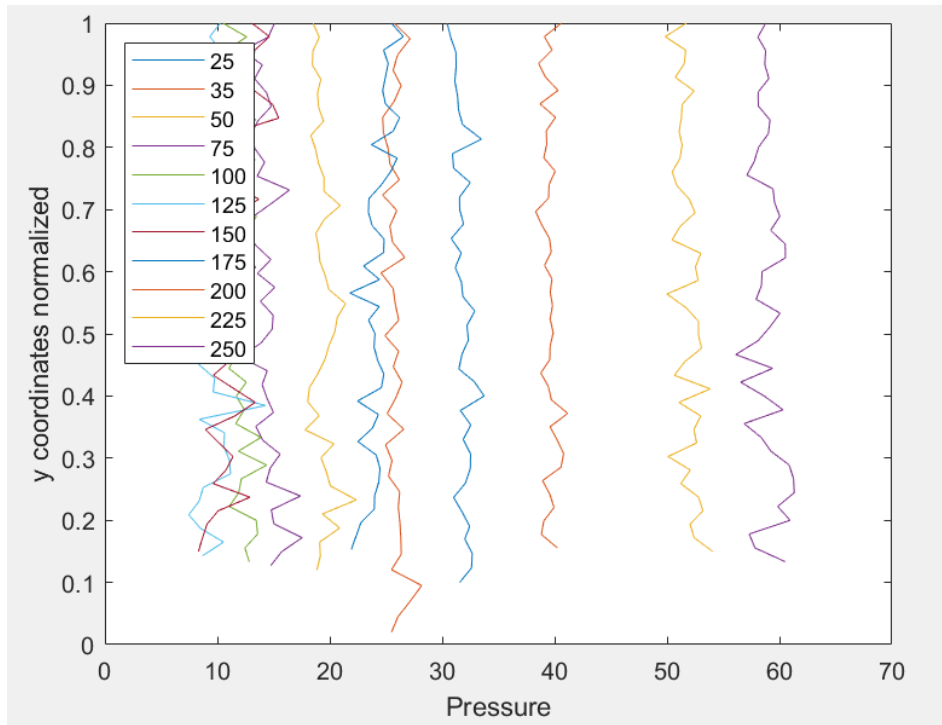


Figure 7.16. Static pressure measurements depending on height normalized and x location in millimeters.

Then, Total pressure was also measured and dynamic pressure was calculated as

$$q = \text{Total Pressure} - \text{Static Pressure}$$

And resulted in figure 7.17:

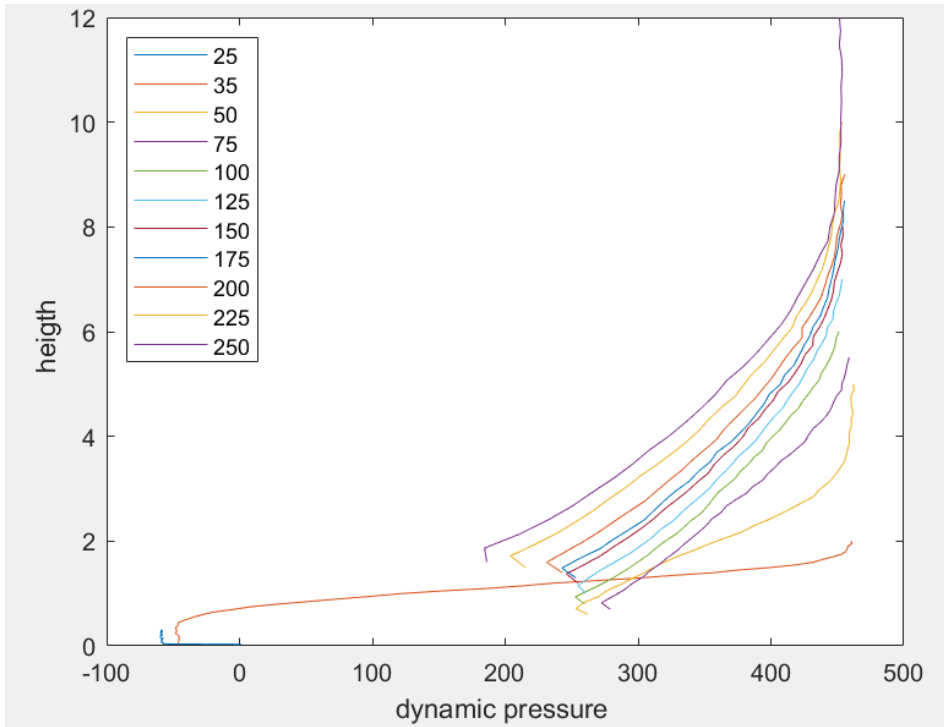


Figure 7.17. Dynamic pressure [Pascals] measurements depending on height and x location in millimeters.

With this results the velocity profile was calculated as  $u = \sqrt{2 \frac{q}{\rho}}$

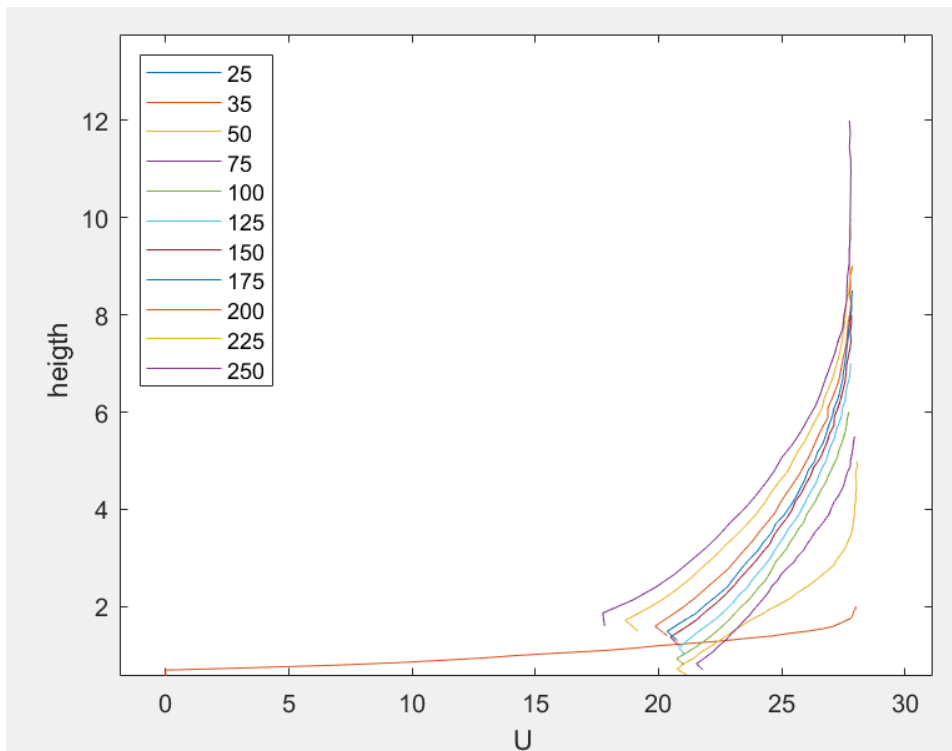


Figure 7.18. velocity profile(m/s) depending on height and x location in millimeters.

In figure 7.18 can be seen how all the velocity profiles converge in almost 28 m/s. this happens because on the experiment design, the aluminum supports form two walls around the flat plate which happens to accelerate the wind speed from 25 m/s to 28 m/s . There is also a separation of the wind current at the beginning of the flat plate that lead to ambiguous measurements and weird results before  $x=75\text{mm}$ .

The velocity profile was normalized taking as free current wind speed  $U_{\infty} = 28 \text{ m/s}$  leading in figure 7.19:

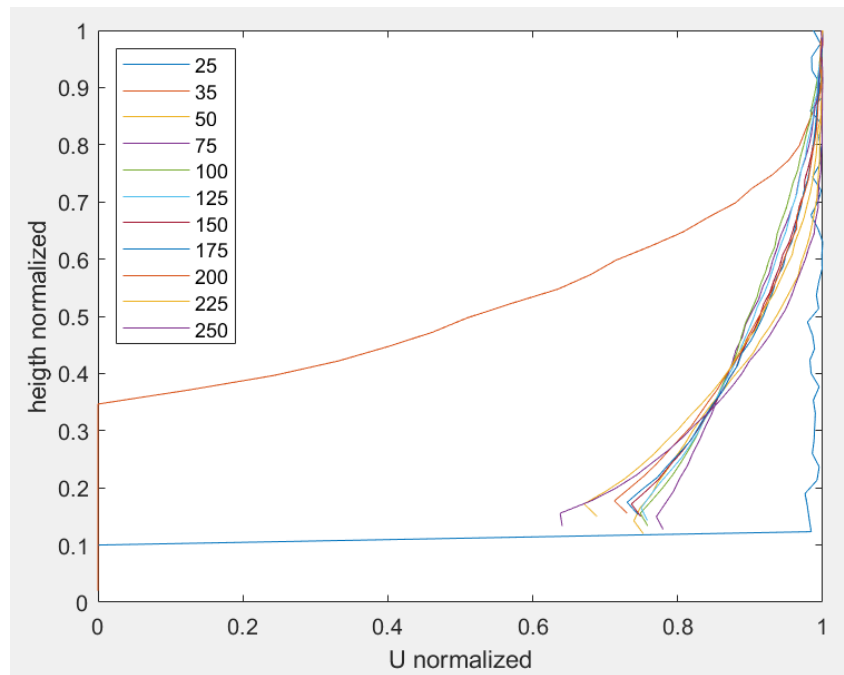


Figure 7.19. velocity profile normalized.

With these values the hydrodynamic boundary layer was calculated from  $x=50$  as the height values where  $\frac{U}{U_{\infty}} = 0.99$  leading to:

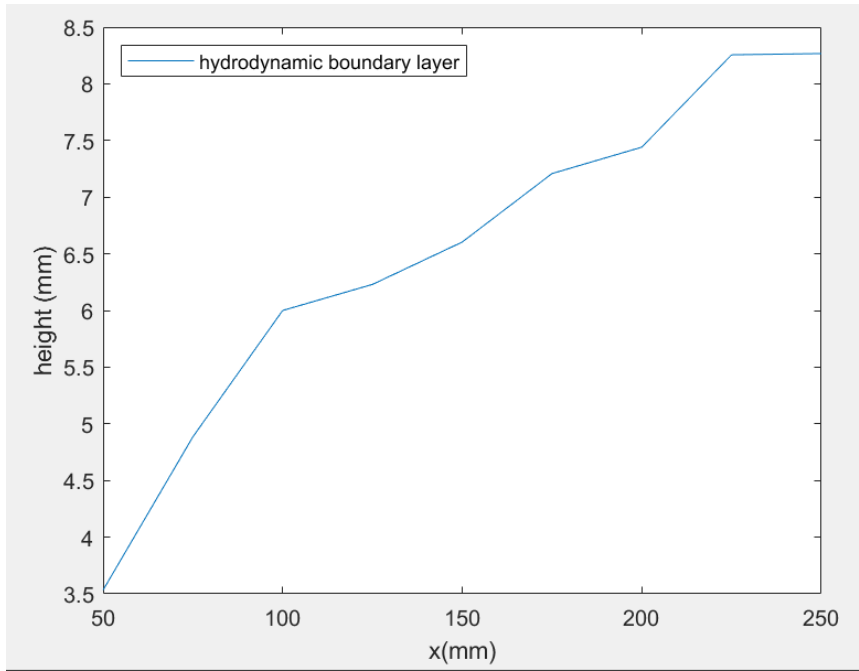


Figure 7.20. Hydrodynamic boundary layer at the flat plate.

## 8. Results

In this chapter the results obtained will be shown. In this project, an experiment to test a special method to measure heat flux was developed. The experiment designed was built and some tests were performed to ensure its utility. The experiment design consists of a flat plate with internal channels where hot water is pumped to heat up the flat plate surface. The flat plate is held by two aluminum supports, each at one side of the flat plate. The flat plate is fitted in the supports by two bosses that come out of the plate. The flat plate channels are connected to copper tubes that close the water circuit through a heater and a pump. The final design and build of the flat plate, the supports and the whole circuit can be found in figures 8.1 to 8.4.



Figure 8.1. Final Experiment Build 1.



Figure 8.2. Final Experiment Build 2.

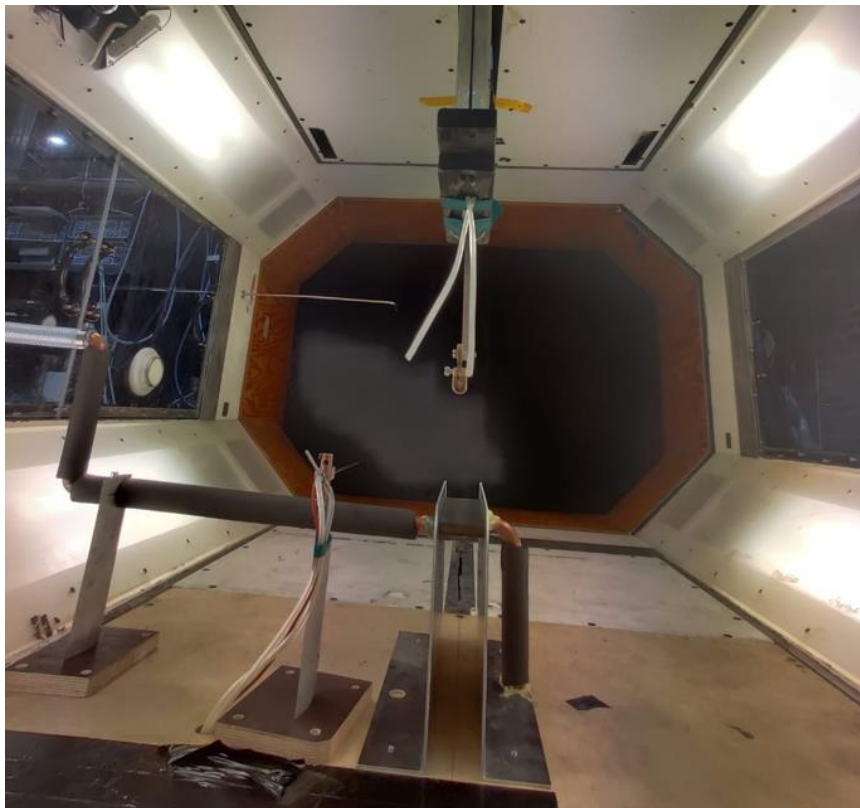


Figure 8.3. Final Experiment Build 3.



Figure 8.4. Final Experiment Build 4.

The designed experiment was done to benchmark an IR based heat transfer measurement method. Some tests were performed on the designed build where flat plate surface temperatures were measured with the IR method and pressure gradient was also measured using a pitot's tube moved through the flat plate surface vicinity.

For the IR tests, different measurements were done with different water speeds and wind speeds.

It was experimentally proved that the inner wall temperature can be assumed to be the same as the water temperature if the water heat transfer coefficient is much higher than the wind heat transfer coefficient:

| Pump Power | 20%    | 40%    | 60%     | 80%    | 100%   |
|------------|--------|--------|---------|--------|--------|
| $T_w$      | 307.11 | 307.13 | 307.046 | 307.12 | 307.22 |
| $T_2$      | 301.5  | 301.42 | 301.21  | 301.11 | 301.59 |

Table 8.1. Water and surface temperatures for varying pump power.

In table 8.1 all the measurements are compared together, the maximum variation on the surface temperature  $T_1$  is of 0.38 K, 1.3% and in the water side,  $T_w$  varies 0.174 K, 0.056% of the maximum  $T_w$ .

This proves the assumption that the inside wall temperature of the flat plate  $T_1 = T_w$  and therefore the surface temperature,  $T_2$  does not depend on the water flow speed. The rest of the experiments where made with full pump power.

With the previously verified assumption:  $T_1 = T_w$  and knowing  $Q_{cond} = Q_{conv Air} + Q_{Rad}$ ,  $h_2$  was calculated with the measurements of the IR camera:

$$h_2 = \frac{1}{T_2 - T_3} \left( \frac{k}{t} (T_1 - T_2) - \sigma (\epsilon T_2^4 - T_3^4) \right)$$

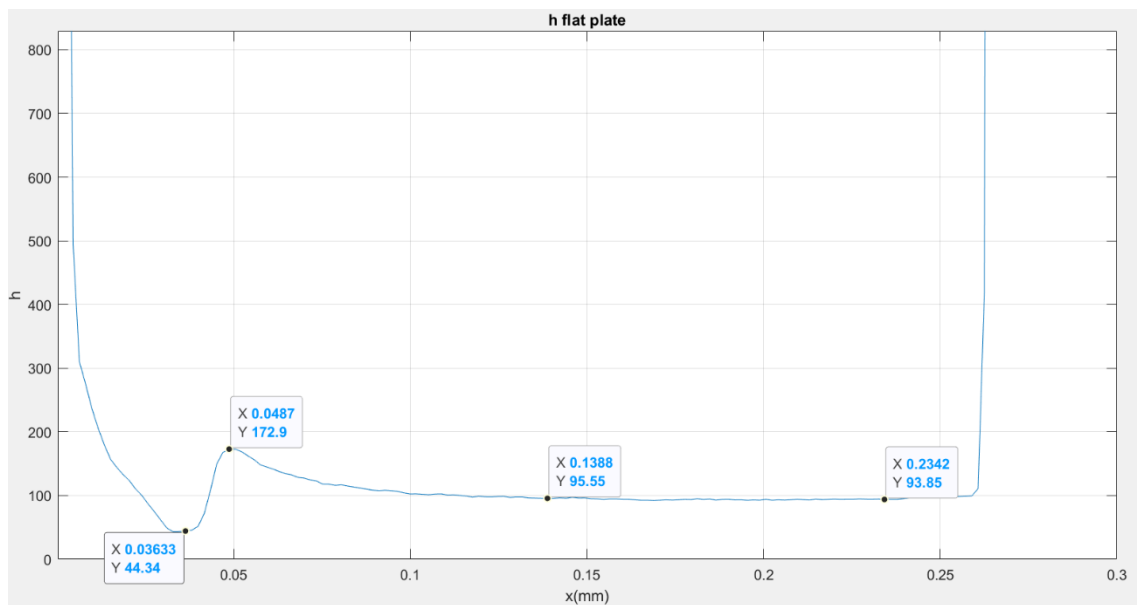


Figure 8.5.  $h_2$  calculated with IR measurements.

By measuring the pressure gradients, the velocity profile was calculated and the hydrodynamic boundary layer.

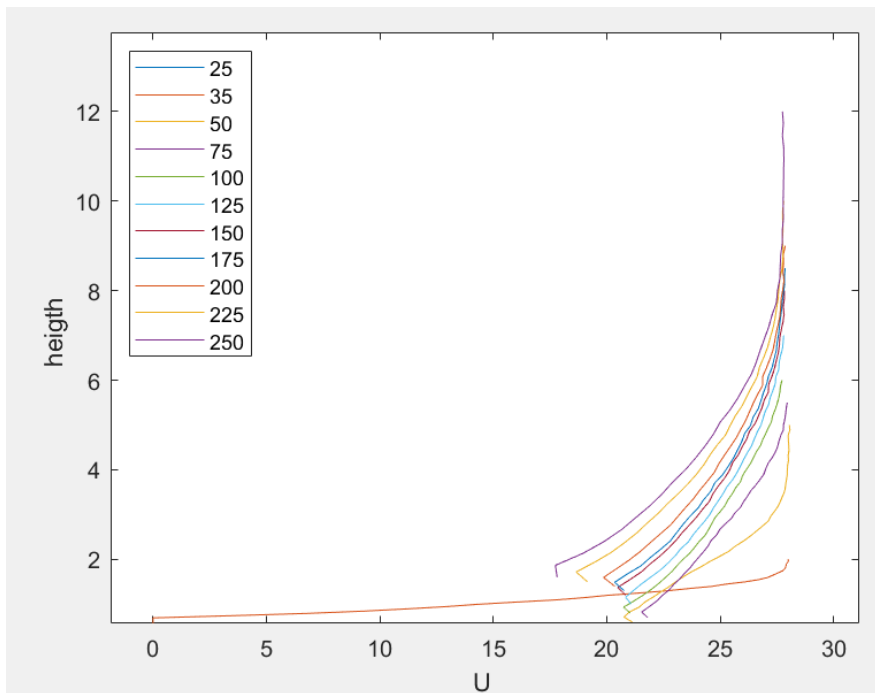


Figure 8.6. velocity profile(m/s) depending on height and x location in millimeters.

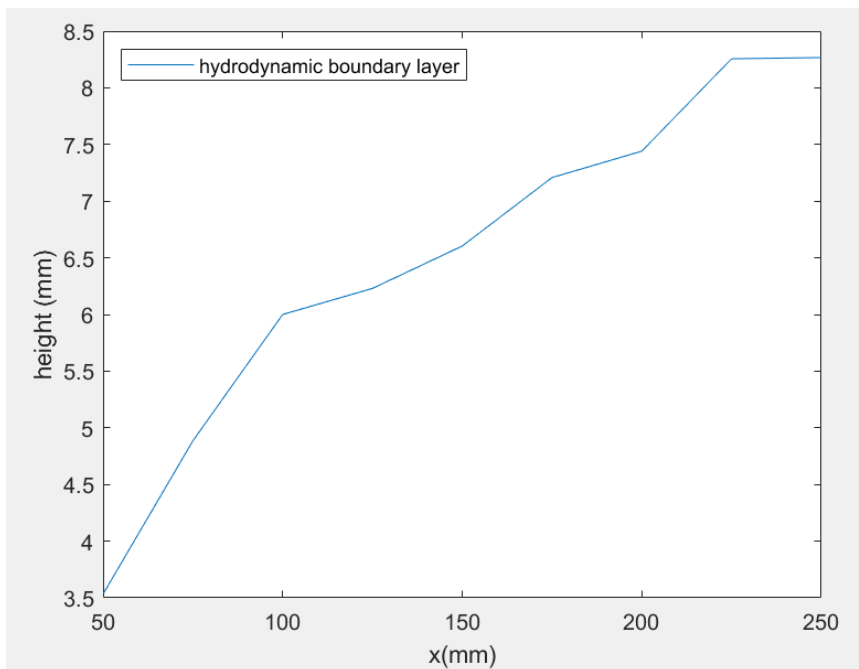


Figure 8.7. Hydrodynamic boundary layer at the flat plate.

# 1. CONCLUSIONS

The experiment was successfully designed and some experiments were tested in the facility built and placed inside the wind tunnel [14]. During these experiments, some issues were found that should be solved for further research and benchmark IR method.

First, as can be seen on the results of the pressure measurements through the flat plate surface, the wind speed goes up to almost 28 m/s. the wind flow was accelerated. The support walls could be interfering on the natural flow of the wind current, accelerating this current and breaking the laminar flow. Therefore the support walls should be cut down so they do not surpass the flat plate surface. This can be done with the already built supports, cutting all the upper part from 4mm over the slot as can be seen in figure 9.1

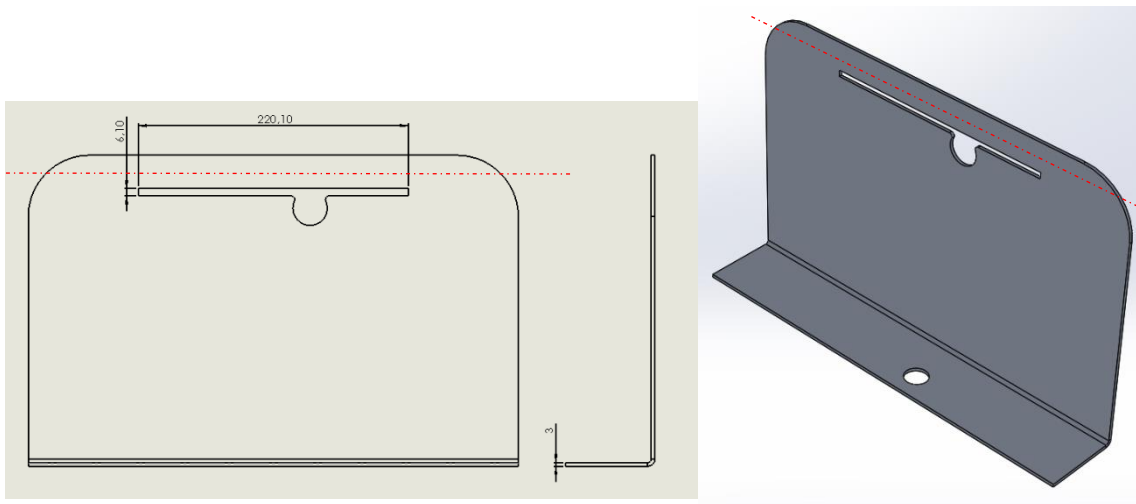


Figure 9.1. Supports top part removal represented with the red line 4mm over the original slot.

Also, as can be seen in figure 9.2, all the measurements that were done showed weird results in the incident edge of the wind flow. This phenomenon could be happening because of the support walls and also because of the fluid crashing in the leading edge. For further research, the flat plate should be redesigned trying to have a sharper leading edge so the wind current follows the flat plate with a flow as similar as possible to a

perfect laminar flow. It is also recommended to elongate the flat plate. It is known that more material increases the flat plates prices but it allows to a full development of the

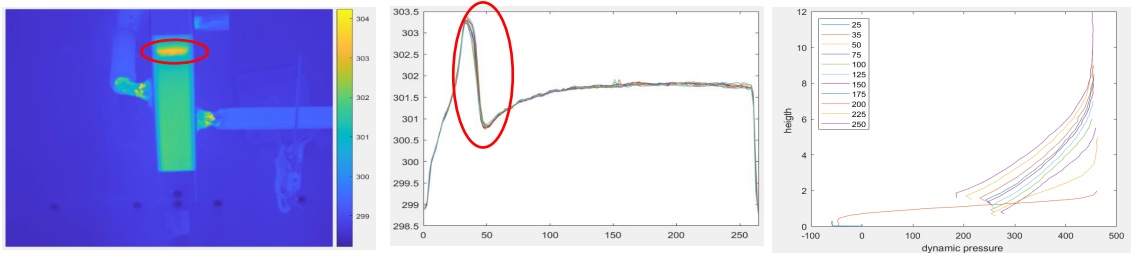


Figure 9.2. Separation / transition of the wind current in the leading edge.

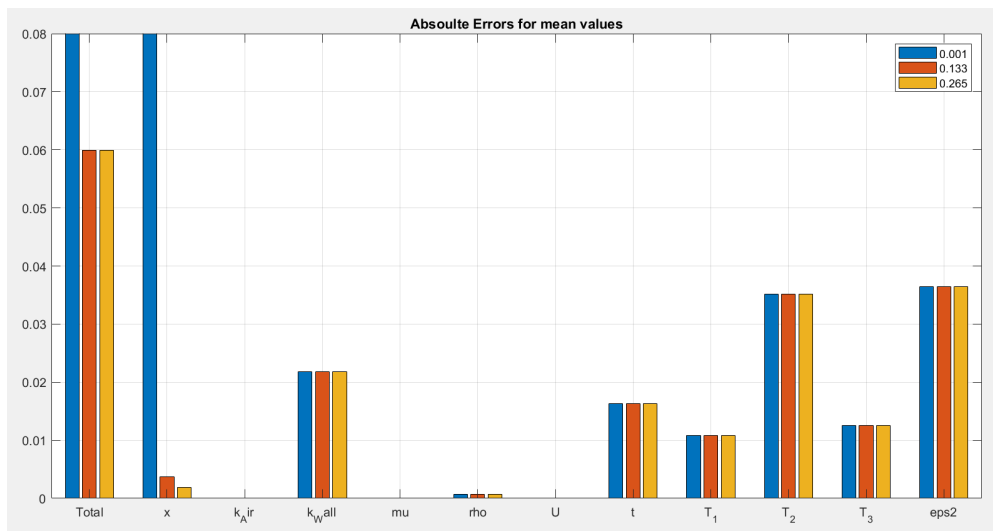


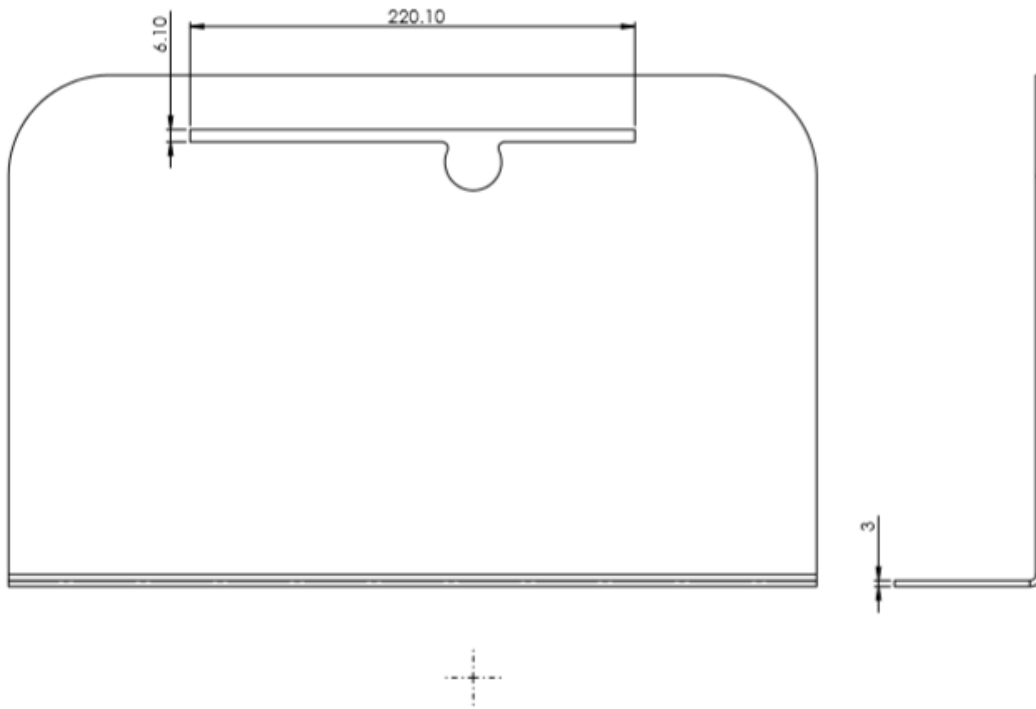
Figure 9.3. Absolute errors for mean values at  $x=0.001\text{m}$ ,  $x=0.133\text{m}$  and  $x=0.265\text{m}$ .

# Bibliography

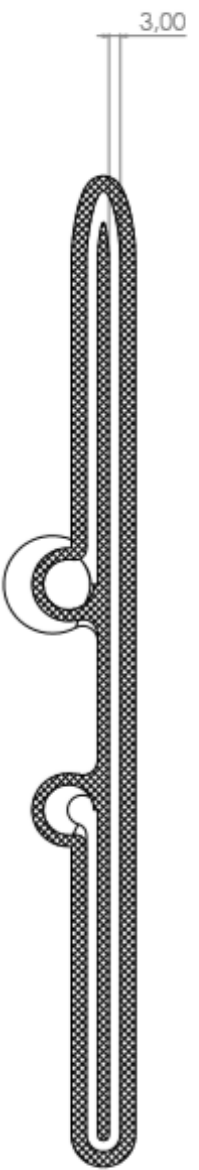
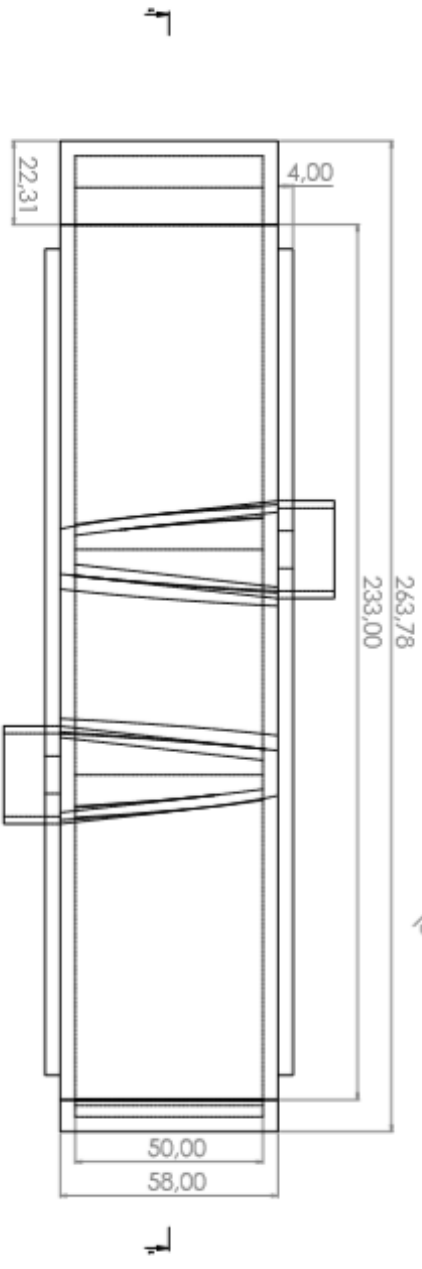
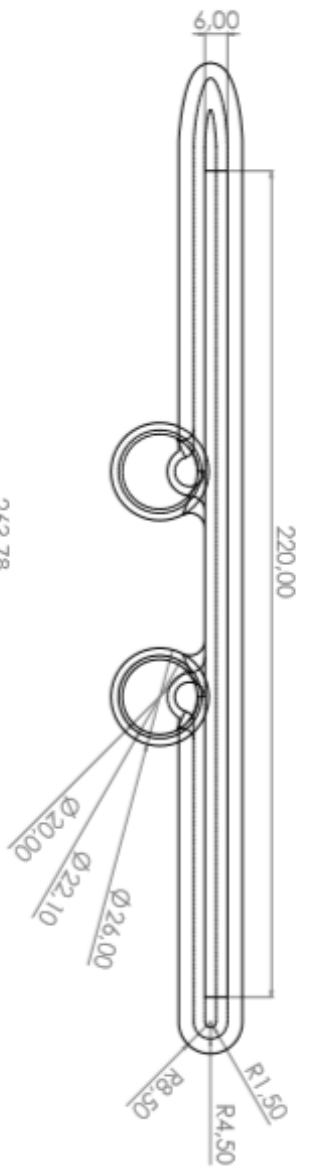
- [1] Benjamin Kirollos; Thomas Povey, «High-accuracy infra-red thermography method using reflective marker arrays,» IOP publishing, Oxford, 2017.
- [2] Isak Jonsson; Valery Chernoray; Radheesh Dhanasegaran, "INFRARED THERMOGRAPHY INVESTIGATION OF HEAT TRANSFER ON OUTLET GUIDE VANES IN AN ENGINE EXIT MODULE," MDPI, Gothemburg, 2020.
- [3] «World unique single turbine stage low-temperature steady-state test facility for TRS and LPT studies,» [En línea]. Available: <https://www.chalmers.se/en/departments/m2/simulator-labs/labs/chalmerswindtunnels/facility/Pages/OGV-LPT.aspx>.
- [4] A. ASME International, «Test Uncertainty PTC 19.1. Technical report,» ASME International ASME, 2005.
- [5] «Sustainable development goals; Climate action,» [En línea]. Available: <https://www.un.org/sustainabledevelopment/climate-change/>.
- [6] «Clean Sky,» [En línea]. Available: <https://www.cleansky.eu/>.
- [7] «Sustainable development Goals; Industries innovation and infrastrucure,» [En línea]. Available: <https://www.un.org/sustainabledevelopment/infrastructure-industrialization/>.
- [8] C. Arroyo Osso, « Aerothermal investigation of an intermediate turbine duct,» PhD Thesis, Chalmers369 University of Technology,, Gothenburg, Sweden, 2009.
- [9] B. Rojo, V. Chernoray, M. Johansson y M. Golubev, « Experimental Heat Transfer Study in an Intermediate371 Turbine Duct,» AIAA-2013-3622, 2013.

- [10] B. Rojo, C. JimenezSanchez y V. Chernoray, « Experimental heat transfer study of end wall in a linear cascade 373 with IR thermography,» In Proc. of EPJ Web of Conferences, Vol. 67., 2014.
- [11] C. Wang, L. Luo, L. Wang, B. Sundén, V. Chernoray, C. Arroyo y H. Abrahamsson, « Experimental and numerical investigation of outlet guide vane and end wall heat transfer with various inlet flow angles,» 2016.
- [12] «3D systems,» [En línea]. Available: <https://www.3dsystems.com/materials/figure-4-hi-temp-300-amb>.
- [13] S. M. Eric Tang Kwor, «Emissivity measurements for Nextel Velvet Coating 811-21 between -36°C and 82°C,» Würzburg, Germany, 1999.
- [14] "Chalmers Large-Scale Low Turbulence Subsonic wind Tunnel," [Online]. Available: <https://www.chalmers.se/en/departments/m2/simulator-labs/labs/chalmerswindtunnels/facility/Pages/Large-Scale-Low-Turbulence-Subsonic-wind-Tunnel.aspx>.
- [15] B. Rojo, « Aerothermal experimental investigation of LPT-OGVs. PhD thesis,» Chalmers University of Technology, Gothenburg, Sweden, 2017.

# Annexes



|  |              |   |   |                            |              |
|--|--------------|---|---|----------------------------|--------------|
| UNLESS OTHERWISE SPECIFIED:<br>DIMENSIONS ARE IN MILLIMETERS<br>TOLERANCES:<br>LINEAR:<br>ANGULAR: |              | ISO 128<br>For angle projection<br>DRAWS AND BREAK SHARP<br>EDGES |  | DD HÖFSCHE DRÄNING         | REVISION:    |
|  |              |   |   | Chalmers Tekniska Högskola |              |
|  |              |   | TITLE   |                            |              |
| DRAWN  | NAME         | DATE  | MATERIAL  | DWG NO.                    |              |
| APP'D  | Isak Jonsson | 10/04/2020  | 1060 Alloy  | Support                    | A3           |
|  |              |   | HOQNT: 101294   | SCALE: 1:0                 | SHEET 1 OF 1 |



2025.04.19  
MUELDA 37

| Item | Description | Quantity | Material |
|------|-------------|----------|----------|
| 1    | Component   | 1        | Aluminum |

## THEORETICAL.M

```
clear all
close all
clc
% Flat Plate constant Ts
%addpath(genpath('D:\Box Sync\Box Sync\Experimenta-
tion\Scripts'))
addpath 'C:\Users\yagog\OneDrive - Universidad Pontificia
Comillas\4°\TFG'

newMC=1;           % want to run Monte Carlo? 1= yes, 0=no
airproperties=1;  % want to use AirProperties? 1= yes, 0=no
% Want to see results for begining, middle and end of the
flat plate
% REP_Points=1; wan to see all the points 3Points=0
REP_Points=0;
z=0.001;          % lower z--> better precision and higher
calculation time
K=273.15;
%% Input values
U_inf=28;         % [m/s] fluid speed
T=25.59+K;       % [°k] air temperature
T_w=35+K;        % [°k] water temperature
%wall parameters
L=0.265;         % [m] flat plate length
t_wall = 4e-3;   % wall thickness [m]
k_wall = 0.225;  % wall thermal conductivity
x=0:z:L;

geo.b=0.058;     % width of the plate
geo.L=L;         % plate Length
geo.h=0.003;     % Channel Height
geo.t=t_wall;    % Wall thickness
geo.k=k_wall;    % Wall Conductive
geo.P=2*(geo.h+geo.b); % Channel Perimiter
geo.A=geo.h*geo.b; % Channel cross section
geo.Atot=geo.L*geo.b; % exposed area

%%Constants (from Incropera, appendix A.4 pag 941) ~(T air,
atmospheric pressure)
if airproperties==false
Cp= 1.007e3;     % [J/(Kg*K)] specific heat capaccity
k=26.3e-3;      % [W/(m*k)] air thermal conductivity
rho=1.1614;     % [Kg/m^3] density
mu = 184.6e-7;  % [kg/(m*s)] dynamic viscosity
nu=mu/rho;      % [m^2/s] kinematic viscosity of air
Pr=Cp*mu/k;     % Prandtl number
```

```

else
[rho,mu,k,Cp,nu,Pr]=AirProperties(T-
K,[],[],'rho','mu','k','c_p','nu','Pr');
end
%%
Rex=(U_inf/nu).*x;
ReL=U_inf/nu*L;

%% Laminar flow
Nux=0.332.*Rex.^(1/2)*Pr^(1/3);      % local Nusselt number
Nu_av=0.664*ReL^(1/2)*Pr^(1/3);     % average Nusselt number
Nu_x_av=0.664*Rex.^(1/2)*Pr^(1/3); % average Nusselt number

hx=k.*Nux.*x.^(-1);                  % local h
h_l=Nu_av/L*k;                        % average h

[T_2d,T_21d,T_3d,Err_1d] = Tempera-
tures(T_w,T,t_wall,k_wall,hx,h_l,geo.Atot,geo.P,geo.h);
Ts=T_2d;                               % [°k] plate temperature

qx=hx.*(Ts-T);
delta_l=((5.*x./(Rex).^(1/2))).*10^3;   % [mm] (7.19 in-
cropera)
delta_T_l=delta_l.*Pr^(-1/3);          % [mm] approx (7.24
incropera)

%% plots
figure
plot(x,Nux)
xlabel('x (m)')
ylabel('Nux')
title('Local Nu flat plate laminar flow')
grid on

figure
plot(x,hx)
xlabel('x (m)')
ylabel('hx')
title('Local h flat plate laminar flow')
grid on

figure
plot(x,qx)
xlabel('x (m)')
ylabel('qx (W/m^2)')
title('Local q flat plate laminar flow')
grid on

```

```

figure
plot(x,Rex)
xlabel('x(m)')
ylabel('Rex')
title('Local Re flat plate laminar flow')
grid on

figure
plot(x,delta_T_l)
xlabel('x(m)')
ylabel('delta_T(mm)')
title('delta_T laminar flow')
hold on
plot(x,delta_l)
legend('delta_t_l', 'delta_l');
grid on
%% Turbulent flow
Nux_T=0.0296*Rex.^(4/5)*Pr^(1/3); %(7.36) incropera
hx_T=k.*Nux_T.*x.^(-1);
qx_T=hx_T.*(Ts-T);
delta_T_T= 0.37.*x.*Rex.^(-1/5).*10^3;

figure
plot(x,delta_T_T)
xlabel('x(m)')
ylabel('delta_T(mm)')
title('delta_T turbulent flow')

figure
plot(x,qx_T)
xlabel('x(m)')
ylabel('qx(W/m^2)')
title('Local q flat plate turbulent flow')
grid on

figure
plot(x,hx_T)
xlabel('x(m)')
ylabel('hx')
title('Local h flat plate turbulent flow')
grid on
%% uncertainties
% Removes the first point(go to inf)
x(1)=[];
hx(1)=[];
Rex(1)=[];
if REP_Points==true
x= [x(1) x(length(x)/2+0.5) x(length(x))];
hx= [hx(1) hx(length(hx)/2+0.5) hx(length(hx))];

```

```

Rex=[Rex(1) Rex(length(Rex)/2+0.5) Rex(length(Rex))];
end
% A row multiplier for individual values so that all variables have the right nr of rows
exdr=ones(1,length(x))';

% conditions
cond.T_air=T;
cond.T_water = T_w;
cond.htc_air = hx;
cond.m = 0.6;

% Errors ( Can introduce more, i just didnt see why now)
error.t=0.02;          % Relative 2%
error.k=0.0002;       % ~ 0.02mm

[totErr, indErr, fs, refVal, var]=HTCErrorCalc_AA(geo,error,cond);

% The location does not scale to the size of the length, its is in absolute
% 1mm = 0.001 m is the assumption as for now.
x_p_err=0.001;

%% Monte Carlo Simulation
% This is a Monte Carlo Simulation, it takes forever

if newMC == true
    noise=randn(10000,1);
    % Temp in C 0.05K          % pressure0.1%          % Accuracy of humidity ~1%
    tests = [(T-K)+noise*0.05  1010+(1010*noise*0.001) 15+noise];

    for ii=1:length(tests)
        [rhoMC(ii), muMC(ii), nuMC(ii), kMC(ii)] = AirProperties(tests(ii,1),tests(ii,2), tests(ii,3), 'rho', 'mu', 'nu', 'k');
    end

    rho_err=2*std(rhoMC);
    mu_err=2*std(muMC);
    nu_err=2*std(nuMC);
    k_err=2*std(kMC);
else
    rho_err=0.0018;
    mu_err=2.9212e-10;
    nu_err=2.2794e-08;
    k_err=3.7483e-06;
end

```

```

end

% U_inf is roughly 0.2% for all span.
U_inf_error = 0.0002;

%% single point Taylor Expansion with Air properties C
syms      x_p      k_air      k_w
mu_p      rho_p      U_p      t
T_1      T_2      T_3      eps2
data =    [ x'      k*exdr      k_wall*exdr
mu*exdr      rho*exdr      U_inf*exdr
t_wall*exdr      T_w*exdr      T_2d*exdr      T_3d*exdr
0.991*exdr      ];
absErr =  [ x_p_err.*exdr      k_err*exdr      k_wall*0.02*exdr
mu_err*exdr      rho_err*exdr      U_inf_error.*exdr
t_wall*0.015*exdr      Err_1d*exdr      0.075*exdr      0.05*exdr
0.991*0.02*exdr ];

% The actual function
C = (1./(T_2 - T_3)).*(((k_w./t).*(T_1 - T_2)) - 5.669e-
08.*( eps2.*T_2.^4 - T_3.^4 ) ) .* x_p.^(1/2) .*
k_air.^(-2/3) .* mu_p.^(1/6) .* rho_p.^(-1/2) .* U_p.^(-
1/2) .* Cp.^(-1/3) ;

[totErr, indErr, Expr, refVal]= ErrorDependentVaria-
bles_BC(C,[x_p k_air k_w mu_p rho_p U_p t T_1 T_2 T_3
eps2],num2cell(data,1),absErr);

% Note that this has to be in the same order as in function
ErrorDependentVariables_BC
varList={'x','k_Air','k_Wall','mu','rho','U','t','T_1','T_2
','T_3','eps2',};
figure()
VarList=[totErr' ;indErr'];./refVal';
bar(VarList)
set(gca,'xticklabel',['Total' varList])
ylim([0 0.08]);
title('Absoulte Errors for mean values')
if REP_Points==true
    legend(cellstr(num2str(x')));
end
grid on

figure
hold on
%plot(x',totErr/refVal)
for ii=1:size(indErr,2)
    plot(x',indErr(:,ii)./refVal);
end

```

```
%plot(x',totErr/refVal)
%legend('C_{err}',varlist)
title('Individual error contribution to C')
legend(varList)
```

# Postproces .m

Code to process pressure measurements.

```
% BOUNDARY LAYER INFO
function [U,c,nrElem,nrOfRow,lim] = postprocess()
addpath 'C:\Users\yagog\OneDrive - Universidad Pontificia
Comillas\4°\TFG'
fileId='YAGO/7_(40_440)25ms_hot/25ms_12slope_BL_pres-
sure_hot'; %chose in each exp

Pa = load([fileId '_m.txt']);
std = load([fileId '_std.txt']);
c = load([fileId '_c.txt']);
fco=load([fileId '_fco.txt']);
rho = fco(:,5);
T=25;
K=273.15;

Pstat = load('YAGO/8_static_pressure/Static_Pres-
sure_m.txt');
Pstat=(Pstat(:,3));
ii=1;
j=1;
%save in P mean static pressure values for each point [25
35 50 75 100 125 150 175 200 225 250]mm;
for i=1:length(Pstat)
    if ii<=3
        V(ii)=Pstat(i);
    end
    ii=ii+1;
    if ii>3
        P(j)= mean(V);
        ii=1;
        j=j+1
    end
end
nrElem=40;
nrOfRow=440;
j=1;
k=1;
% calculate q. P is a vector with the mean P static value
for each point
% repeated the number o measurements of that point
for i=1:length(P)
    for ii=j:nrElem
        q(k) = (Pa(k,2) - P(i));
        j=j+1;
    end
end
```

```

        k=k+1;
    end
    if j>nrElem
        j=1;
    end
end

figure
for ii=1:nrElem:(nrOfRow-nrElem+1)
    plot(Pa(ii:ii+nrElem-1,2),c(ii:ii+nrElem-1,2))

    hold on
    % loopname = [loopname {num2str(c(ii,1))}];

end
%x= pressure y= altura
%xlim([0 1])
% legend(loopname,'location','northwest')
xlabel('Total pressure ')
ylabel('height ')
%calculate U drag force with dynamic pressure
https://en.wikipedia.org/wiki/Drag\_equation
U = sqrt(2.*q./transpose(rho)); loopname=[];

figure
for ii=1:nrElem:(nrOfRow-nrElem+1)
    plot(q(ii:ii+nrElem-1),c(ii:ii+nrElem-1,2))

    hold on
    loopname = [loopname {num2str(c(ii,1))}];

end
%x= pressure y= altura
%xlim([0 1])
legend(loopname,'location','northwest')
xlabel('dynamic pressure ')
ylabel('height ')
figure

for ii=1:nrElem:(nrOfRow-nrElem+1)
    plot(U(ii:ii+nrElem-1)./max(U(ii:ii+nrElem-1),c(ii:ii+nrElem-1,2))./max(c(ii:ii+nrElem-1,2)))

    hold on
    loopname = [loopname {num2str(c(ii,1))}];

end
%x= velocity y= altura
xlim([0 1])

```

```

legend(loopname,'location','northwest')
xlabel('U normalized')
ylabel('heigth normalized')
% figure
% for ii=1:nrElem:(nrOfRow-nrElem+1)
%     plot(U(ii:ii+nrElem-1),c(ii:ii+nrElem-1,2))
%
%     hold on
%     loopname = [loopname {num2str(c(ii,1))}];
%
% end
% %x= velocity y= altura
% %xlim([0 1])
% legend(loopname,'location','northwest')
% xlabel('U ')
% ylabel('heigth ')
% loopname=[];
% figure
%
% for ii=1:nrElem:(nrOfRow-nrElem+1)
%     plot(Pa(ii:ii+nrElem-1,3),c(ii:ii+nrElem-1,2)./max(c(ii:ii+nrElem-1,2)))
%     hold on
%     loopname = [loopname {num2str(c(ii,1))}];
% end
% %x= presion y= altura
% %xlim([0 1])
% legend(loopname,'location','northwest')
% xlabel('Pressure');
% ylabel('y coordinates normalized');

j=1;
Max_U=max(U(1:40));
k=0;
for l=1:nrOfRow
    if l-k > 40
        k=k+40
        Z=U(k:k+40);
        Max_U=max(Z);
    end
    if U(l)/Max_U >= 0.99 && k>0
        lim.U(j)=U(l);        % todos los U>=0.99
        lim.c(j)=c(l,2);      % la h de los U>=0.99
        lim.index(j)=l;      % posicion de los U cojidos en el
vector U original
        lim.point(j)=c(l);    % posicion en x de los U cojidos
        j=j+1;
    end
end

```

```

end

l=1;
for j=1:length(lim.U)
    if j>1 && lim.point(j)~=lim.point(j-1)% coje solo el
primer U>= 0.99
lim.H_bound_layer(l)=lim.c(j); %altura de los U>=0.99
lim.Rpoint(l)=lim.point(j); % posicion en x de los U
cojidos
lim.Rindex(l)=lim.index(j); % posicion de los U cojidos en
el vector U original
lim.RU(l)=lim.U(j); % valor de los U>= 0.99
l=l+1;
    end
end
[Pr]=AirProperties(T-K,[],[],'Pr');
lim.T_bound_layer=lim.H_bound_layer.*Pr^(-1/3); %altura de
los T>=0.99

figure
plot(lim.Rpoint,lim.H_bound_layer)

xlabel('x (mm) ');
ylabel('height (mm) ');

legend('hydrodynamic boundary layer','location','north-
west')

end

```

# LocalQuickRead3.m

Code to process IR camera information

```
%% CAMERA INFO  %% 25 M/S FULL POWER
% each folder in yago0 has different measurements, the
camera was moved so
% the extraction of the information in the middspan of the
flatplate is
% different. this means the coordinates need to be changed.
%%
function [A,Z,x] = LocalQuickRead3()
load('20180626_Calibration_13mm.mat');
A=load('camera/3/10dots_25ms_2559C.mat');
close all
    % Temporal average, BP, NUC and calibration
    X_i_phi_BP(:, :) = BadPixel(mapBP, mean(A.imd3D, 3));
    T_i_raw = polyval(pC(:, end), X_i_phi_BP.*Gi(:, :, 2) + Offset(:, :, 2));

    pcolor(T_i_raw); shading interp
colorbar
%caxis([300 305])
%xline(166)
%temperatures in the middle of the flat plate
%%
figure
plot(T_i_raw(1, :))
%temperatures in the middle of the flat plate flipped
Z=(T_i_raw(:, 166));
Z(231:end)=[];
Z(1:80)=[];
Z=flipud(Z);
figure
plot(Z)
%rescale Z L=265--> pixel 151
x=1:265/length(Z):265;
figure
plot(x, Z)
xlim([0, 265])
%%
ii=1;
for i=160:172

    W=T_i_raw(:, i);
    W(231:end)=[];
```

```

        W(1:80)=[];
        W=flipud(W);

        F(:,ii)=W;
        ii=ii+1;
end

figure
plot(x,F)
xlim([0,265])

%%
figure
countvar=std(A.imd3D,[],3);
plot(flipud(countvar(:,166)))

end

```

# Experimental.m

Code for calculations with experimental data

```
close all
clear all
clc
K=273.15;
%% Input values
U_p=28;           % [m/s] fluid speed

% [°k] plate temperature. specify local quick read number(DIFF EXP)
[A,T_2,x]=LocalQuickRead3(); % T_2 = wall temperature --> camera
T_2m=mean(T_2);
Rpt100_57=A.Rpt100_57; Rpt100_58=A.Rpt100_58;
Rpt100_59=A.Rpt100_59;

T_3=25.59+K; % T_3 = air temperature-->measured in the wind tunnel --> sensor (wrote it down)
T_1=RTDtoTemp(Rpt100_59); % T_1 water temperature --> sensor
%% wall parameters
L=0.265;           % [m] flat plate length
t_wall = 4e-3;     % wall thickness [m]
k_wall = 0.225;    % wall thermal conductivity
eps2= 0.991;
%% Laminar flow
[rho_p,mu_p,k_air,Cp,nu,Pr]=AirProperties(T_3-K,[],[], 'rho', 'mu', 'k', 'c_p', 'nu', 'Pr');

x=x*10^-3;
Rex=(U_p/nu).*x;
ReL=U_p/nu*L;

Nux=0.332.*Rex.^(1/2)*Pr^(1/3); % local Nusselt number
Nu_av=0.664*ReL^(1/2)*Pr^(1/3); % average Nusselt number
Nu_x_av=0.664*Rex.^(1/2)*Pr^(1/3); % average Nusselt number

exdr=ones(1,length(T_2))';
T_1=T_1*exdr;
T_3=T_3*exdr;
k_wall=k_wall*exdr;
t_wall=t_wall*exdr;
eps2=eps2*exdr;
```

```

k_air=k_air*exdr;
mu_p=mu_p*exdr;
rho_p=rho_p*exdr;
U_p=U_p*exdr;
Cp=Cp*exdr;

h1=(1./(T_2 - T_3)).*(((k_wall./t_wall).*(T_1 - T_2)) -
5.669e-08.*( eps2.*T_2.^4 - T_3.^4 ));

figure
plot(x,h1)
xlabel('x (mm) ')
ylabel('h')
title(' h flat plate ')
grid on
[U,c,nrElem,nrOfRow,lim] = postprocess();
T_2_norm=(T_2./298.5); %-1)*100;

figure
plot(x,T_2_norm)
title(' surface temperature normalized ')
grid on

delta_T_T= 0.37.*x.*Re_x.^(-1/5)*10^3;

figure

plot(lim.Rpoint,lim.H_bound_layer)
hold on
plot(x*10^3,delta_T_T)

xlabel('x (m) ')
ylabel('delta_T (mm) ')
title('delta_T turbulent flow')

figure
plot(lim.Rpoint,lim.H_bound_layer./8.1771)

xlabel('x (mm) ');
ylabel('height (mm) ');

legend('hydrodynamic boundary layer','location','north-
west')

```